FARAMIR
Mapping Your Radio Environment

2007 - 2013

# Flexible and Spectrum Aware Radio Access through Measurements and Modelling in Cognitive Radio Systems

FARAMIR

D5.2

## Evaluation of Selected Measurement-based Techniques

| | |
|---|---|
| Project Number and Acronym: | 248351 - FARAMIR |
| Editor: | Jordi Pérez-Romero (UPC) |
| Authors: | Ramon Agustí (UPC), Ian F. Akyildiz (UPC), Jordi Pérez-Romero (UPC), Oriol Sallent (UPC), Faouzi Bouali (UPC), Andreas Achtzehn (RWTH), Xia Li (RWTH), Petri Mähönen (RWTH), Jad Nasreddine (RWTH), Janne Riihijärvi (RWTH), Andreas Zalonis (IASA), Nikos Dimitriou (IASA), Andreas Polydoros (IASA), Lorenzo Iacobelli (TC), Christophe Le Martret (TC), Sebastien Herry (TC), Tao Cai (HWSE), Tim Farnham (TRL), Fengming Cao (TRL), Siva Subramani (TRL) |
| Participants: | UPC, RWTH, IASA, TC, TRL, HWSE |
| Workpackage | WP5 |
| Security: | PU |
| Nature: | R |
| Version: | 1.0 |
| Total number of pages: | 139 |

Abstract:

This deliverable presents the performance evaluation results of the measurement-based optimization techniques for solving the identified radio resource management problems developed within the project. The different techniques are classified depending on the scenarios of applicability, namely intra-operator spectrum management, LTE TVWS, non-coordinated spectrum access between primary and secondary users and ad hoc networks. The document illustrates the benefits of using the REM as a support to the optimization techniques.

Keywords: Radio Resource Management, Optimization, Radio Environment Map, Resource Allocation, Cognitive Radio, Intra-operator spectrum management, LTE, TVWS, Spectrum sharing, Ad hoc networks.

Document Revision History

| *Version* | *Date* | *Author* | *Summary of main changes* |
|---|---|---|---|
| 0.1 | 26.7.2011 | UPC | ToC proposal |
| 0.2 | 09.11.2011 | UPC | ToC after comments received from IASA, RWTH and after Ohrid meeting discussion |
| 0.3 | 16.12.2011 | UPC, IASA, RWTH, TCF | First integrated version with the received contributions from IASA, RWTH, TCF and UPC. |
| 0.4 | 10.01.2012 | TREL | Sections 2.2 and 4.6 |
| 0.5 | 07.02.2012 | UPC, TCF, HWSE | Full draft version with contributions and updates in sections 3.1, 4.1, 4.2 and chapter 5. Introduction and conclusions have been added. |
| 0.6 | 22.02.2012 | UPC, RWTH, HWSE, TCF, IASA | Minor updates in sections 2.1, 2.3, 3.1, 4.5, 5.2, and chapter 6.<br>Editorial revision. |
| 1.0 | 28.02.2012 | Janne Riihijärvi (RWTH) | Final integrated version |
| 1.0f | 29.02.2012 | Petri Mähönen (RWTH) | Coordinator review and approval |

# Table of Contents

1. Introduction ..... 7

2. Optimization techniques in Intra-operator Spectrum Management scenarios ..... 8

2.1. Solutions for multi-tier co-channel cellular networks, enhanced with multi-level REMs ..... 8
2.1.1. Summary of the optimization problem ..... 9
2.1.2. Optimization techniques ..... 10
2.1.3. Evaluation methodology ..... 11
2.1.4. Results ..... 12
2.1.5. Conclusions ..... 14

2.2. Resource optimization for macro-femto network ..... 15
2.2.1. Summary of the optimization problem ..... 15
2.2.2. Optimization techniques ..... 15
2.2.3. Evaluation methodology ..... 18
2.2.4. Results ..... 19
2.2.5. Conclusions ..... 21

2.3. Enabling spectrum sharing in OFDMA-based network using Robust channel Assignment 21
2.3.1. Summary of the optimization problem ..... 21
2.3.2. Optimization techniques ..... 23
2.3.3. Evaluation methodology ..... 25
2.3.4. Results ..... 26
2.3.5. Conclusions ..... 28

3. Optimization techniques in LTE TVWS scenario ..... 29

3.1. Femtocell radio resource usage optimization based on REM for intra-operator spectrum management ..... 29
3.1.1. Summary of the optimization problem ..... 29
3.1.2. Optimization techniques ..... 31
3.1.3. Evaluation methodology ..... 34
3.1.4. Results ..... 34
3.1.5. Conclusions ..... 35

4. Optimization techniques in scenarios with Non-Coordinated Spectrum Access between PUs and SUs ..... 36

4.1. Out-of-band (Cognitive) Femtocells ..... 37
4.1.1. Summary of the optimization problem ..... 37
4.1.2. Optimization techniques ..... 40
4.1.3. Evaluation methodology ..... 42
4.1.4. Results ..... 43
4.1.5. Conclusions ..... 48

4.2. Cognitive RRM exploiting heterogeneous PU types ..... 48
4.2.1. Summary of the optimization problem ..... 48
4.2.2. Optimization techniques ..... 50
4.2.3. Evaluation methodology ..... 54
4.2.4. Results ..... 55
4.2.5. Conclusions ..... 61

4.3. Spectrum selection based on PU transmission patterns ..... 61
4.3.1. Summary of the optimization problem ..... 61
4.3.2. Optimization techniques ..... 62
4.3.3. Evaluation methodology ..... 67
4.3.4. Results ..... 68
4.3.5. Conclusions ..... 71
4.4. Using Geolocation Information for DSA ..... 72
4.4.1. Summary of the optimization problem ..... 72
4.4.2. Optimization techniques ..... 75
4.4.3. Evaluation methodology ..... 76
4.4.4. Results ..... 77
4.4.5. Conclusions ..... 82
4.5. Opportunistic Access Technique using Stochastic Models ..... 83
4.5.1. Summary of the optimization problem ..... 83
4.5.2. Optimization techniques ..... 86
4.5.3. Evaluation methodology ..... 88
4.5.4. Results ..... 90
4.5.5. Conclusions ..... 92
4.6. Hidden node detection and avoidance ..... 93
4.6.1. Summary of the optimization problem ..... 93
4.6.2. Performance evaluation methodology ..... 96
4.6.3. Results ..... 97
4.6.4. Conclusions ..... 99
5. Optimization techniques in Ad hoc Networks scenario ..... 101
5.1. REM population protocol ..... 101
5.1.1. MAC Frame ..... 101
5.1.2. Local REM population protocol ..... 102
5.2. Fast reactive autonomous networks ..... 103
5.2.1. Summary of the optimization problem ..... 103
5.2.2. Optimization techniques ..... 103
5.2.3. Evaluation methodology ..... 108
5.2.4. Results ..... 109
5.2.5. Conclusions ..... 116
5.3. Networks with high data rate point-to-point links ..... 116
5.3.1. Summary of the optimization problem ..... 116
5.3.2. Optimization techniques ..... 117
5.3.3. Evaluation methodology ..... 119
5.3.4. Results ..... 120
5.3.5. Conclusions ..... 122
5.4. Mobile networks in primary environment ..... 122
5.4.1. Summary of the optimization problem ..... 122
5.4.2. Optimization techniques ..... 123
5.4.3. Evaluation methodology ..... 125
5.4.4. Results ..... 125
5.4.5. Conclusions ..... 129
6. Conclusions ..... 130

Acronyms ..... 134

References ..... 136

# 1. Introduction

One of the objectives of the FARAMIR project is the development of technologies that improve the efficiency of future wireless systems by enhancing the awareness that the different network elements have about the radio environment. This is achieved by exploiting the Radio Environmental Map (REM) concept. Specifically, environmental information stored in REM can be used by smart Radio Resource Management (RRM) strategies to ensure that the scarce radio resources available can be used efficiently to provide the desired quality of service to the different network elements in different scenarios. Similarly, by properly exploiting the REM information, resource management mechanisms should be able to increase the overall system capacity.

Specific scenarios where REM information can be exploited were first identified in deliverable D2.2 [1] and classified into three main groups: intra-operator scenarios, hierarchical access in licensed bands and spectrum sharing on unlicensed bands. This goes beyond the usual existing solutions and proposals tending to focus on limited scenarios, such as TV White Spaces (TVWS). Then, in deliverable D5.1 [2], a set of different RRM optimization problems for these scenarios were identified and formulated. This deliverable relies on these previous works, and takes into consideration the final FARAMIR system architecture developed in deliverable D2.4 [3] that defined the functional elements of the REM and the interactions between them. Based on this, this deliverable presents on the one hand the REM-based optimization techniques that have been selected for solving the identified RRM optimization problems, and provides an evaluation of these techniques to illustrate the benefits of using the REM in terms of resource efficiency.

This deliverable is organized in four main chapters according to the optimization techniques for the general scenarios identified in [1] and associated architectures in [3]. In particular, Chapter 2 deals with the intra-operator spectrum management scenarios in which the REM is used to support the resource allocation inside the network of an operator. Then, Chapter 3 focuses on the particular scenario of a Long Term Evolution (LTE) network deployed using TVWS and addresses the intra-operator spectrum management problems. Chapter 4 deals with scenarios in which Secondary Users (SU) share the same spectrum as Primary Users (PU) without any coordination among them and thus the secondary network relies on the REM information to make the RRM decisions. Finally, Chapter 5 addresses the optimization techniques for ad hoc networks scenarios, together with the data dissemination protocol to build the local and global REM.

In each of the chapters, specific sub-sections are devoted to present the different solutions and their performance evaluation. In all cases, a short description of the optimization problem is given, with reference to previous deliverable D5.1 [2], the optimization techniques to solve it are presented, emphasising the information used from the REM, and a performance evaluation is provided, trying to quantify the role of the REM in terms of performance improvements.

# 2. Optimization techniques in Intra-operator Spectrum Management scenarios

This chapter addresses the RRM optimization problems that have been identified in the context of the scenarios dealing with intra-operator spectrum management for OFDMA cellular networks, with the main objective of perform the allocation of resources in terms of power and frequencies. The key differentiating element with respect to state-of-the-art approaches is the introduction of the REM database as supporting element of the different procedures.

Based on the above considerations, the chapter is organised according to three different problems:

- Section 2.1 focuses on the problem of multi-tier cellular networks, composed by macro and femtocells that share the same channel, and proposes a power allocation algorithm to ensure the adequate level of protection to macrocell users.
- Section 2.2 also deals with the problem of cellular networks composed by macro and femtocells but from the perspective of the frequency domain. In particular, it proposes an efficient mechanism of dynamic spectrum allocation to the different cells.
- Section 2.3 presents a channel assignment solution that enables a network operator to allow certain channels to be shared with a secondary network without degrading the QoS of the primary network. As a difference from the solutions that will be presented in Chapter 4, the strategy presented here focuses on the primary network and assumes that primary and secondary networks operate in a coordinated way.

## 2.1. Solutions for multi-tier co-channel cellular networks, enhanced with multi-level REMs

A reliable way to increase the capacity of a cellular network is to reduce the distance between the transmitter and the receiver, thus achieving higher quality links. In that direction, the deployed networks are enhancing their infrastructure with the addition of femtocells as a second tier under the macrocells. Femtocells are low power radio access points, providing cellular services to users in the home and small-office environments through the Femtocell Access Points (FAPs). The latter are deployed by the end-users and thus their locations with respect to the Macrocell Base Stations (MBSs) are dynamic and random. Interference Management (IM) and RRM procedures have the important role to control, with an efficient and robust manner, the various resources (power, channel allocation, rate, etc.) in order for the femtocells to be seamlessly integrated into the network architecture.

Context information stored in REMs can be used in order to enhance the performance of IM and RRM algorithms for co-channel femtocell deployments. The main difference between a REM-based approach versus a traditional one is that the information used by the optimization algorithm is not only related to Channel State Information (CSI) feedback from a User Equipment (UE) to its serving Base Station (BS), but also includes information obtained by accessing REMs at various levels of the infrastructure [4], where the information is collected using different approaches (sensor networks, localization techniques [6], [7] etc). The objective here is to highlight and assess the benefits of

using REMs in controlling the interference in two-tier networks. The 3GPP LTE network [5] with femtocells is considered.

### 2.1.1. Summary of the optimization problem

Herein, the use of "rich" context information stored in REMs is considered in order to enhance the performance of pragmatic Power Control (PC) algorithms for the FAP's downlink transmission in co-channel femtocell deployments. In [8] the Femto Forum identified the various scenarios where interference impacts the performance of a two-tier network when co-channel allocation is considered. The focus here is on the downlink interference from the FAP to the Macrocell User Equipment (MUE). In this scenario the MUE is located in the same area with the FAP and uses the same channel for the downlink communication with the MBS. Closed access FAP is considered, which means that the MUE cannot use the FAP to access the network. The MUE can be inside the house where the FAP is deployed, or it can be outside in a small distance from it. The interference from the FAP will result in coverage holes in the macrocell where the MUE will not have the necessary SINR to communicate with the MBS. In Figure 1 the selected interference scenario is depicted.

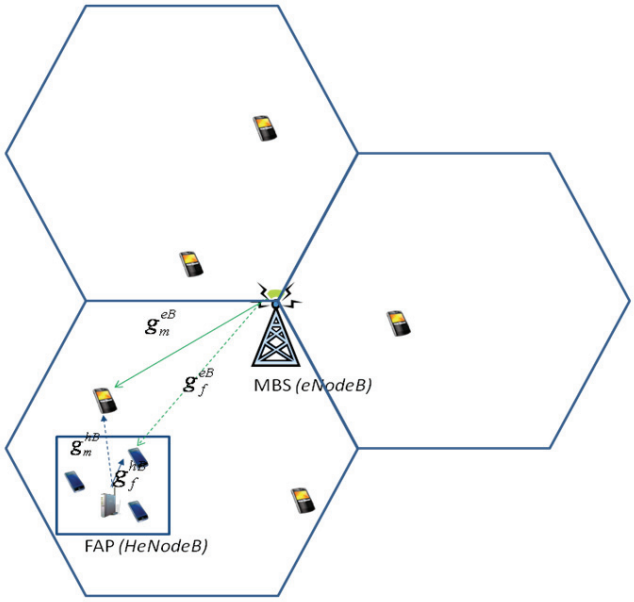


Figure 1: Femtocell to Macrocell UE interference.

The macrocell is considered as a primary infrastructure, and the femtocell as a secondary one. The focus in this study is to assess the effectiveness of the protection that can be provided to the MUE from the FAP's downlink interference with the use of downlink PC, without considering the effect to the FAP connections to the Femtocell User Equipments (FUEs).

Table 1 summarizes the optimization problem related information.

Table 1: Optimization Problem: Femtocell downlink power control.

| Femtocell Downlink Power Control | |
|---|---|
| Scenario(s) of applicability | Femtocells deployed within a macrocell (2-tier networks) |
| General description | The MUE is located in the same area with the FAP and uses the same channel for the downlink communication with the MBS. The MUE can be inside the house where the FAP is deployed, or it can be outside in a small distance from it (a radius of 50m). |
| Assumptions | Closed access FAP is considered. Co-channel allocation. |
| Optimization target | MUE's protection; FAP transmit at a certain power level allowing the MUE to meet its SINR target |
| Tunable parameters | FAP's Tx DL power |
| Input parameters | REM's related information, MUE's SINR target |
| Constraints | MBS Tx power (fixed) |
| REM information | MBS, FAP location, MUE detection and location, path loss term, shadowing term |

### 2.1.2. Optimization techniques

In [9], [10] for 3G and in [11] for LTE femtocells, the following algorithm was proposed for the protection of the MUE (we will refer to this as the *baseline*):

- The FAP (HeNB) measures the Reference Signal Received Power (RSRP) and the SINR from the macro BS and neighboring FAPs.
- Upon detection of a neighboring victim MUE the FAP reduces its transmission power aiming to maintain a predefined SINR target for the MUE (calculated by using a fixed predefined assumption for pathloss distance)
- In case the target cannot be achieved, the FAP transmits at a predefined minimum power level.

In this algorithm, various assumptions had to be taken into consideration. Because of the lack of direct communication between the victim MUE and the FAP, the exact downlink received power measured at the MUE from its connected MBS is unknown to the FAP. In [11] it was proposed that the FAP will measure its received power (RSRP) from the MBS, and it was assumed that a close by MUE will have the same RSRP measurements. Another assumption was a fixed path loss distance in dB between the MUE and the FAP for the calculation of the interference (80 dB). This algorithm has been shown in [11] to reduce MUE outage with respect to the case when the existence of a neighborhood victim MUE is unknown.

The use of information stored in REM can improve the effectiveness of this algorithm. A modified version of this algorithm is proposed where the location of both the FAP and the MBS is known, along with the existence and the location of a neighbourhood victim MUE. The information for the path loss and shadowing models of the area are also stored in the REM allowing the FAP to estimate the expected MUE's SINR. The REM-based procedure can then be described in the following way:

- The FAP accesses the REM to update the available path loss and shadowing models for its area (based on building characteristics and geographical data) and the positions of the other neighbouring network elements (MBS, FAPs, MUEs).
- After detecting the presence of a neighbouring victim MUE, the FAP calculates its transmission power aiming to maintain a predefined SINR target for the MUE by using the context information collected in the first step.
- In case the SINR target cannot be met, FAP transmits at a predefined minimum power.

In the above REM-based PC algorithm we assumed complete knowledge of the network components' locations, the path loss and shadowing terms. While the location of MBS is known in advance, the FAP location needs to be estimated since the user may place the FAP randomly inside the house. The victim MUE's position relative to the FAP and the building also has to be estimated. We assume herein that these locations are determined either from the FAP and MUEs themselves, or from a dedicated sensor network deployed near the house from the operator. The path loss term for the calculation of the channel gains between the network elements is also assumed to be stored in the REM for a specific area based on long term operator's measurements. A sensor network could also be used to estimate the shadowing term, but this is not an easy task and it may result in inaccurate estimates. Assuming that the victim MUE's distance to the FAP is smaller than the MBS shadowing correlation distance, the FAP will be able to estimate the MBS-to-MUE shadowing term based on its power measurements from the MBS. For the FAP-to-MUE shadowing term - on the other hand - we have to rely on the accuracy of the sensing results.

Here we also propose a modified version of the REM-based PC where the FAP-to-MUE shadowing term is unknown and we only know the statistics of the shadowing, which is a lognormal distribution with zero mean and known standard deviation σ that characterizes the area. In this case we use this knowledge to calculate a back-off term for the total channel gain estimate between the FAP and the MUE based on a target outage level. In our assessment we assume that the standard deviation for the femtocell area is 4 dB (stored in REM). Thus for an outage of 2% in the channel gain estimate we have a Back-Off (BO) term of about -8 dB. In following subsections we will refer to this version of the algorithm as REM-based-PL (REM-based power control with accurate Path Loss knowledge and statistical knowledge for the shadowing).

### 2.1.3. Evaluation methodology

The objective here is to highlight the potential gain of using the rich context information in a two-tier network deployment. This gain can serve as an upper bound for pragmatic REM-based algorithms, considering that the inaccuracies in the stored REM's data will result in reduced performance figures. The metric used for assessment is the MUE outage that is observed when the FAP transmits at a power level such that –due to the generated co-channel interference – the MUE cannot satisfy its SINR target.

Specifically we compare the baseline PC based on the detection of the presence of a victim MUE, with the REM-based PC (with the accurate knowledge for the location, the path loss and the shadowing). We also examine the more realistic REM-based-PL where only the standard deviation of the shadowing is available in the REM.

The simulation setup is based on the Orthogonal Frequency Division Multiple Access (OFDMA) Interference Scenario Evaluation Methodology for LTE femtocells presented in [11] for the suburban case. The parameters used in our simulation are summarized in Table 2.

Table 2: Simulation parameters.

| Parameter | Value |
|---|---|
| Cell Layout | Hexagonal grid, 3 sectors per cell |
| Inter-MBS distance | 1732 m |
| Carrier Frequency | 2000 MHz |
| LTE bandwidth | 10 MHz |
| MBS Shadowing standard deviation | 8 dB |
| MBS Auto-correlation distance of shadowing | 50m |
| Wall penetration loss | 10 dB |
| MBS Tx power | 46 dBm |
| MUE Noise Figure | 9 dB |
| Minimum distance between MUE and BS | 35m |
| MUE distribution | Uniformly distributed within a circle 50 m around the FAP |
| Minimum distance between MUE and FAP | 20 cm |
| Min/Max Tx FAP Power | -10/20 dBm |
| FAP Auto-correlation distance of shadowing | 3m |
| Thermal noise density | -174 dBm/Hz |
| Simulation Scenario | Suburban |
| House size | 12x12 m |
| Number of victim MUEs | 1 |
| Placement of FAP inside the house | Random uniform |
| Path loss models | See [11] |
| Antenna pattern | See [11] |

## 2.1.4. Results

### 2.1.4.1. Illustrative examples

In this section two characteristic examples of femtocell deployments are presented. In the first case the femtocell is deployed in an area where the macrocell signal is weak, while in the second case the femtocell is deployed in an area with a strong macrocell signal. The baseline and the ideal REM-based strategies are compared. The MUE SINR target in this example is set to 3dB. The objective here is to identify the conditions where the use of the REM information is more beneficial for the protection of the MUEs.

- *Case 1: Femtocell in an area with relatively weak macrocell signal*: This is the case according to which the femtocell is deployed in an area at the edge of the cell and/or outside of the center direction of the antenna beam. We simulated 1000 MUE random positions in the vicinity of the

FAP (at a maximum distance from the FAP of 50m) and calculated the average outage experienced from the MUE. For the REM-based PC the measured outage was calculated at 35.1%, while for the baseline PC it was 45.5%, therefore we observed a difference of about 10%. The FAP Tx power distribution based on the REM-based PC (in blue) is depicted in Figure 2. In the same figure the red column depicts the constant Tx power of -6 dBm calculated from the baseline PC based on the predefined assumptions for the channel gain estimates. We see that the REM-based PC algorithm was forced to select the minimum Tx level more than 40% of the times causing the increased outage. This highlights the fact that any minimal provision for the FAP coverage, which is represented in our scenario with the minimum Tx power of -10 dBm, will inevitably result in high probability of outage for the victim MUE. That means that if we want to have an acceptable outage for the MUE in this area we have to reduce the Tx power level below the minimum Tx level of -10dBm.

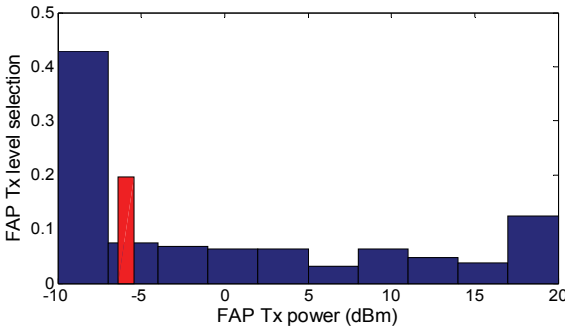


Figure 2: FAP Tx Power profile in weak macro-signal.

- *Case 2: Femtocell in an area with relatively strong macrocell signal:* This is the case when the femtocell is deployed in an area at the center of the sector's antenna beam and/or relatively close to the MBS. The measured outage now was found to be equal to 4.5% for the REM-based PC and 45.8% for the baseline PC. The reason for this increased gain of REM-based PC over the baseline is the significantly lower selection of the minimum Tx level (less than 10%; see Figure 3), since the victim MUE receives strong signal from the MBS and therefore the FAP power margin is larger.

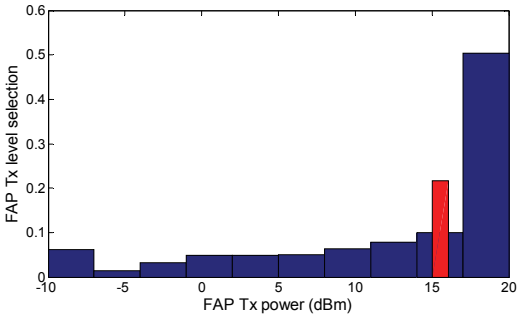


Figure 3: FAP Tx Power profile in strong macro-signal.

### 2.1.4.2. Overall comparison

In Figure 4 we present the average MUE outage when we have random femtocell deployment in specific distances from the MBS (cell radius in Figure 4), for the three PC algorithms (baseline, the

ideal REM-based, the REM-based-PL), and for two different SINR targets for the MUE (3, 9 dB). Here the aim is to average out the effects of MBS shadowing and the antenna pattern; thus the distance from the MBS will be the only parameter that will characterize the MBS signal strength.

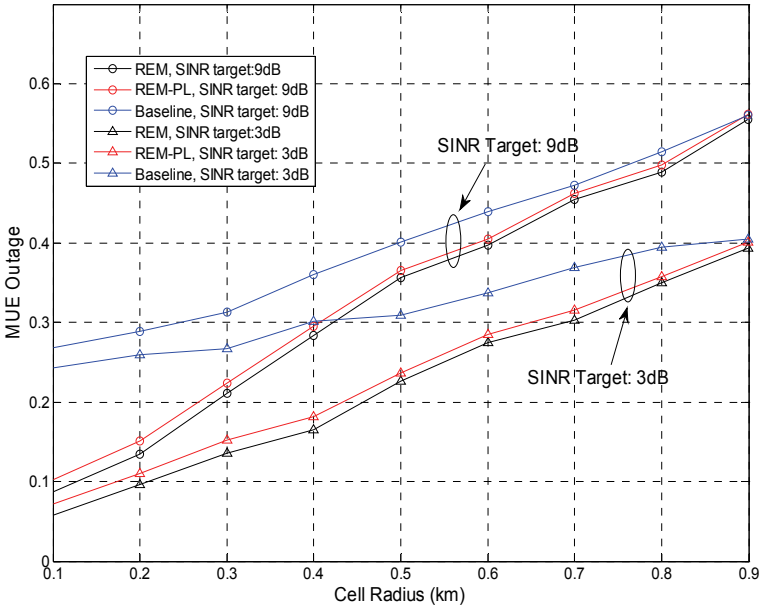


Figure 4: FAP Tx Power profile in strong macro-signal.

The benefit of using "rich" context information is clearly presented in this figure. As the femtocell is deployed closer to the cell edge, the outage gain is reduced. This is expected since the lower threshold for the FAP Tx power has a bigger effect when the MBS signal is weaker. This is most evident in the most demanding SINR target of 9 dB. Also as expected, the outage increases as the MUE's SINR target increases, since the interference generated by the FAP has a bigger effect in the SINR calculation. The REM-based-PL algorithm achieves a clear gain in the MUE's measured outage over the baseline algorithm, and it is slightly worst from the ideal REM-based algorithm. The difference in the outage from the baseline is mainly attributed to the knowledge of the location, since - for example - the path loss term varies substantially if the MUE is inside or outside the house. The small difference in the outage of the REM-based-PL versus the ideal REM-based is accomplished because of the conservative approach of using a fixed back-off loss in the estimation of the channel gain between the FAP and the MUE. This approach has the drawback that the FAP is forced to transmit at a lower level than needed to protect the MUEs, which results in femtocell coverage loss.

### 2.1.5. Conclusions

An ideal REM-based PC was proposed and compared with a baseline PC algorithm designed for LTE femtocell deployment scenarios. It was shown that the use of stored context information increases the effectiveness of a PC algorithm to protect a co-channel MUE. A version of the REM-based PC without the knowledge of the shadowing term was also proposed and compared to the previous algorithms. The estimation of the shadowing term with the use of a back-off term, based on the standard deviation, was shown to protect the MUE almost as good as the ideal case, at the expense of a lower FAP's transmission power level that may lead to smaller femtocell coverage.

## 2.2. Resource optimization for macro-femto network

Femtocells are typically deployed by the subscribers via plug-and-play and could be everywhere within the macrocell, which will result in potential interferences between the femtocell and macrocell especially when both the femtocell and the macrocell operate in co-channel. To address the interference problem, resource/spectrum allocation are widely studied and regarded as an efficient means for interference mitigation considering that the vast majority of femtocells are Closed Subscriber Group (CSG)-based femtocells (not suitable for handover). While tremendous efforts have been taken on spectrum allocation for the interference problem, most of them indeed don't take the practical constraints into account. According to the system architecture in LTE and Wimax, there are no direct links between macro BS and femto BS and any communication between the two has to be via backhaul, which literally imposes two critical constraints: efficient backhaul signalling and delay resistance. The information exchanged between the macro BS and femto BS has to be kept as low as possible, otherwise the backhaul will be overburden with the exchanged information due to numerous femtocells deployed within one macrocell. A practical spectrum resource allocation is of particular interest.

### 2.2.1. Summary of the optimization problem

Here we focus on the downlink interference between macro layer and femto layer, i.e. the interference from macro BS to femto users and the one from femto BS to macro users, and come up with a spectrum allocation solution to mitigate the interference between the femtocell and macrocell by using Dynamic Fractional Frequency Reuse (DFFR) and Dynamic Spectrum Allocation (DSA), taking into account of the requirement of delay-resistance and low backhaul-signaling overhead. Here we consider an OFDMA-based macro-femto system. The conventional hexagonal macro network is used for the study, where a network is formed. Within the macro coverage area, the macro users and femtocells are distributed randomly with a uniform distribution, subject to minimum separation to macro BSs. Macro users choose their anchoring macro BSs by cell searching selection: when a macro user enters the network, the macro user will anchor to a BS from whom the macro user receives highest SINR. In each femtocell, users are randomly dropped to communicate with their corresponding femto BSs. For the simplification of the study and without loss of the generality, we assume universal frequency reuse scheme is used among macrocells and will focus on the area covered by the central macrocell.

Table 3 presents a summary of the main elements of the optimization problem considered in this section.

### 2.2.2. Optimization techniques

#### 2.2.2.1. Macro-to-Femto interference mitigation: DFFR

Firstly, the macro BS gets the REM information from REM database and calculates the averaged SINR for k-th femto user of n-th femtocell with/without the central macro interference as $\mathrm{SINR}_{\mathrm{n,k}}^{\mathrm{F}}$ and $\mathrm{SINR}_{\mathrm{n,k}}^{\mathrm{F}\prime}$. The averaged SINRs for a user are only related to the received power from the BSs to the given user and the received power can be easily derived from the REM information, i.e statistical propagation characteristics from BSs to users, BS TX power, radiation pattern.

Table 3: Optimization Problem: Downlink Spectrum allocation for macro-femto networks.

| Downlink Spectrum allocation for macro-femto networks | |
|---|---|
| Scenario(s) of applicability | Heterogeneous macro-femto network |
| General description | Distributed indoor femtocells within macrocells<br>Distributed macro users within macrocells<br>Distributed femto users within femtocellss<br>Hexagonal macro formed with 19 macrocells |
| Assumptions | CSG typed femtocells and co-channel with macrocell |
| Optimization target | Averaged user and cell throughput |
| Tunable parameters | Frequency resource |
| Input parameters | Inter-BSs level: REM information<br>Intra-BS level: instantaneous CSI, i.e. SINRs |
| Constraints | Fixed TX powers,<br>No direct radio link between macro BS and femto BS |
| REM information | Statistical propagation characteristics from BSs to users: propagation factor (pathloss, shadowing, etc), BS TX power, radiation pattern. |

Then the macro BS divides each femtocell's users into two sets: one set $F_i'$ is composed of the outage users, whose averaged SINR with central macro interference cannot meet the minimal QoS requirement, while their averaged SINR without central macro interference meets the minimal QoS requirement; the other set $F_i''$ includes other users. The macro BS will simply partition the spectrum into two parts as *F*1 and *F*2 as shown in Figure 5, where the *F*1 is exclusive for femtocells and is intended to be used for the femto users of the set $F_i'$. The size of *F*1 can be derived as

$$F1=ceil\left(\frac{\max_i(|F_i'|)}{\max_i(|F_i'|)+K}N\right) \quad (1)$$

where $\max_i(|F_i'|)$ is the largest number of the users of the sets $F_i'$ among the femtocells and $ceil(x)$ rounds the elements of $x$ to the nearest integers towards infinity. In turn, $F2=N-F1$.

It could be seen that the *F*1 is calculated assuming that the outage users of the femtocell mostly affected by the macro interference will share the spectrum with the macro users. The reason to calculate *F*1 like that is to make sure that the outage users of femtocells should at least have the same user experience as macro users. Since this spectrum allocation only relies on the number of outage femto users from each femto cell, the partition scheme will be quasi-static, delay-tolerant. On the other hand, the partition dynamically depends on the distribution of the femtocells and femto users. Therefore, the spectrum allocation is kind of dynamic fractional frequency reuse (DFFR) among the macrocell and femtocell. After the spectrum partition, each femto BS will schedule the frequency resources to its users, where the outage users will be assigned in the part *F*1. Since the *F*1 is computed based on the number of the outage users in the most macro-interference affected femtocell, it is not necessary for each femtocell to allocate the whole *F*1to its outage users. How many resources within *F*1 will be allocated to its outage users depends on this number of outage users.

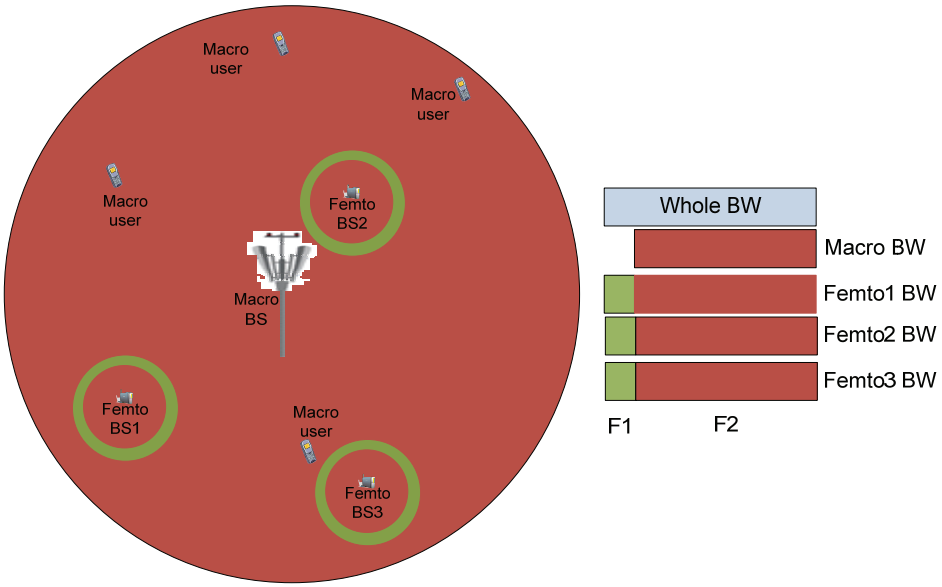


Figure 5: Dynamical fractional frequency reuse.

### 2.2.2.2. Femto-to-Macro interference mitigation: DSA

For the case of the interference mitigation from femto BS to macro user, one challenge is that normally the femto BS doesn't know whether there are any macro users in its territory or the femto BS has no capability to detect the presence of any macro users. However, with help of the REM, the femto BSs can regularly access the REM database to get the updated REM information. Via the REM information, each femto BS can have an idea if there are macro users in or approaching its vicinity. By knowing the presence of the victim macro users, a simple dynamic spectrum allocation (DSA) is proposed to tackle the interference.

Assume $a$ is the number of subcarriers required to meet the minimal QoS requirement, with which the macro user can communicate with the macro BS. Each femto BS will calculate the resources needed for the victim macro users in its vicinity as $a_i = a \times \mathrm{I}_i$, where $\mathrm{I}_i$ is the number of the macro users falling into the vicinity of the $i^{th}$ femtocell. After that, each femto BS will reserve $a_i$ subcarriers for the macro users by leaving $a_i$ distributed subcarriers unused.

At the side of the victim macro users, each macro user estimates the SINRs across the subcarriers and as usual feeds them back to the macro BS. Obviously, only the subcarriers left unused by the femto BS are good enough and according to the feedbacks, the macro BS then can assign the unused subcarriers to the interfered macro users.

Figure 6 shows an example of how to reduce the interferences by randomly distributing the unused subcarriers. Suppose there are 3 femtocells and there are 2 macro users , 1 macro user and 1 macro user falling in the femtocell #1, femtocell #2 and femtocell #3 respectively, and each interfered macro user has to use 2 subcarriers to communicate with macro BS to meet the minimum QoS requirement. Based on this assumption, the femtocell #1, #2 and #3 should randomly distribute 4, 2 and 2 un-used subcarriers respectively. Normally, the number of subcarriers needed per interfered macro user will be much less than the whole available subcarriers, hence the possibility of overlay of the unused subcarriers among the femtocells is rather low and the macro BS can easily schedule the unused subcarriers to the interfered macro users.

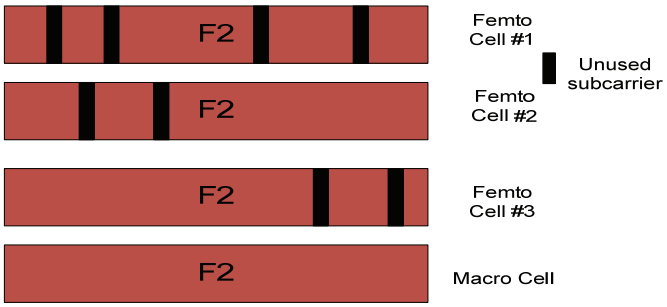


Figure 6: Distribution of unused subcarriers in the femtocells.

### 2.2.3. Evaluation methodology

The main parameters used in the evaluation are listed in Table 4.

Table 4: System parameters.

| Parameters | Value |
|---|---|
| Carrier frequency | 2 GHz |
| Carrier bandwidth | 10 MHz |
| Transmit power (Mcro BS/Femto BS) | 43dBm/18dBm |
| Antenna gain (Mcro BS/Femto BS/User) | 14dBi/0dBi/0dBi |
| Noise figure in User | 9 dB |
| Minimum distance | 20 meters for macro users and macro BS<br>20 cm for femto user and femto BS |
| Lognormal shadowing standard deviation (macrocell/femtocell) | 10dB/4dB |
| Scheduler | Round Robin |
| Inter-macro BS distance | 500 meters |

Once the users are dropped in the macrocell or femtocell, radio propagation fading will be calculated with the following path loss and fast fading models. The path loss between the users and the macro BS can be calculated as:

$$\mathrm{PL_{macro}(dB)} = \begin{cases} 15.3 + 37.6\log_{10}\mathrm{R} & \text{outdoor user} \\ 15.3 + 37.6\log_{10}\mathrm{R} + \mathrm{L_{ow}} & \text{indoor user} \end{cases} \quad (2)$$

where $\mathrm{R}$ is the distance between the UE and the macro BS in meters and $\mathrm{L_{ow}}$ is the penetration loss of an outdoor wall, which is 10 dB.

When the user is connected with a femto BS, the path loss can be calculated as

$$\mathrm{PL_{femto}(dB)} = \begin{cases} 38.46 + 20\log_{10}\mathrm{R} & \text{indoor user} \\ \max(15.3 + 37.6\log_{10}\mathrm{R}, 38.46 + 20\log_{10}\mathrm{R}) + 0.7\mathrm{d_{2D}} + \mathrm{L_{ow}} & \text{outdoor user} \end{cases} \quad (3)$$

We assume that per-subcarrier capacity is used for link-to-system mapping, where the capacity of the $\mathrm{k^{th}}$ subcarrier in a user is given by

$$\mathrm{C_n} = \begin{cases} 0 & \text{if } \gamma_\mathrm{n} < -2dB \\ \alpha\log_2(1 + \beta\gamma_\mathrm{n}) & \\ 4.4 & \text{if } \alpha\log_2(1 + \beta\gamma_\mathrm{n}) > 4.4 \end{cases} \quad (4)$$

where $\alpha$ and $\beta$ are parameters (between 0 and 1) selected to match the link level performance (here $\beta = 1, \alpha = 0.6$ for simulation study), and $\gamma_n$ is the SINR at the $n^{th}$ subcarrier. The capacity is a "backed-off" Shannon channel capacity, taking into account of the non-ideal receiver structure without the need to simulate MCS selection. The overall capacity for a user can be attained by summing the per-subcarrier capacity over all the subcarriers.

### 2.2.4. Results

A simulation was carried out to evaluate the proposed solution. The number of femtocells is varied between 20, 30, 40 and 50. They are deployed indoor, and each femtocell has 2 femto users. There are a total 10 macro users. Figure 7 and Figure 8 show the performance of the proposed methods, where Figure 7 illustrates the performance for DFFR and Figure 8 presents the performance for DSA. The performances are illustrated in terms of CDF of the throughputs of macrocell, macro user, femtocell and femto user respectively in the case of 40 femtocells. With DFFR only in Figure 7, it can be seen that the femtocell and femto user throughputs indeed are improved at the cost of the degradation of macrocell and macro user throughput. In Figure 8, it is obvious that macro users and subsequently the macrocell can have benefits with higher throughput, while femtocell and femto users remain almost unchanged simply because the unused subcarriers left by the femtocells for the interfered macro users in the vicinity of femtocells don't count too much comparing the whole subcarriers available for the femtocells.

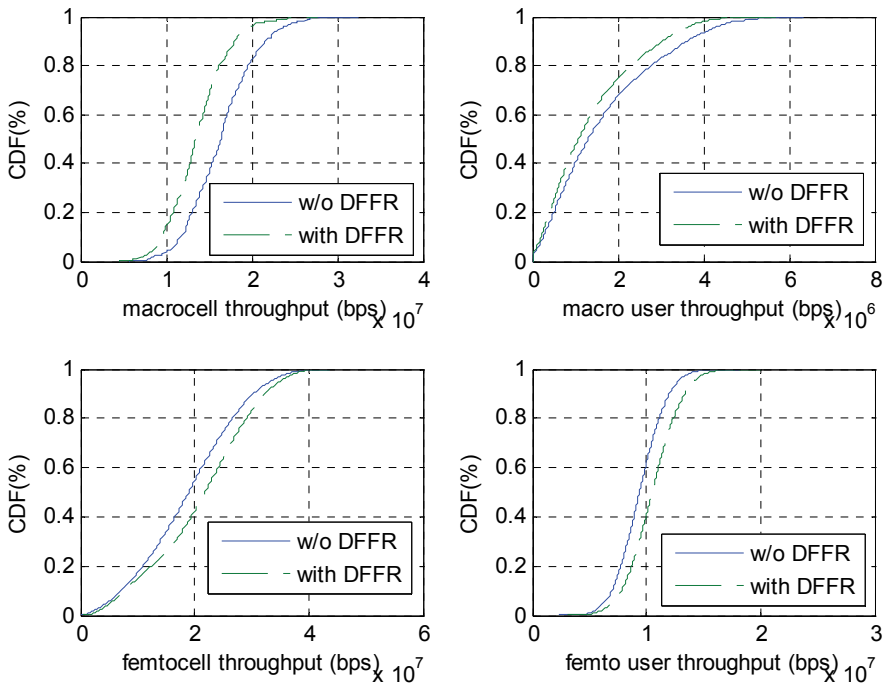


Figure 7: CDF comparison of averaged throughput with/without proposed DFFR for the case of 40 femtocells.

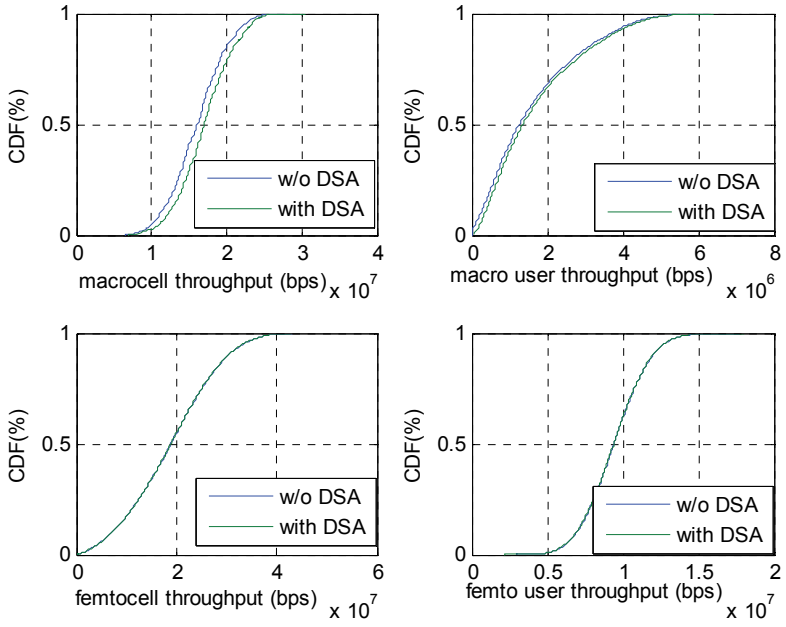


Figure 8: CDF comparison of averaged throughput with/without proposed DSA for the case of 40 femtocells.

Table 5 provides average throughputs of the macrocell and femtocells with different number of femtocells, where the "normalized" means normalization over the benchmark. With DFFR, the macrocell throughput has about 17 percent degradation, while the average femtocell throughput will obtain 11% gain. At the same time, with DSA, the macrocell can increase 3 to 7% depending on the number of femtocells, while there is almost no loss for femtocell average throughput. The simulation results show that using the proposed method, the downlink interferences indeed can be mitigated. Considering the overall system throughput as the sum of the throughputs of the macrocell and all the femtocells, it clearly shows that the overall system throughput can be greatly improved by using the proposed DFFR and DSA, especially for the deployment with more femtocells.

Table 5: Average throughput of macrocell and femtocells.

| | | Number of femtocells | | | |
|---|---|---|---|---|---|
| | | 20 | 30 | 40 | 50 |
| Macrocell average throughput | Benchmark No DFFR and DSA (Mbps) | 17.257 | 16.901 | 16.487 | 15.923 |
| | With DFFR (Mbps) | 14.690 | 14.143 | 13.691 | 13.116 |
| | Normalized DFFR | 0.8513 | 0.8368 | 0.8305 | 0.8237 |
| | DSA(Mpbs) | 17.785 | 17.866 | 17.485 | 17.136 |
| | Normalized DSA | 1.0306 | 1.0571 | 1.0605 | 1.0762 |
| Femtocell average throughput | Benchmark No DFFR and DSA (Mbps) | 19.532 | 19.228 | 18.922 | 18.699 |
| | DFFR | 21.923 | 21.572 | 21.088 | 20.763 |
| | Normalized | 1.1224 | 1.1219 | 1.1145 | 1.1104 |
| | DSA (Mpbs) | 19.502 | 19.079 | 18.876 | 18.684 |
| | Normalized DSA | 0.9985 | 0.9923 | 0.9976 | 0.9992 |

### 2.2.5. Conclusions

A spectrum allocation method using REM information is proposed to address the downlink interference problem, considering the delay-resistance and low signaling overhead requirement. The proposed DFFR decides an exclusive part of the resources to be used for femtocells dynamically based on the number of outage users interfered by the macro BS, to reduce the inference from macro BS to femtocell. At the same time, by using the proposed DSA, the interference from the femto BS to macro users can be effectively reduced.

## 2.3. Enabling spectrum sharing in OFDMA-based network using Robust channel Assignment

Most of the work in the context of Dynamic Spectrum Access (DSA) focuses on the exploitation by secondary users of the unused primary resources. Although a significant amount of these works consider a primary network with ON-OFF patterns [12][13], it is rarely mentioned that these networks are cellular networks. Therefore, only few papers study, though implicitly, the problem of defining primary constraints and the development of mechanisms to allow secondary activity [14]-[18]. Most of these works consider a primary TV broadcasting network, where secondary users' activity is enabled by a reduction in geographical coverage. In [18], however, a reduction of rate is considered as a possibility for cellular primary networks.

Since FARAMIR project does not only focus on white space scenarios but considers the general case of wireless networks, we conducted studies on the possibilities of opportunistic access to primary cellular networks. More specifically, in this section, we consider an OFDMA-based primary network with $T$ frequency channels. Our objective is to develop a mechanism that allows a secondary user to opportunistically access a set of these channels without degrading the QoS provided by the primary network [19]. The proposed mechanism is enabled by the presence of a REM where the primary information can be stored and then accessed by the secondary.

### 2.3.1. Summary of the optimization problem

Cellular operators place in their higher priority serving their users with the expected services wherever these users are. Therefore, reducing the coverage, as in the case of TV white space, to allow secondary activities will not be allowed by cellular operators. Hence, another approach guaranteeing that the pervasive coverage is provided is needed in such scenario. In the following, we discuss a solution to this problem, which exploits the flexibility of OFDMA-based networks through flexible planning and channel assignment.

The dimensioning of cellular networks is generally designed to guarantee that the probability of having an unsatisfied user is lower than threshold $\varepsilon$, where an unsatisfied user can appear due to coverage or cell capacity problems. In most cases, users at the edges of the cell are the ones that are most affected by these problems. Hence network planning tools are designed to guarantee that the average Signal to Interference and Noise Ratio (SINR) over time at the edges of the cell is higher than a given threshold $\gamma_{\text{min}}$. The average SINR in dB at the edge of the cell is given by

$$\gamma_{\text{edge}} = P - L_{\text{max}} - 10\log_{10}\left(10^{I_{S,\text{max}}/10} + 10^{P_N/10}\right) \quad (5)$$

where $P$ is the transmitted power by the base station for one user, $L_{max}$ is the maximum allowed path loss in the cell, $I_{S;max}$ is the interference generated by the other primary cells and $P_N$ is the power of background noise.

We assume that all primary channels are orthogonal and show the same propagation characteristics. It is also assumed that the secondary network will respect the interference constraint of the primary network. The latter is represented by a maximum allowed interference $\iota_{max}$. This interference is determined such that it can be tolerated by any primary receiver, especially the ones at the cell boundaries [12]. Furthermore, any approximation in the computation is considered keeping in mind a more protective situation for the primary network. This will guarantee that, in the worst case, the performance of this network is the one predicted by the model. Finally, we assume that all base stations have the same activity pattern that is defined by the probability of activity $\alpha$. In other words, $\alpha$ is the ratio between the number of active users in the cell and $T$, reflecting the cell load.

Due to secondary activity, the SINR of primary users will be affected by additional interference. At the edge of the cells, the minimum SINR can be written as

$$\gamma_s = P - L_{max} - 10\log_{10}\left(10^{I_{S,max}/10} + 10^{P_N/10} + 10^{\iota/10}\right) \quad (6)$$

where $\iota$ is the experienced interference due to secondary transmission. If traditional planning and resource management techniques (i.e., without considering secondary activity) are applied, primary users will suffer from unacceptable degradation in their QoS. Users' QoS can be kept at the acceptable levels by either increasing transmit power or the number of primary base stations. However these solutions are expensive and should be avoided.

In order to maintain the same base station distribution and configuration while providing the required QoS for their users, the primary network has to implement more sophisticated planning combined with a channel assignment algorithm guaranteeing that a high percentage of users in the otherwise dead zone will be able to maintain reliable communication. This will lead to more robust primary networks against secondary interference for the same available secondary opportunities, or more opportunities for the same robustness in comparison to other solutions.

The proposed approach is based on interference mitigation in OFDMA or TD-CDMA based systems where each cell is divided into two regions as depicted in Figure 9: inner zone and protected zone. In this approach the secondary users will be allowed to share channels with the primary users in the inner zone of the cell. The border between the two zones is defined by the region where the SINRs $\gamma_s$ are equal to $\gamma_{min}$. Since it is difficult to extract secondary interference from primary one especially if they are weak, the primary receiver estimating its SINR will not be able to know if it already includes secondary interference and thus cannot estimate if it is in the inner or protected zone. Hence the border between the two zones can be mapped to a threshold $L_{th}$ on the measured path loss.

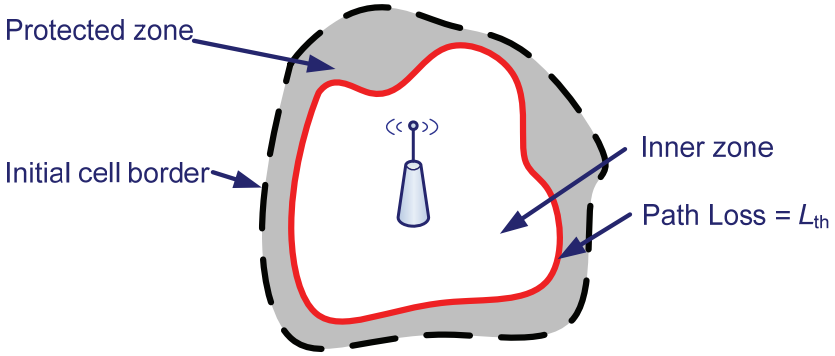


Figure 9: Division of the cells in inner and protected zones separated by path loss threshold $L_{th}$.

In the proposed approach, the channel allocated to the primary network will be divided into two sets: shared channels allocated to primary users in the inner zone and secondary users, and restricted channels that can be used only by primary users in the protected zone and if required by the primary users in the inner zone. The number of restricted channels $\tau$ is determined by the primary network. Therefore the primary network has to find the tuple $(\tau, \iota_{max})$ that enables secondary activity while keeping the unsatisfied user probability due to secondary activity is lower than $\varepsilon_s$. It should be noted that the threshold $\varepsilon_s$ should be lower than $\varepsilon_s$. In fact, the primary network should change system planning in order to have a probability of unsatisfied users lower than a threshold $\varepsilon_p$ satisfying the condition $\varepsilon_s + \varepsilon_p = \varepsilon$.

The unsatisfied user probability due to secondary activity can be also defined as the probability of having at least one user from the protected zone associated to a shared channel. Therefore we can write

$$\varepsilon_s = \mathbb{P}\{\exists(i \in \Pi \text{ and } f \in \Theta) \text{ such that } a_{if} = 1\} \quad (7)$$

where $a_{if} \in \{0; 1\}$ is a variable that reflects the binding of channel f to user i (i.e., it is equal to 1 if channel f is assigned to user i and 0 otherwise), $\Pi$ is the set of users in the protected zone and $\Theta$ is the set of shared channels.

### 2.3.2. Optimization techniques

In the following we assume that at any time we can reassign channels in order to preserve availability of the restricted channels to users in the protected zone. More practical algorithms and their performance can be derived from the following analysis. The approach is divided into two phases:

- Planning phase: In this phase the tuple of the number of restricted channels and interference threshold are computed in addition to the path loss threshold. This phase can be performed in a periodic way or when significant changes appear in primary traffic.
- Channel assignment phase: This is the real time phase where the channels are dynamically allocated to the primary users.

#### 2.3.2.1. Planning phase

In the planning phase the configuration of the primary network is established. First the path loss threshold is estimated for each cell using the fact that the SINR at the initial cell border without

secondary activity should be equal to the SINR at the inner zone border with secondary activity. By combining (5) and (6) we can write

$$L_{\text{th}} = L_{\text{max}} + 10\log_{10}\left(10^{I_{S,\text{max}}/10}+10^{P_N/10}\right) - 10\log_{10}\left(10^{I_{S,\text{th}}/10}+10^{P_N/10}+10^{\iota_{\text{max}}/10}\right) \quad (8)$$

where $I_{S;\text{th}}$ is the estimated internal interference experienced by the users at the border of the inner zone. $L_{\text{max}}$ and $I_{S;\text{max}}$ are in general given by the planning tool and depend on the deployment of the base stations. $I_{S;\text{th}}$ does not only depend on the position of the primary user inside the cell but also on the distribution of the base stations and their activity. Since a protective scheme is adopted for the primary network, we assume that $I_{S;\text{th}} = 10\log_{10}(\alpha) + I_{S;\text{max}}$. The parameter $\alpha$ is introduced in order to take the impact of cell loads into account. Although this approach is not optimal for increasing spectrum opportunities it guarantees that the primary users will always be satisfied. By using this assumption, we can write

$$L_{\text{th}} = L_{\text{max}} + 10\log_{10}\left(\frac{10^{I_{S,\text{max}}/10}+10^{P_N/10}}{\alpha 10^{I_{S,\text{max}}/10}+10^{P_N/10}+10^{\iota_{\text{max}}/10}}\right) - 10\log_{10}\left(10^{I_{S,\text{max}}/10}+10^{P_N/10}+10^{\iota/10}\right) \quad (9)$$

After computing the path loss threshold the primary network can compute the tuple $(\tau, \iota_{\text{max}})$. From (7) we can write

$$\mathbb{P}\{N_P \leq \tau - 1\} \leq \varepsilon_S \leq \mathbb{P}\{N_P \leq \tau\} \quad (10)$$

where $N_p$ is the number of users in the protected zone. The probabilities in (10) can be computed numerically based on the distribution of the primary users inside the cell, their number $N$, $L_{\text{th}}$ and by considering a known propagation model with log-normal shadowing as it shown in [19]. Since $L_{\text{th}}$ depends on $\alpha$ and $\iota_{\text{max}}$, the planning tool will provide the channel assignment algorithm with a table that gives the number of restricted channels as a function of $\alpha$ and $\iota_{\text{max}}$. It should be noted that the value of $\iota_{\text{max}}$ is used by the secondary network in order to estimate its allowed power and tune its detection mechanisms [20].

Since the value of $N$ can change on a millisecond scale, it is not practical to use instantaneous values of $N$. Instead, the planning tool will provide the channel assignment with a table that gives the total number of users $N$ as a function of the period of day, the day in the week, etc. The value of $N$ will be estimated as the maximum number of users that the cell can have at a given period of time since we are adopting conservative mechanisms to protect primary networks. Another possibility is to consider $N$ equal to the maximum number of users in the cell over all time periods. However, this will limit the opportunities for the secondary network since in some periods of time the cell load can be very low (e.g., cells in an industrial zone will be less loaded at night or at the weekend).

#### 2.3.2.2. Channel Assignment phase

The primary network will reserve $\tau$ channels for the users in the protected zone based on the period of time and the table provided by the planning tool. Each time a primary user from this zone requests a connection, the primary network will try to assign a restricted channel. If there is no restricted channel available and some of these channels are allocated to users in the inner zone, one of these channels will be allocated to the new user and a shared channel will be allocated to the user that was originally associated to the restricted channel. Otherwise, a shared channel will

be associated to the user until a restricted channel is released. Moreover, if the system does not have any available channel from the *T* channels, the user will be dropped.

For each period of time, the primary network will inform the secondary network about channels that can be used for secondary communications and the value of $\iota_{\max}$ that is needed to compute the maximum allowed power. In order to compute this power, the secondary needs to know the boundaries inside which the primary users in the shared channels are. In theory, this should be the circle that contains the inner zone. Since this depends on the shadowing factor which follows a normal distribution, we can estimate the radius rs of this cell by considering the tail of the distribution. Another more conservative approach is to assume that it is equal to the radius of the cell that contains the full coverage area of the cell, which is the approach that we have taken in this work.

### 2.3.3. Evaluation methodology

We evaluate the performance of the proposed mechanism using Xia-Bertoni propagation model [21]. The path loss *L* in dB between two transceivers separated by a distance *d* (in meters) can be written as

$$L = 10\eta \log_{10} d + C + \chi \tag{11}$$

where *C* and $\eta$ are constants specific to the propagation environment, and $\chi$ is a normal random variable of zero mean and standard deviation $\sigma$ to account for shadowing. Simulation parameters are summarized in Table 6.

Table 6: Simulation parameters.

| System parameter | Value |
|---|---|
| Bandwidth *W* | 10MHz |
| Number of channels *T* | 50 |
| Cell radius *r* | 500m |
| Path loss threshold $L_{\max}$ | 128.65 dB |
| Noise power $P_N$ | 121 dBm |
| Transmitted power per channel *P* | 29 dBm |
| Internal interference $I_{S;\max}$ | 110 dBm |
| Propagation exponent $\eta$ | 3.76 |
| Propagation constant $C$ | 15.65 |

We consider two types of user distribution inside the cell. In the first one, the users are uniformly distributed inside a cell of radius *r*. In the second type, the distance between the user and the base station follows a truncated Gaussian distribution between 0 and *r* with mean 0 and standard deviation *r*/3. The second type of distribution corresponds roughly to the case of microcells or hotspots [22].

### 2.3.4. Results

We shall first study the variation of the number of restricted channels as a function of cell load $\alpha$ and the probability threshold $\varepsilon_s$ for a fixed value of $\iota_{max}$, which is depicted in Figure 10. As expected, $\tau$ is an increasing function of $\alpha$ and a decreasing function of $\varepsilon_s$ since an increase in $\alpha$ will lead to an decrease in $L_{th}$ (see (9)), which will increase the number of users in the protected zone, whereas an increase in $\varepsilon_s$ will lead to a less protective scenario for the primary network allowing more opportunities to the secondary. It should be noted here that the proposed mechanism allows the secondary network to use more than 70% of its channels even when the system is fully loaded and with an allowed interference $\iota_{max}$ that is 21 dB higher than the noise power. We note that the value of $L_{th}$ varies only in the interval [118.54 dB; 118.94 dB] when $\alpha$ decreases from 1 to 0.02. It is also clear that the number of restricted channels is much lower when we have the Gaussian distribution because the users will be mainly concentrated around the base station. In this case the shared channels can reach 95% of the primary channels when the primary network is fully loaded.

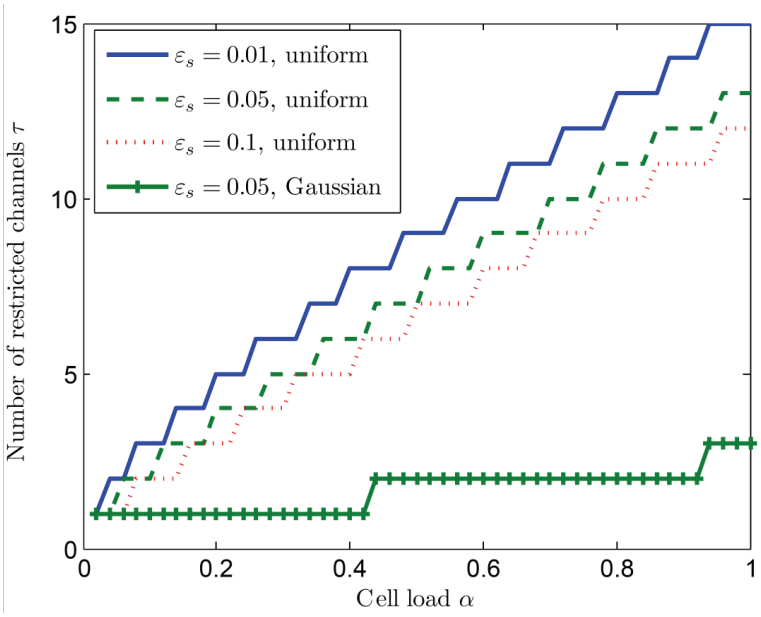


Figure 10: The variation of the number of restricted channels as a function of the cell load for different values of $\varepsilon_s$ and $\iota_{max}$ = -100 dBm [19].

In Figure 11, we show the variation of $\tau$ as a function of the maximum allowed interference $\iota_{max}$ and the probability threshold $\varepsilon_s$ for a fully loaded cell. First, we note that the value of $L_{th}$ varies in the interval [69 dB; 128.65 dB] when $\iota_{max}$ varies between -150 dBm and -60 dBm. When $\iota_{max}$ reaches -120 dBm the value of $L_{th}$ becomes 128 dB, which is equal to $L_{max}$ and therefore it stabilizes at this value for the lower values of $\iota_{max}$. Figure 11 shows that there is a limit of $\iota_{max}$ (i.e., -75 dBm for the uniform distribution and -40 dBm for the Gaussian distribution) over which no channels can be shared. Moreover the figure shows that the proposed algorithm can allow sharing more than 90% of primary channels when it is fully loaded and for $\iota_{max}$ lower than -120 dBm.

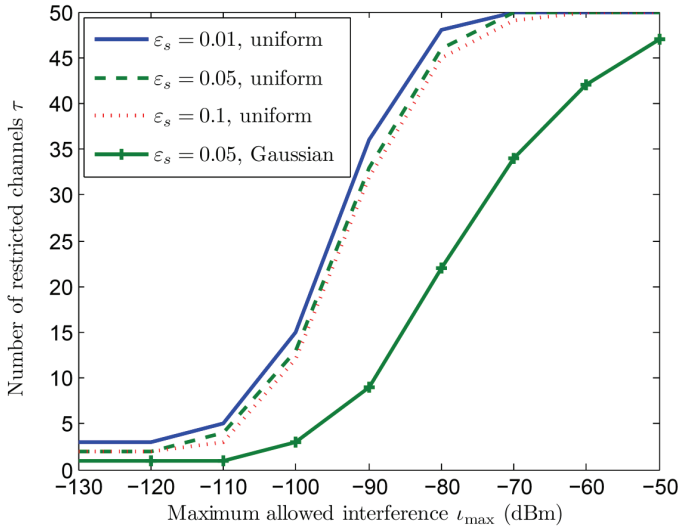


Figure 11: The variation of the number of restricted channels as a function of the maximum allowed interference for different values of $\varepsilon_s$ and a fully loaded cell (i. e., for $\alpha = 1$) [10].

Table 7 is the configuration table that will provided by the planning tool of the primary network for $\varepsilon_s$ = 0.05. This table gives the number of restricted channels as a function of $\iota_{\max}$ and $\alpha$. If the primary network knows the range of its load at a given period, it can choose the highest bound in the table for a given $\iota_{\max}$. For instance, if $\iota_{\max}$ is -90 dBm and the load changes between 0.3 and 0.5 at night time, the primary network will reserve 9 restricted channels for uniform distribution and 2 channels for Gaussian distribution. In operational network the values of the cell load (i.e. $\alpha$) can be replaced by the periods of time where the load appears in order not to reveal sensitive information of the primary network. In addition, the number of the channels will be replaced by the set of the shared channels. The table can be then stored in the REM and queried by the secondary network to know the shared channels and the corresponding allowed interference threshold. Two cases can appear for the table. In the first case, the different levels of the interference threshold can be provided so that the secondary network can have more flexibility in choosing the best channel and transmit power. In the second case, only one level of interference threshold can be given. This can be required by the primary network in order to have more and easier control on interference management.

Table 7: Configuration table for $\varepsilon_s$ = 0:05 for the uniform (the first number in the parenthesis) and the Gaussian (the second number in the parenthesis) user distributions [10].

| | $\iota_{\max}$ | | | | |
|---|---|---|---|---|---|
| $\alpha$ | -130 dBm | -110 dBm | -90 dBm | -70 dBm | -50 dBm |
| 0.2 | (1,1) | (1,1) | (4,1) | (10,6) | (10,10) |
| 0.4 | (1,1) | (1,1) | (6,1) | (19,10) | (20,18) |
| 0.6 | (1,1) | (1,1) | (9,2) | (28,14) | (30,26) |
| 0.8 | (2,1) | (2,1) | (11,2) | (37,18) | (40,34) |
| 1 | (2,1) | (2,1) | (13,3) | (46.22) | (50,42) |

### 2.3.5. Conclusions

In this section we have designed a planning tool to estimate the number of channels an OFDMA-based primary system must reserve for exclusive use in order to keep its quality of service requirements. From the derivation of the probability of primary users to face interference above the system-dependent tolerable threshold we were able to provide upper boundaries on the overall system performance.

Simulation results are promising: with the proposed reservation scheme a significant amount of spectrum still remains available for secondary sharing. The algorithms developed are lightweight, yet for practical deployments may be replaced by an even simpler lookup table. The approach we have taken is flexible enough to account for many different deployment scenarios.

# 3. Optimization techniques in LTE TVWS scenario

This chapter focuses on the radio resource optimization for a particular scenario in which an LTE network is deployed using the available TVWS. In particular, the problem of frequency and power allocation in a LTE femtocell network is considered.

## 3.1. Femtocell radio resource usage optimization based on REM for intra-operator spectrum management

For this scenario, it is assumed that LTE based femtocell access points (HeNBs) and user terminals (UEs) are able to utilize TVWS, in order to provide extra data communication capacity, in addition to the capacity provided with licensed spectra.

According to a FARAMIR study on available TVWS in Europe [23], the usable TVWS in the UHF 470-790 MHz band will be at the level of 100-150 MHz in many European countries. The key questions for this scenario are then how the available TVWS, as well as other system parameters, can be managed to achieve optimal capacity.

### 3.1.1. Summary of the optimization problem

Normally for one mobile access network, there are large quantities of parameters, from physical layer to upper layer, that need to be tuned to facilitate optimal system performance. However, compared with macrocell scenarios, femtocell scenarios have specific characteristics which can be taken into account to simplify RRM. Very often simple RRM is must-have for offering a low-cost femtocell solution.

First the number of users for one femtocell will vary very little within a range, e.g. 0-5 and also service fairness is less of an issue. Then, the scheduling function, which would be the pivotal function for a commercial LTE network, can be implemented in simple Round Robin (equal chance of access) or FIFO (First In First Out) manner.

Secondly the mobility for femtocell users is limited and they are fixed or moving with very low-speed. Then, handover optimization is also less important issue.

The optimization focus will be then on the coverage/capacity considering how the power and carrier bandwidth of HeNBs/UEs can be set in femtocells. The main challenge is that, as femtocell networks are user-deployed/less well-planned and frequently subject to network topology changes (e.g. new HeNB switch on and/or switch off for energy saving), the RRM and optimization have to be adaptive and autonomous. REM, which can reside in operator OAM system or HeNB Gateway, can help with geo-location information and other system information and assist such management and optimization. Figure 12 illustrates the considered problem.

On the other hand, we assume the UEs in the femtocell can carry out measurements and provide measurement reports to be used in build-up of REM and in turn in the optimization processes. It is envisaged that current LTE terminal capabilities, with addition of a wide-band scanner module if necessary, can satisfy such measurement requirements on the UHF TVWS [3].

Table 8 summarizes the main elements of the considered optimization problem.

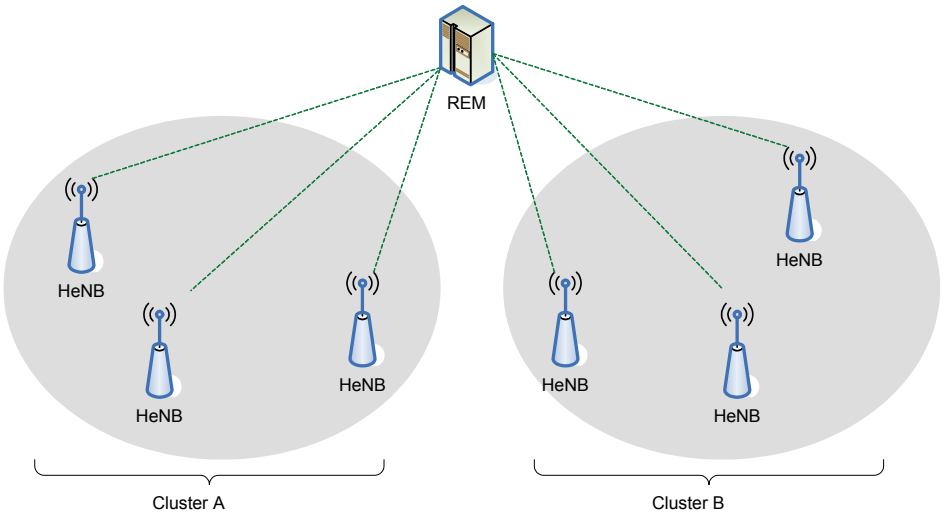


Figure 12: Cluster A and Cluster B can re-use the available spectrum resource if they are spatially separated. Within one cluster where inter-femto interference needs to be considered, the power and spectrum shall be optimized based on the REM information.

Table 8: Optimization problem: femtocell radio resource optimization based on REM for intra-operator spectrum management.

| Femtocell power and spectrum resource usage optimization based on REM | |
|---|---|
| Scenario(s) of applicability | This problem is mostly relevant to the scenario groups "Intra-Operator Spectrum Management" and "LTE in TV White Space" from Deliverable D2.2 [1], with focus on:<br>-Power/carrier bandwidth usage management<br>-REM based optimization |
| General description | Femtocells are in general less well-planned and subject to frequent topology changes when cells are turned on/off. The power of transmitters has to been managed to achieve optimal coverage and capacity. The utilization of TVWS needs to be optimized to maximize network/user throughput. |
| Assumptions | Power of transmitters, both downlink and uplink, can be tuned by a controlling entity; however the focus is HeNB power, i.e. for downlink.<br>Spectrum usage of femto cells can be coordinated in an operator network which is different from a random access ISM band network.<br>Measurements by the access point and user terminal can be used to build the REM and assist RRM and optimization.<br>REM can be built and embedded in the network and can be accessed by the controlling entity. We assume REM can be built into operator OAM system or into a HeNB gateway. |
| Optimization target | Maximize the network/user throughput by managing power and spectrum setting and optimizing interference coordination |

| | |
|---|---|
| Tuneable parameters | Spectrum/Carrier bandwidth that one femtocell and its served mobile can use. The power that the HeNB transmitter can use on that spectrum band. Our evaluation will be based on LTE-TDD system however only downlink will be studied. |
| Input parameters | Information collected by mobile measurements and other means, stored in REM and used for the optimization, include:<br>Location of the access points (HeNBs)<br>Location of the mobiles: this will be used for calculation of system performance. However the RRM algorithms will not depend on the UE locations.<br>Total interference level measurement (e.g. RSSI in LTE) and pilot channel power value measurement (e.g. RSRP in LTE) from serving cell and neighbouring cells by the UEs.<br>The input below can be used by controlling entity (e.g. REM manager) also:<br>Historical record of traffic and QoS statistics, and/or the policy set by regulator on the use of TVWS. |
| Constraints | No direct link between femto cells, i.e. no X2 interface can be used.<br>The localization of mobile can only be done in slow loop meaning low accuracy. |
| REM information | The input parameters, collected by mobile and other means, shall be all possible to be stored in REM, plus a network operator or a regulator shall be able to impose and input policy into the REM. |

### 3.1.2. Optimization techniques

The optimization techniques that we propose to be used in a real femtocell network shall be subject to constraints of HeNB and user terminal capabilities. According to [5], without Carrier Aggregation capability, a LTE Rel-8/9 UE can receive on a single Component Carrier and transmit on a single Component Carrier. An advanced LTE Rel-10 UE with reception and/or transmission capabilities for Carrier Aggregation can simultaneously receive and/or transmit on multiple Component Carriers. Carrier Aggregation is supported for both contiguous and non-contiguous Component Carriers with each Component Carrier limited to a maximum of 110 Resource Blocks in the frequency domain (corresponding to 20MHz spectrum bandwidth). The highest supported transmission bandwidth is up to 100MHz.

Considering one TV channel bandwidth is 8MHz in European area [23], we envisage that one LTE HeNB Access Point and its serviced LTE terminal will have the capability to aggregate and utilize two TV channels. This is constrained by the abovementioned Rel-10 LTE terminal capability and practical terminal design limitation (e.g. multi-mode RF chains and antenna). Within each TV channel, we assume LTE HeNB access point and LTE terminal can use one 5MHz spectrum band, which is centred at the middle of the TV channel.

Our optimization techniques for using LTE HeNBs and terminals in TVWS are designed under such assumption that the LTE femto network will have a 10MHz system bandwidth while the available TVWS will be on the level of 100-150MHz. The spectrum allocation among LTE femto networks will

be very similar to the GSM system frequency planning problem, which is a narrow band allocation problem.

Except spectrum allocation, the maximum downlink transmission power for LTE HeNB can be optimized to minimize interference in the networks, when two adjacent LTE HeNBs are using the same TV channel. Uplink power of LTE terminals can be controlled with standard LTE power control methods. Considering that optimizing spectrum allocation and power allocation will be NP-hard problem in general [29], we design a two step optimization technique (see Figure 13) in which the spectrum of TVWS will be allocated first among LTE HeNBs, then maximum power of LTE HeNBs can be tuned. These two steps can be coordinated by a REM manager and with the support of REM information.

The spectrum allocation algorithm is similar to one map-colouring algorithm.

For a network comprising m clusters where each cluster comprises n HeNBs, we assume available TVWS is $X$ MHz such that the number of available TV channels is $k = X/10$. RRM optimization algorithms will be run independently for each cluster as clusters are isolated from the perspective of interference. The identification of clusters can be done with help of REM information. Within one cluster, the first HeNB randomly picks one TV channel from k channels, and the second HeNB picks one TV channel from residual $k$ - 1 channels and so on. Apparently within one cluster, there might be non-zero number of HeNBs which are using the same TV channels if $n > k$ and zero number of HeNB using the same TV channels if $n = k$ or $n < k$.

The power optimization technique (see Figure 14) is a simulated annealing algorithm similar to [24] and the cells (i.e. HeNBs) which are involved in the power optimization algorithms are those HeNBs which are using the same TV channels.

When the transmission powers of HeNBs are changed, the received power from these nodes at the user terminal and the user experienced Signal to Interference Ratio (SIR) will change. This in turn will lead to a change in the coverage and the capacity of the different femtocells. The capacity of a femtocell is represented by the transmission throughput and potential long-term transmission delay of user terminal on the downlink.

The optimization objective is then to minimize the sum of the potential long-term transmission delays of all user terminals in the group of femtocells which are using the same TV channel. The potential long-term transmission delay is defined as the inverse of long term-user throughput, which is decided by user terminal's experienced SIR.

The simulated annealing algorithm is based on LTE terminal measurements and reporting mechanism. The terminals can measure the received power from other HeNB on the same TV channel and report such measurement to its serving HeNB.

In the step for power optimization, for each sampling cycle of the simulated annealing algorithm, every HeNB takes turn to sample a power value according to a probability and tune to that power value. The calculation of probability in each HeNB depends on the measurement assistance from user terminals and the information transferred from other same TV channel HeNBs. A cost function of one HeNB is defined by taking into account all the long-term transmission delays of all user terminals which are connected to this HeNB. Also, the cost function comprises contribution parts

from the co-channel HeNBs. The objective of the scheme is thus to minimize this cost function. Further, a forced cooling element is added upon the sampling process. The system is gradually "cooled down" as time elapses. We assume that REM manager can take record on each HeNB status (long-term transmission delay and power value) and decides when to start/stop the optimization process.

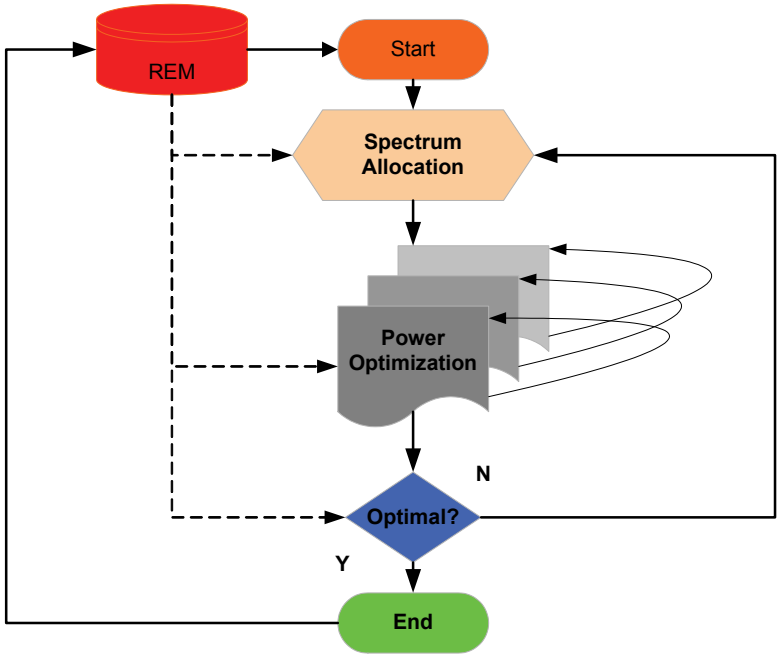


Figure 13: Two step resource allocation scheme.

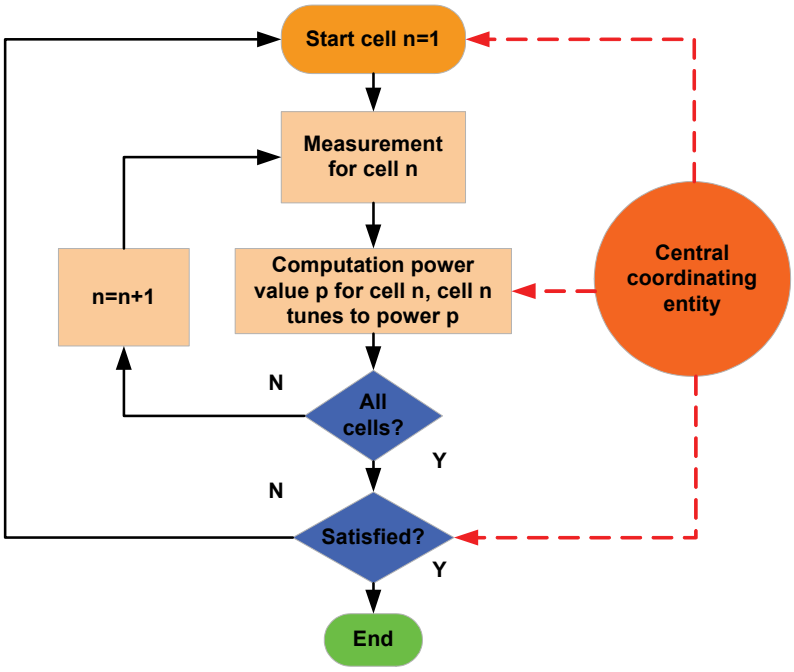


Figure 14: Power optimization based on simulated annealing.

### 3.1.3. Evaluation methodology

The following table lists the parameters that are used in the evaluation of the optimization schemes.

Table 9: Simulation parameter settings.

| | |
|---|---|
| No. of cells per cluster | 5,10,20 |
| Average No. UEs in one cell | 4 |
| Inter-cluster distance | 100m |
| Cell radius | 10m |
| Distance attenuation model | Dual strip model/Urban deployment [25] |
| FAP output power | 20 mW |
| Power tuning range | [-3 3]/[-5 5]dB |
| Power adaptation granularity | 0.5/1dB |
| Shadowing standard derivation | 8dB |
| UE mobility | 0 |
| System bandwidth | 10MHz |
| Cooling speed in annealing method | 0.02/0.1/0.2/0.5/1/2/5 |
| Total No. of annealing sampling cycles simulated | 2000 |
| UE received power offset (PO) between serving cell and its interfering cells | 3dB/8dB |

### 3.1.4. Results

Simulation results show that, for the spectrum allocation, the relation between the number of HeNBs within one cluster and the available TV channels will impact the system performance. If the number of HeNBs within one cluster is small, compared with available TV channels, the system performance is similar to the base line method where each HeNB, either intra-cluster or inter-cluster, randomly picks one TV channel. When the number of HeNBs is large, the interference between co-channels HeNBs can be decreased by the simulated annealing algorithm.

Since the start of sampling process, the average long-term delay of a HeNB can be optimized gradually and converged into a stable state. The network is monitored by the REM manager and the scheme can be stopped when the expected optimization threshold is reached. Considerable (10-15 dB) gain on long-term delay can be obtained especially for the case that some user terminals experience severe interference (see Figure 15).

On the other hand, the user terminals which are located favourably will experience slight throughput loss on the scale of 0.2 dB (see Figure 16). It shows that, while the edge users (or the users experiencing e.g. bad signal coverage and shadowing) can benefit from the scheme, the central users' SIR is decreased. Simulation results show that the worst-case users will be able to achieve 10dB throughput gain and the cost is that the total HeNB throughput will be slightly decreased by about 5%.

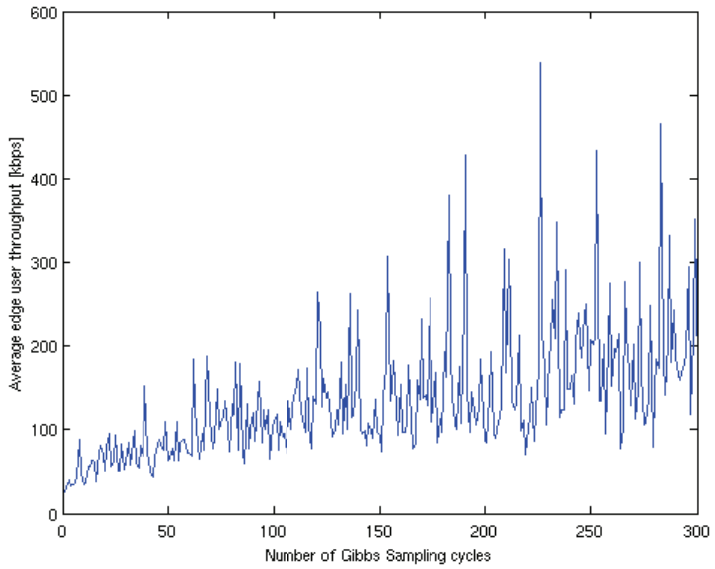


Figure 15: Outage (edge) user throughput improvements with Gibbs Sampling.

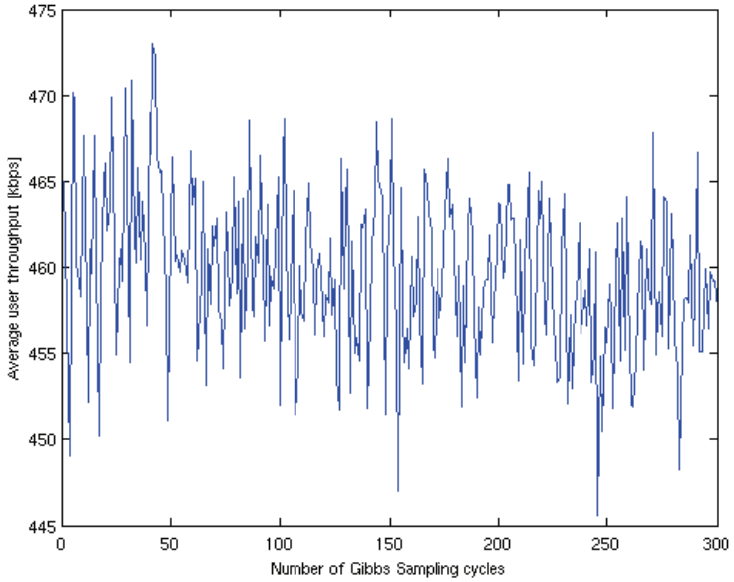


Figure 16: Marginal change of average user throughput during Gibbs Sampling optimization.

### 3.1.5. Conclusions

A two step spectrum and power optimization scheme based on central coordination (through REM manager) and simulated annealing for LTE femto network on TVWS is evaluated. Evaluation is based on an LTE downlink indoor network configuration. It shows that this scheme is able to improve worst case user terminal throughput when the number of HeNBs is bigger than the available TV channels, meanwhile causing slightly negative impact on the other users. This scheme can be used as an effective method for interference coordination in dense urban deployment scenario. A REM manager is used to collect reports from involved HeNBs and carry out simulated annealing process and then control the maximum transmission power of HeNBs in a centralized manner. When inter-HeNB interface (e.g. a X2 interface) is available, the optimization method can be implemented in a distributed way where the HeNBs can take the task of calculation and the REM manager will decide when the process is started/stopped.

# 4. Optimization techniques in scenarios with Non-Coordinated Spectrum Access between PUs and SUs

This chapter presents the performance evaluation of optimization problems identified for the general type of scenarios in which a secondary network shares the spectrum with a primary network and no coordination exists between the two. In this case, the information stored in REM database about the different PU features and the environmental characteristics is used to determine under which conditions the secondary transmission can be carried out without interfering the PU network. Under this general framework, this chapter is organized according to the following optimization problems:

- Section 4.1 considers the so-called out-of-band or cognitive femtocells in which a femtocell network is deployed making use of the spectrum left available by a number of primary networks. In particular the problem deals with finding the adequate power and channel assignment to femtocell users that ensures their QoS and that no interference is created to the PU. Note that this problem can be seen as a generalisation of the one presented in section 3.1 that dealt with the case of using TVWS and that femtocells were using the LTE, while the problem presented here deals with any type of PU. Similarly, as compared to the femtocells problems in chapter 2, note that the focus here is placed on the RRM for the SU.
- Section 4.2 addresses the situation when a number of heterogeneous PUs exists, exhibiting different features, and leaving different capacities available for SUs. The problem then consists in doing a smart RRM control over the SUs so that, depending on their rate requirements, they can use the remaining capacity left by PUs in the most efficient way. Correspondingly the problem is subdivided into an admission control and a resource allocation.
- Section 4.3 focuses on the exploitation of the PU statistics in the temporal dimension to perform an efficient assignment of idle channels to a number of SUs with different service requirements. The main focus here is on reducing the rate of spectrum handovers (and corresponding signalling) needed by SUs due to the appearance of the PU in a used channel. This can be achieved by exploiting REM information about the PU statistics.
- Section 4.4 deals with the problem of opportunistic spectrum access when the primary is a cellular network. In particular, the detection of the closest active primary base station to a given cognitive node is considered, making use of a maximum likelihood estimator. The resulting detection is used to determine the transmit power that can be allowed to the cognitive node transmitter not to interfere with the PU.
- Section 4.5 also focuses on the case that the primary is a cellular network and explores a new approach for dynamic spectrum access (DSA) based on stochastic models, suitable if the primary activity patterns are very fast where traditional DSA techniques based on sensing and localization fail to allow any transmission. The objective is to find the best secondary activity patterns over different primary channels leading to the highest possible capacities while satisfying primary constraints.
- Section 4.6 will focus on the hidden node detection problem, which constitutes a classical problem in different scenarios, such as the case when the hidden node is a PU that needs

to be detected by a SU network to avoid interference. The REM is used to make interference predictions that help in the detection of hidden nodes.

## 4.1. Out-of-band (Cognitive) Femtocells

In this scenario, several coexisting cognitive femtocell networks share the spectrum to provide wireless services to their associated wireless terminals without direct cooperation among femtocells. Additionally, several PU networks with different bandwidth and coverage areas may coexist with these femtocells. The coexistence mechanism is based on overlay spectrum sharing approach [26], where each cognitive femtocell has a pool of available frequency bands obtained from REM database. The available bands are those that are not currently in use by the PU network in the coverage range of the femtocell. Furthermore, the shared bands may have different bandwidths and utilization efficiencies and they are divided further into sub-bands (channels) of identical bandwidth.

It should be noted that any reference to the term femtocell in this section is meant to be for a cognitive femtocell, also denoted as out-of-band femtocell following the terminology of D2.2 [1].

### 4.1.1. Summary of the optimization problem

The optimization framework in this scenario aims to minimize the wireless resources utilization to achieve specific QoS requirements of femtocell users under certain femtocell transmission power constraints. The spectral resource utilization is quantified by the *product of bandwidth and transmission power*. Also, the study focuses on the downlink resource allocation. Similar analysis can be conducted for uplink resource allocation.

The space-bandwidth product, which is defined as the multiplication of the bandwidth utilization and transmission power (an alternative measurement for coverage space), is similar to the transport capacity defined in [27] to study capacity scaling laws in large wireless networks. This metric can be used to capture the efficiency of spectrum utilization. In cognitive radio networks, the gain of spectrum sharing comes from the heterogeneity in space consumption of different types of wireless devices with different bandwidth [28]. In this context, a user with large bandwidth demand is allocated first to achieve better utilization. In cognitive femtocell environment, it is likely that femtocell coverage area is smaller than any PU network. Therefore, cognitive femtocell networks can achieve better utilization of space, which can be captured by the space-bandwidth product.

Let us denote $\mathcal{F}$ as the set of femtocells and $\mathrm{T}$ as the set of all wireless Cognitive Radio (CR) terminals operating in these femtocells. The available spectrum for all nodes in the network is modelled as a set of unequally sized bands. Let us denote $\mathcal{M}$ as the set of these bands and $\mathcal{M}_{\mathrm{i}} \subseteq \mathcal{M}$ the set of available bands at femtocell $i \in \aleph$, which can be different from the available bands at another femtocell. $W(m)$ refers to the bandwidth of band $m \in \mathcal{M}$. It is further divided into K($m$) sub-bands (channels) of equal bandwidth $B^{(m)}$.

Let $x_{ij}^{(m,k)}$ be a binary variable, which is equal to *one* if channel $(m,k)$ is allocated for CR user $j$, and is equal to *zero* otherwise. Also, let ${p_{ij}}^{(m,k)}$ be a continuous real variable that represents the power transmission of the femtocell on channel $(m,k)$ to user $j$ in femtocell $i$. The optimization problem is formulated as follows:

$$\min \sum_{i\in\mathcal{F}} \left( \sum_{m\in\mathcal{M}_i} \sum_{j\in S_{R_i}} \sum_{k=1}^{K^{(m)}} \frac{1}{1-\omega^{(m,k)}} \; B^{(m)} \, x_{ij}^{(m,k)} \right) \left( \sum_{m\in\mathcal{M}_i} \sum_{j\in S_{R_i}} \sum_{k=1}^{K^{(m)}} {p_{ij}}^{(m,k)} \right) \tag{12}$$

where $x_{ij}^{(m,k)} \in \{0,1\}$ and $p^{(m,k)} \in \mathcal{R}$ are the optimization variables.
The problem is subject to the following constraints:

$$\sum_{m\in\overline{\mathcal{M}_j}} x_{ij}^{(m,k)} = 0 \tag{13}$$

$$\sum_{j\in S_{R_i}} x_{ij}^{(m,k)} \leq 1 \tag{14}$$

$$x_{ij}^{(m,k)} + \sum_{a\in S_{I_i}} \sum_{b\in S_{R_a}} x_{ab}^{(m,k)} \leq 1 \qquad i \neq a \tag{15}$$

$$\sum_{j\in S_{R_i}} \Lambda_{ip}^{(m,k)} \leq \Gamma_{PU}^{(m,k)}, \qquad when \;\; \omega^{(m,k)} > \omega_{th} \tag{16}$$

$$\sum_{m\in\mathcal{M}_i} \sum_{k=1}^{K(m)} g_{ij}^{(m,k)} . p_{ij}^{(m,k)} \geq \Gamma_{ij} \tag{17}$$

$$\sum_{m\in\mathcal{M}_i} \sum_{k=1}^{K(m)} B^{(m)} . x_{ij}^{(m,k)} . \log_2 \left( 1 + \frac{g_{ij}^{(m,k)} p_{ij}^{(m,k)}}{\eta + \sum_{p\in P} \Lambda_{pj}^{(m,k)}} \right) \geq \phi_{ij} \tag{18}$$

The following definitions hold in the above expressions:

- $S_{R_i}$ is the total number of wireless terminals associated with the i-th femtocell
- $S_{I_i}$ is the total number of interfering femtocells in the interference range of femtocell i.
- $\overline{\mathcal{M}_{ij}}$ is the set of inaccessible bands by user j in femtocell i due to hardware limitations
- $g_{ij}^{(m,k)}$ is the channel gain between femtocell i and terminal j at sub-band k of band m.
- $\Gamma_{ij}$ is the minimum required power for successful reception at terminal j of femtocell i
- $\eta$ is the ambient noise power
- $\phi_{ij}$ is the minimum QoS requirement of user j expressed in terms of average data rate.
- $\Lambda_{ip}^{(m,k)}$ is the interference caused by femtocell i on the primary user p on channel (m,k)
- $\omega_{th}$ is the PU activity threshold over which the power upper bound constraint is activated.
- $\Gamma_{PU}^{(m,k)}$ is the maximum tolerable interference at PU at channel (m,k).

The constraints described in inequalities (13)-(18) are divided into several categories.

*The channel allocation constraints* regulate the channel assignments at the terminal level, femtocell level, and multi-femtocell level. At the terminal level, the first constraint (13) takes into consideration the hardware specification of wireless terminals. It assures that no allocation is made to a wireless terminal *j* outside the range of bands that the wireless terminal is capable of accessing. At the femtocell level, inequality (14) implies that each channel should not be allocated to more than 1 user within the reception range of a femtocell *i*. At multi-femtocell level, inequality (15) sets the constraints on allocating the same channel for more than once among interfering sets of femtocells.

The *power constraints* determine the upper and lower bounds of the transmission power that can be transmitted. The upper bound is set by (16) which implies that the power is bounded at each channel k by the PU interference limit if its activity exceeds a certain level. The lower bound is governed by (17) where each power allocated for the j[th] wireless terminal at a given channel should be higher than the sensitivity limit $\Gamma_{ij}$.

The *QoS constraint* in (18) assures meeting the minimum average data rate requirements $\phi_{ij}$ by the channel allocation $x_{ij}^{(m,k)}$ and power allocation $p_{ij}^{(m,k)}$.

In order to accommodate for the PU spectral activities in the optimization process, the bandwidth footprint is adjusted by $\omega^{(m,k)}$. This coefficient is the primary user activity index and captures the impact of PU activities on the resource allocation process. This is achieved by applying a cost factor to a channel *k* that is proportional to the level of PU activity on that channel. As a result, the optimization framework aims to avoid allocating channels with high PU activities.

The network optimization problem and its corresponding variables are summarized in Table 10.

Table 10: Optimization problem: out-of-band (cognitive) femtocells.

| Power and spectrum allocation in Out of Band (Cognitive) Femtocells | |
|---|---|
| Scenario(s) of applicability | - Out-of-band (Cognitive) Femtocells |
| General description | - The proposed optimization framework addresses the problem of power and spectrum resource allocation among several femtocells. The shared spectrum is comprised of multiple bands of different bandwidth. Each band is further divided into smaller sub-bands. |
| Assumptions | - Femtocell coverage is small enough to assume homogeneous local spectral activities.<br>- The spectrum sharing approach is overlay.<br>- A femtocell can be in the coverage area of more than one PU network.<br>- A femtocell base station has two transceivers, one for data transmission and reception, and one for CR sensing tasks.<br>- Femtocell nodes can operate at different bands of different bandwidth.<br>- Control channel:<br>  o Inter-femtocell control channel: No direct communication between femtocells exists. Instead, each femtocell maintains a local REM database of its system information and measurements. The data of local REMs are synchronized through their content update mechanism with the global REM.<br>  o Intra-femtocell control channel: measurements and control signals are exchanged within the femtocell between the base station and associated femtocell users. |
| Optimization target | - The framework objective is to minimize the spectral and power utilization of a set of femtocells using joint channel and power resource allocations given by (12) |
| Tunable parameters | - $x_{ij}^{(m,k)}$ binary indicator to mark the utilization of sub-band (m,k) in link (i, j).<br>- $\mathrm{p}^{(\mathrm{m,k})}$ the power of the transmitted signal on kth sub-band in band m |

| | |
|---|---|
| Input parameters | - Set of femtocells and terminals associated to each femtocell.<br>- Total number of available bands,associated bandwidth and total number of sub-bands in each band.<br>- Set of interfering femtocells in the interference range of femtocell i.<br>- QoS requirements expressed in terms of average data rate. |
| Constraints | - *Channel allocation constraints*: to ensure that each sub-band is assigned to only one wireless terminal within the interference range.<br>- *Power constraints:* to assure that interference to PUs is bounded and that received power at the terminal is above sensitivity level.<br>- *QoS constraint*: To ensure the required data rates for each terminal. |
| REM information | - PU-related information: PU locations, transmission power, interference threshold, activity index<br>- Femtocell-related information: Adjacent femtocells, Bandwidth budget, CR sensing measurements (to build and update the PU activity index), power and channel allocations<br>- Terminal-related information: Interference measurements, user locations, CR user accessible bands, data rate requirements |

### 4.1.2. Optimization techniques

The formulated optimization problem is a mixed integer non-linear programming problem, which is NP-hard to solve in general. One method to solve such problems is using decomposition theory [29][30]. The overall optimization problem is decomposed into a master problem and a sub-problem as follows (see

Figure 17).

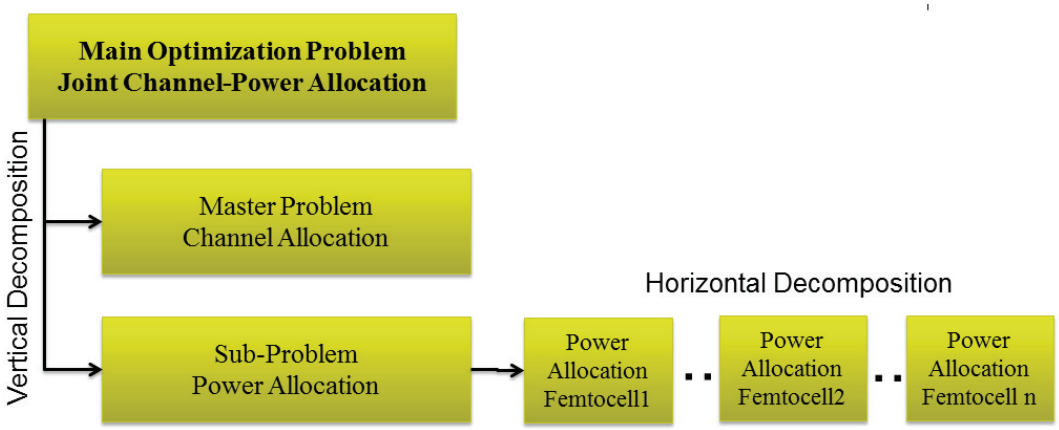


Figure 17: Optimization decomposition.

The master problem is channel allocation, in which a feasible fixed transmission power is assumed. The channel allocation problem can be formulated as a binary integer programming problem which can be solved in different ways. One way is to reduce the problem into a linear programming problem by relaxing the integrity condition of the binary indicator variable x so that it becomes a continuous variable from 0 to 1. The obtained linear programming problem can be solved in polynomial time. However, the solution obtained is the upper bound for the optimization objective function.

The sub-problem is the power allocation problem, in which the power is determined for the allocated channels in the master problem. The power allocation problem can be solved using dual-decomposition method, where the Lagrangian variables are calculated in a distributive fashion using iterative gradient algorithm.

REMs are used to support the optimization process, using the local and global REM architecture from the FARAMIR architecture [3]. Each femtocell maintains its local radio environment information in a local REM. This includes the signal-to-noise and interference ratio measured at each wireless terminal associated with the femtocell and the available sub-bands as observed by the femtocell-base-station. The optimization scenario assumes that the local spectral map within the femtocell is homogeneous. This assumption is justified by the small spatial footprint of femtocell compared to the macrocell size typically covered by primary user networks.

The global REM obtains the information stored in the local REM(s) and analyses the measurements stored in them to extract the global information. The synchronization between local and global REMs takes place periodically to assure coherent operation among all the cognitive femtocells.

The channel allocation is performed in a centralized fashion in the global REM, while the power allocation is performed in a distributive fashion at each femtocell using its local REM information.

Figure 18 shows the message exchange using REM for channel and power allocation for cognitive femtocells. The global REM obtains the measurements and local REM information to build the interference map and to allocate the channels for each femtocell. The channel allocation and interference map is synchronized with the local map. Then, a local power control can be performed based on the information obtained by the global REM.

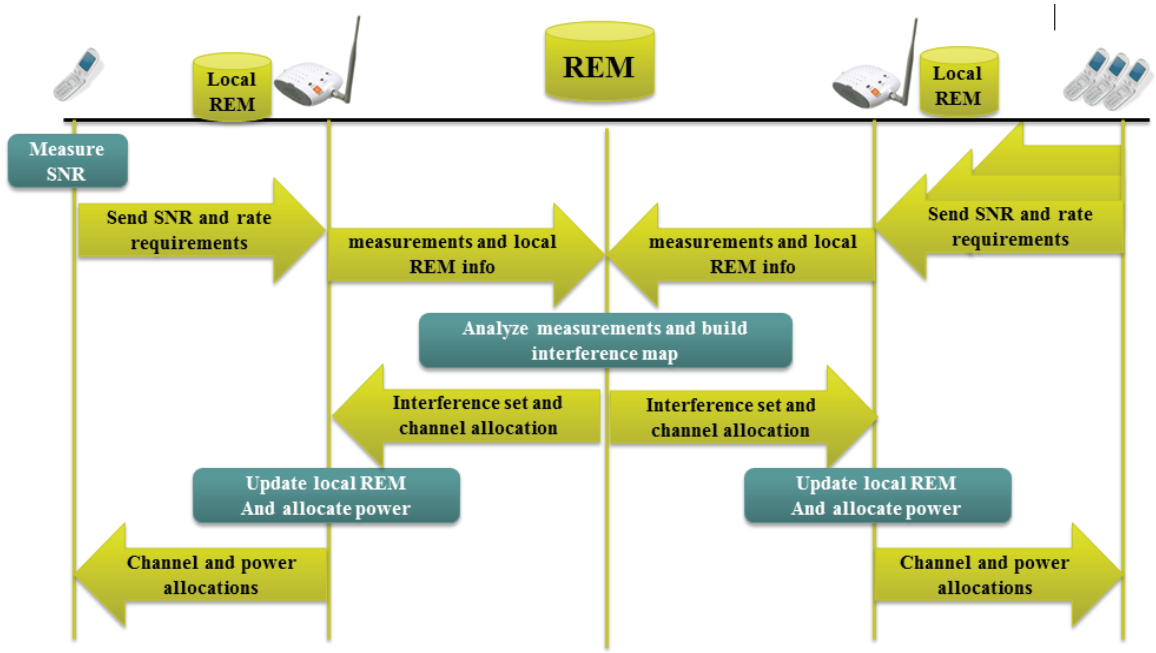


Figure 18: Information exchange using REM for femtocell resource allocation optimization.

Besides the application of REM architecture (local/global) in resource allocation optimization, the following applications are enabled by the REM architecture:

- Femtocell Initialization: Upon turning on the femtocell base station, it first senses the spectrum environment to identify available spectral resources and logs it to the local REM database. Each femtocell is responsible of allocating resources to its users, and regulating their transmission power.
- Spectral Handover:
    - Handover from Macrocell to Femtocell: Whenever a femtocell user moves from macrocell to femtocell, it detects the existence of a femtocell by listening to the control channel information and switches to the femtocell network.
    - Handover from Femtocell to Macrocell: If a femtocell user moves out of the femtocell into the macrocell area, it examines the signal strength of macrocell and switches to it if the macrocell signal strength is higher than that for femtocell

### 4.1.3. Evaluation methodology

In this section, we evaluate the performance and convergence of the proposed resource allocation framework based on simulations. We investigate the performance for each individual user to validate the theoretical results. The impact of system parameter settings on the allocation results is also analyzed. Additionally, we examine the convergence of the power control scheme for multiple users.

In the simulation, we consider the cases: single-user, multi-user resource allocation of a single femtocell and a multi-cell resource allocation. The wireless channel model used in our simulation study is Rayleigh fading channel with Doppler shift $f_D = 6$ Hz. The bandwidth of each channel is 15 kHz. The minimum received power for CR users is -100dBm. The maximum interference threshold for PU is calculated based on minimum received SINR of 15 dB. The average background noise power is -110dBm. CR users are placed randomly on a distance of 100 - 1000m from CR-BS. The simulation results are the average of the results of 1000 iterations of Monte-Carlo simulation method.

#### 4.1.3.1. Single User Resource Allocation

In the single-user case, we compare the efficiency of different resource utilization metrics in allocating channel and power resources to fulfil different data rates and under different wireless channel conditions. The metrics are (1) power, (2) summation of power and bandwidth and (3) the product of bandwidth and power. The first metric is used as a benchmark since it captures the behaviour of widely used margin-adaptive power allocation based on waterfilling technique. The second metric applies equal ”importance” to power and channel resources. The third metric is the one proposed in our resource allocation framework and it captures the utilized spectral footprint. The number of channels considered for this case is K = 8, and the CR rate requirement varies from 100 bps to 500 kbps. In this study, two channel models are considered: the first one is frequency-flat channel model (identical signal to noise ratio for all channels) and the second one is frequency-selective channel model (varying SNR values for each channel).

#### 4.1.3.2. Multi-User Resource Allocation

In the second simulation case, we compare the performance of our framework with the performance of iterative waterfilling resource allocation scheme for three users under different channel conditions and rate requirements. The performance is demonstrated in the absence and presence of primary user activities.

#### 4.1.3.3. Multi-Cell Resource Allocation

The simulation scenario in this case is composed of 9 PU BSs with equal transmission power as shown in Figure 19. Also, 50 CR-femtocells are distributed uniformly across the whole coverage area of PU BSs. These femtocells share 512 channels with PU. Channel bandwidth is 15 kHz. Each femtocell has a random number of associated users that range from one to four. The QoS is represented in terms of a minimum data rate and it ranges randomly between 1,2 and 4 Mbps. The PU activity is simulated at each PU BS by utilizing 10%, 50% and 90% of the shared channels, representing low, medium and high PU activities. For each PU activity profile, 1000 simulation iterations were conducted. At each iteration, a complete iterative resource allocation cycle is performed for all femtocells.

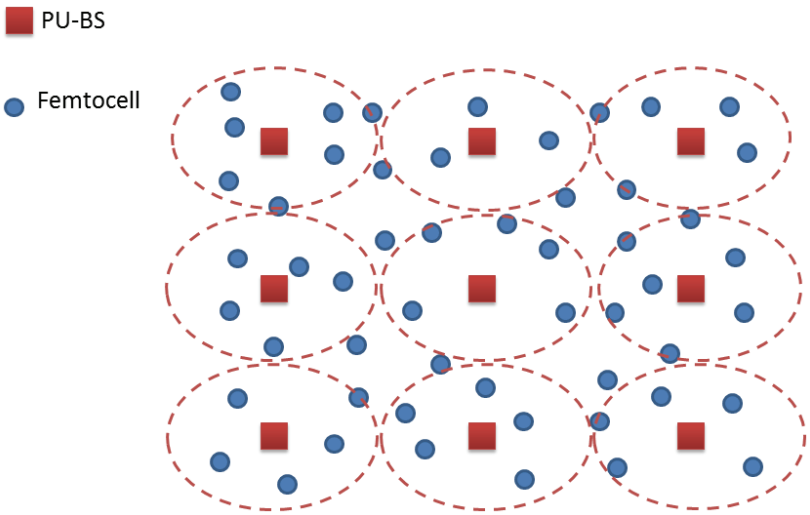


Figure 19: Multi-Cell Simulation Scenario.

### 4.1.4. Results

#### 4.1.4.1. Single User Resource Allocation

Figure 20 shows the allocated channels, power, and total bandwidth-power product values obtained for a single user under different data rate requirements and flat fading wireless channel. The SNR values of all channels are 10 dB. Under such wireless channel conditions, the resource optimization based on power minimization tends to consume all available channels. This is the expected behaviour of waterfilling power allocation mechanism. The bandwidth-power product metric consumes less number of channels compared to the power or the power-bandwidth summation metrics at the expense of slight increase in the transmission power. However, the behaviour of the resource allocation under different metrics converges under high data rate requirements because all available channels are consumed. In this case, the only degree of freedom available for the resource allocation is transmission power. Nevertheless, the flat fading channel is the worst case scenario for the power-metric in terms of the consumed channels.

Figure 21 presents the results for the case of single user allocation with variable channel SNR values. In this case, the performance difference between the metrics is smaller. Yet, the use of bandwidth-power metric decreases the number of allocated channels.

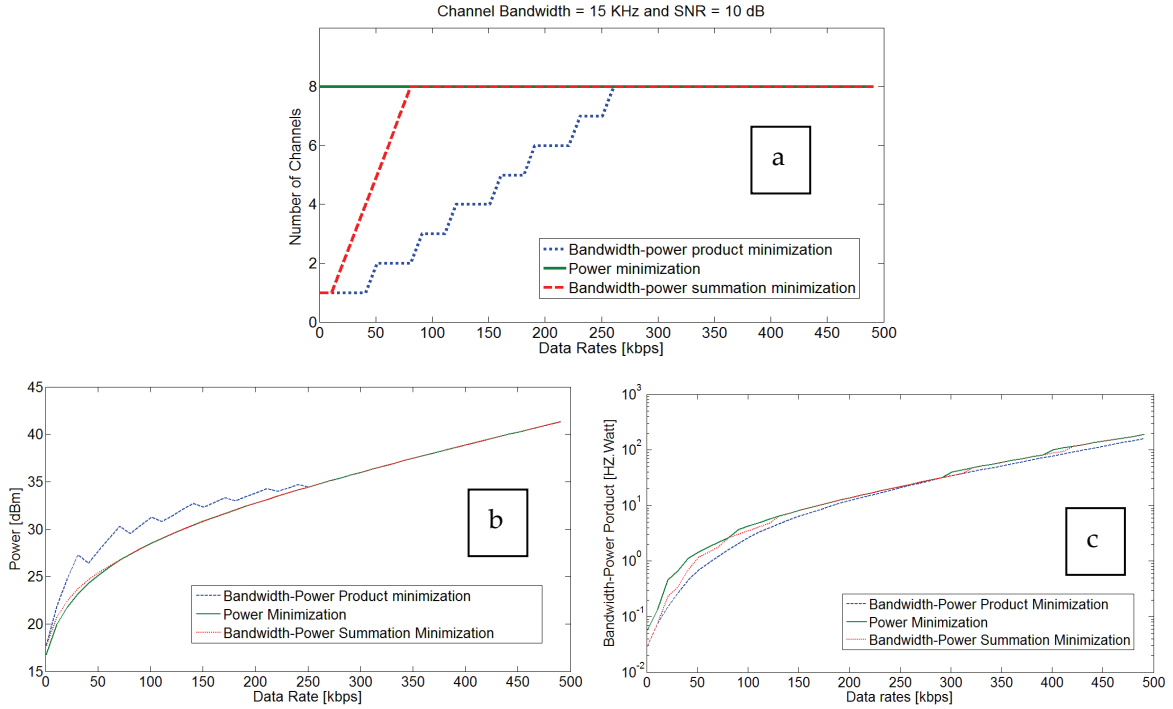


Figure 20: (a) Number of channels, (b) transmission power, and (c) bandwidth-power product vs. data rates with SNR = 10 dB and channel bandwidth 15 kHz.

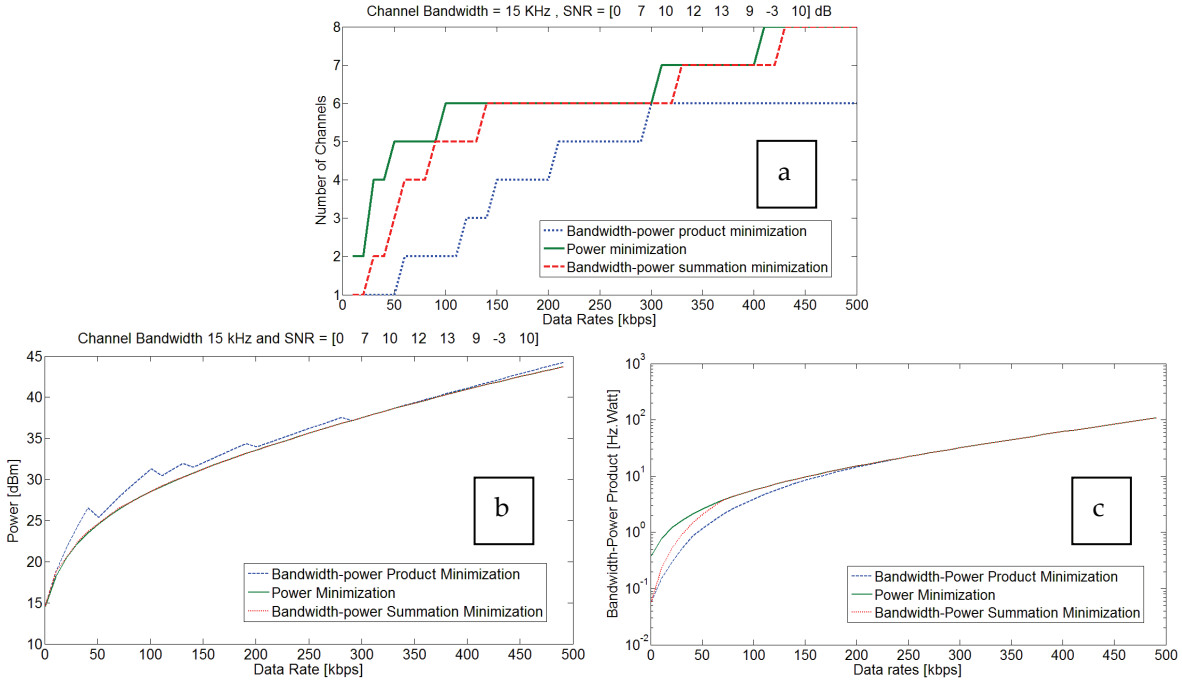


Figure 21: (a) Number of channels, (b) transmission power, and (c) bandwidth-power product vs. data rates with SNR = [0, 7, 10, 12, 13, 9, -3, 10] dB and channel bandwidth 15 kHz.

### 4.1.4.2. Multi-User Resource Allocation

First, we demonstrate the performance of the channel allocation algorithm in the absence of PU activities as depicted in Figure 22(a), where three CR users are considered with data rate requirements of 2, 4 and 6 Mbps. It can be seen that the channel allocation algorithm seeks high SINR values (low 1/SINR values as shown in the figure). However, upon the existence of PU activities at the channel resources, the channel allocation algorithm avoids as much as possible assigning channels with high PU activity profile. This behaviour, which is shown in Figure 22 (b) with the inaccessible band constraints applied to two CR users, is a result of the cost value associated with each channel which scales the SINR value based on the PU activity index. In Figure 23, we compare the behaviour of our proposed resource allocation framework to multiuser waterfilling resource allocation technique. In this figure, the waterfilling technique allocates more channels compared to our proposed resource allocation framework, leaving much less spectral opportunities to adjacent CR networks that operate based on the overlay spectrum sharing technique. The convergence of the iterative power allocation scheme is depicted in Figure 24. In each iteration, the power allocation is updated. The results show that our power allocation scheme converges by a few iterations, e.g., around 20.

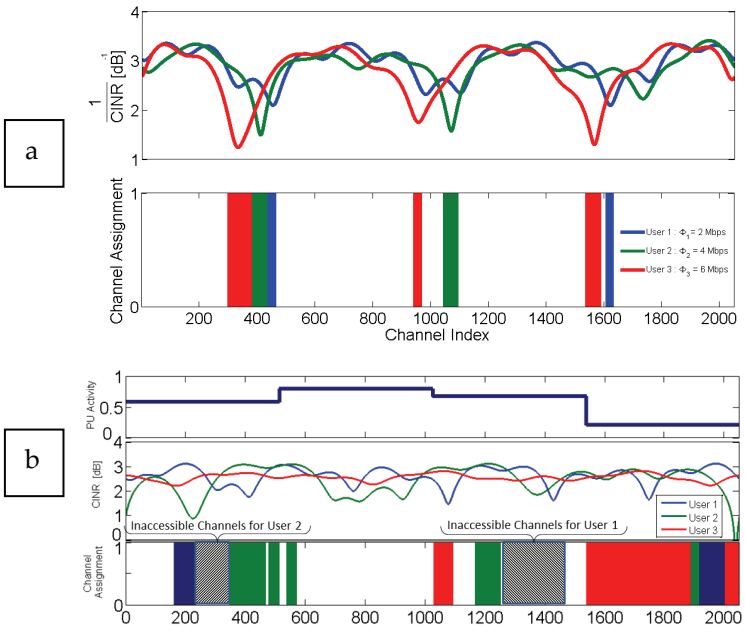


Figure 22: Channel assignment behaviour with (a) no existing PU activities and (b) different PU activity levels and inaccessible bands constraints.

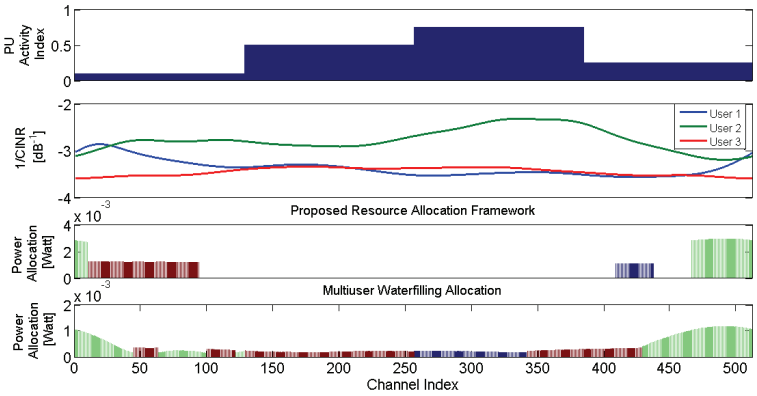


Figure 23: Resource allocation behaviour at different levels of PU activities.

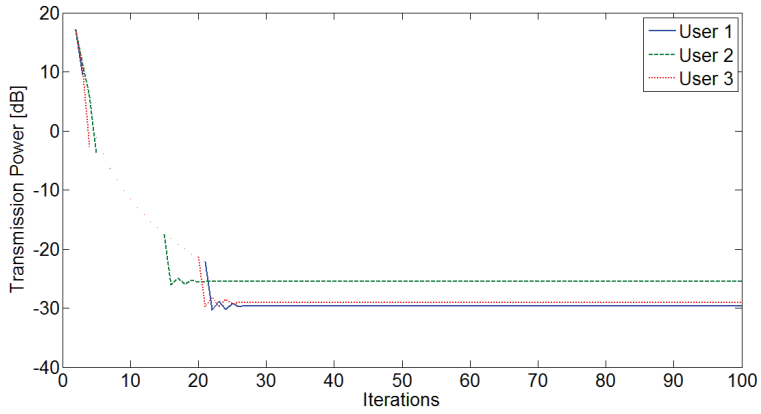


Figure 24: Convergence of power allocation for each CR user.

### 4.1.4.3. Multi-Cell Resource Allocation

We conduct three measurements based on this described simulation scenario. The first one is performed to obtain a resource allocation performance benchmark. This benchmark is presented in terms of the utilization percentage of available spectral resources that could be achieved using the space-bandwidth product metric. Based on [28], it was found that only 45% of the spatial resources can be utilized by random packing of PUs as much as possible in a given area with fixed transmission coverage. If the radii of secondary users are much smaller than that of a PU, secondary users can occupy μ=45% portion of the unoccupied space of primaries. In other words, SUs can occupy $\mu \cdot (1 - \mu) \approx 0.25$ portion of the total space. This results in a total space utilization of 70%. By considering a heterogeneous network with TV stations, WLAN devices, and pico sensors, then the overall utilization is around 82% instead of 45% with only PUs. In the first result in Figure 25, we show the resource allocation percentage for up to 15 different levels of heterogeneity. The level of heterogeneity means how many different transmission power levels are allocated among all femtocells. Level = 1 means that all femtocells are of equal transmission power, two means that there are two different transmission power values, and so on. Also, we consider the cases where the detection performance of cognitive radio is at 90% and 95% probability of successful detection. It can be observed how the spectral utilization improves when having multiple transmission power levels.

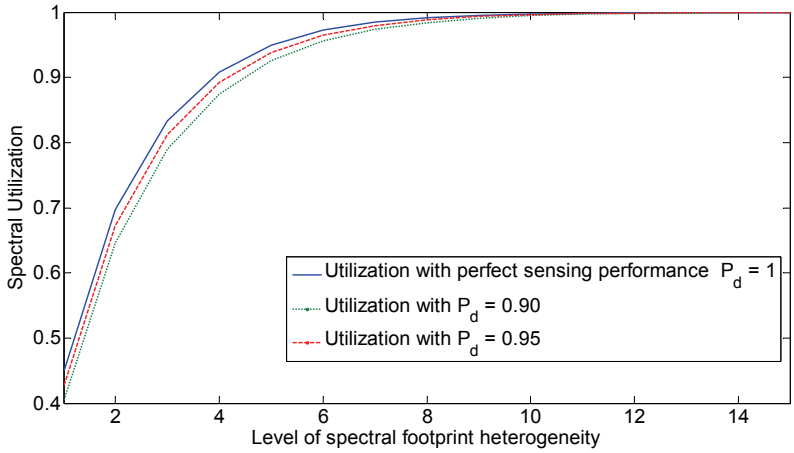


Figure 25: Resource utilization limits.

In the second performance measurement, shown in Figure 26, the rate of REM updates is obtained. A REM update is incremented by one if the interference list changes between two different simulation iterations (with resource allocation framework based on adaptive interference list). The number of updates is averaged across all femtocells. The results are normalized to the maximum number of updates occurred (i.e. when PU activities are high).

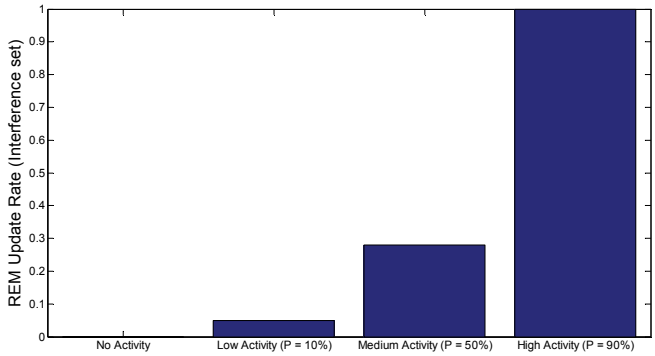


Figure 26: Rate of REM updates.

The third performance measurement (Figure 27) is the convergence rate, defined as the number of iterations required on average by the iterative algorithm to resolve the conflict of channel allocations among various femtocells. It can be seen that the complexity of the iterative algorithm grows considerably as the size of interference list increases.

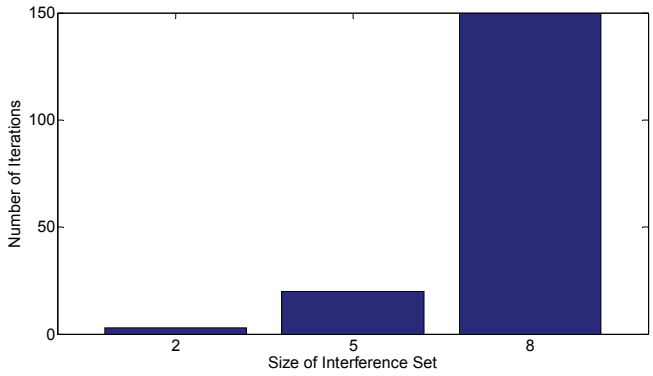


Figure 27: Convergence performance.

### 4.1.5. Conclusions

A new resource allocation optimization framework for cognitive femtocells is developed. The framework aims to minimize the spectral footprint of the Cognitive Radio Network (CRN) through the bandwidth-power product metric. The protection of PUs from harmful interference is incorporated in the framework through primary user activity index. In addition, several hardware limitations of CR users are considered in the proposed framework. The framework implementation is illustrated based on the REM architecture. Based on the performance evaluation results presented in this work, the proposed framework improves the utilization of spectrum by striking a balance between the consumed power and bandwidth. This achievement allows for further spectral opportunities compared to what can be obtained by resource allocation based on waterfilling in CRN based on overlay spectrum sharing mechanism. The proposed framework thus provides an efficient mechanism of resource allocation for CRN in the presence of one or more primary user networks. Simulation results show that performance of adaptive REMs relies on the activities of primary users and the complexity of the network (number of interference cells). Further studies are required to characterize the tradeoff between resource allocation improvements obtained by adaptive REMs and the complexity of its implementations.

## 4.2. Cognitive RRM exploiting heterogeneous PU types

In this scenario, there is no coordination between PU and CR networks. Therefore, CRs access the spectrum in an opportunistic manner depending on the information provided in the REM. We consider a RRM system which takes into account heterogeneous PUs with different spectral features. By exploiting these features, the RRM system can improve the efficiency of spectrum sharing in CR networks and, thus, enhance their capacity. In this context, the RRM calculates the available capacity of the CR network based on the different PU types identified by the CRs. We propose a RRM control mechanism to regulate the sharing of the total available capacity among CRs with variable data rate requirements.

### 4.2.1. Summary of the optimization problem

The optimization framework in this scenario aims to minimize the difference between the available capacity left by PUs and the achievable data rate while satisfying CR demands and interference constraints. The existence of a specific PU type in a CR network influences the amount of available capacity left for the CRs. Assuming heterogeneity of PU types, CRs sharing the same available resources than a certain PU type will be referred to as a “cluster”, whose capacity is formulated

based on the influencing PU type. Note that clusters are not determined by the location of their nodes but by a specific PU type.

Based on the above, the proposed RRM will identify different PU types by exploiting REM information, and will determine how CR users are associated to clusters depending on their requirements. The formulation of the optimization problem [33] was detailed in D5.1 [2] and is summarized in the following Table 11.

Table 11: Optimization problem: Cognitive RRM exploiting Heterogeneous PUs.

| Cognitive RRM exploiting Heterogeneous Primary Users | |
|---|---|
| Scenario(s) of applicability | Hierarchical spectrum access on licensed band:<br>Non-coordinated spectrum access between PUs & SUs |
| General description | A system that takes into account heterogeneous PUs with multiple features is considered. By exploiting this diversity, it is possible to improve the adaptability in CR networks and, thus, to design an efficient Cognitive RRM. An optimization framework is developed by considering heterogeneous PUs and variable CR demands while assuring interference protection towards PUs. A suboptimal solution is proposed by involving the ability of CR users to vary their transmission parameters as well as an Admission Control Policy among CR users. |
| Assumptions | - Coexistence among PUs & CRs<br>- Heterogeneous PUs with several features (i.e., bandwidth, allowable interference level and activity pattern)<br>- Infrastructure-based CR network with a centralized entity (such as a CR base station)<br>- CR resources allocation based on OFDMA<br>- Variable CR demands |
| Optimization target | The objective of the optimization framework is to minimize the difference between the sum of the available capacities left by PUs and the sum of the CR achievable data rates<br>$\min_{P_k, B_k, T_{txk}, R_k^*, c_{k,n}} \sum_{j=1}^{J} \sum_{k=1}^{K} C_{av}^{j} - R_k$<br>$C_{av}^{j}$ is the capacity for the recognized j[th] PU type<br>$R_k$ is the achievable data rate for the k[th] CR<br>$P_k, B_k, T_{tx_k}, R_k^*, c_{k,n}$ are the CR tuneable parameters |
| Tuneable parameters | - $P_k$ is the transmission power of the k[th] CR<br>- $B_k$ is the bandwidth of the k[th] CR<br>- $T_{txk}$ is the transmission time of the k[th] CR<br>- $R_k^*$ is the data rate requirement for the k[th] CR<br>- $c_{k,n}$ is the subcarrier assigned index indicating whether the k[th] CR occupies the n[th] subcarrier or not, in the j[th] cluster |

| | |
|---|---|
| Input parameters | - *Capacity* $C_{av}^{j}$ : The CR sensing information is sent to the CR base station, which elaborates it to identify the PU type(s). Then, the PU features associated to the PU type are extracted, i.e. bandwidth, allowable interference level, and activity index. The identified PU features are used for the calculation of the available capacity<br>- *CR data rate requirements*<br>- *Propagation Model* (used for Interference calculation) |
| Constraints | - *Subcarrier allocation:* to ensure that each subcarrier is assigned to only one user.<br>- *Power allocation to assure Interference protection towards PUs:* if CRs do not detect any PU, CRs are allowed to transmit with their maximum power; if a PU is detected, CRs change their transmission power depending on the allowed interference level of the PU type.<br>- *Transmission time:* it is connected to the PU activity index, which represents the traffic patterns on a certain band at a given time instant.<br>- *CR rate requirements:* We consider a system with CRs transmitting different types of video stream with the capability of changing the rate requirement depending on available resources. |
| REM information | - *PU Allowed Interference levels*<br>- *PU bandwidth and activity pattern*<br>- *Propagation features (propagation factor, etc)*<br>This information is valid for the geographical area where CRs operations are carried out. |

### 4.2.2. Optimization techniques

The considered optimization problem is difficult to solve. It involves binary variables $c_{k,n}$ for subcarrier assignment, continuous variables $P_{k,n}$ for power allocation, and discrete time slots to allocate the transmission time $T_{tx\,k}$. In fact, the resource allocation problem consists of assigning a CR to a cluster and then allocating time slots to a subset of the subcarriers available to meet CR demands and minimize the objective function. The time interval over which these demands must be satisfied can be interpreted as a time horizon over which the QoS requirements must be met. The discrete version of the problem, where the time axis is divided into a number of discrete time slots, is in general NP-hard [32]. The additional constraint to meet the demand $R_k^*$ further increases the difficulty in finding the optimal solution because the feasible set is not convex. Ideally, the CR assignment to a cluster, the subcarrier and power allocation inside the cluster, along with the time interval, should be carried out jointly which leads to high computational complexity. Therefore, a low complexity algorithm with acceptable performance is much preferable than the complex optimal solution.

In this section, we describe a low complexity algorithm for Cognitive RRM. The key factors exploited by our solution are the different values of the available capacities, according to the features of heterogeneous PUs, and the CRs capability of changing their rate requirements. Specifically, the suboptimal solution consists in decomposing the overall optimization problem into two different sub-problems: the CRs assignment to the clusters, according to their rate requirements, and the resource allocation inside the cluster, in terms of subcarriers, power and

time slots allocation. We call the first sub-problem Admission Control Policy and the second one Resource Allocation inside the cluster.

The objective of the overall optimization framework is to minimize the function according to the constraint. In the two sub-problems we consider the constraints separately:

- In the first sub-problem we deal with the assignment of CRs to clusters only according to their requirements. For this reason, $R_k$ in the minimization function must be replaced by $R_k$*.
- After assigning the CRs to the clusters, in the second sub-problem we allocate subcarriers, power and time slots, so that the data rate $R_k$ meets the requirement $R_k$*.

Figure 28 illustrates the developed suboptimal cognitive RRM process highlighting the information stored in the REM and the two sub-problems, i.e. admission control policy and resource allocation inside the cluster. Specifically, the sensing information is sent by the CR node to the CR base station, which processes it to detect the PU types. The details on how this process is done can be found in [31]. The information on the detected PU types is then stored in the REM along with the PU features. The CR base station utilizes these PU features (allowed interference level, bandwidth, activity pattern) and the propagation features (propagation factor, etc.) to calculate the available capacities $C_{av}^{j}$, as formulated in D5.1 [2]. Then, through the admission control policy, CRs are assigned to the cluster according to the available capacities $C_{av}^{j}$ and CR rate requirements. After this process, the resource allocation inside the cluster is carried out. The two sub-problems are described in detail in the following sections.

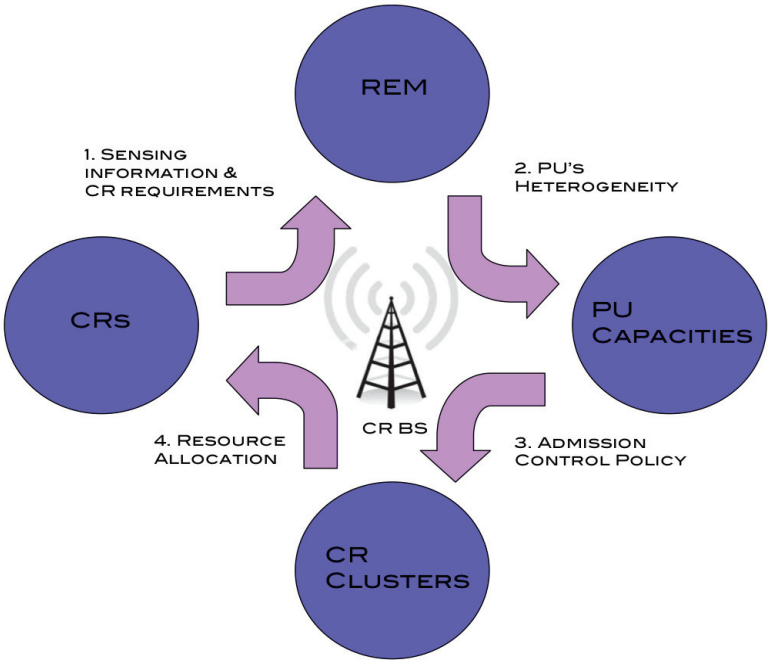


Figure 28: Cognitive Radio Resource Management exploiting Heterogeneous PUs.

#### 4.2.2.1. Admission Control Policy

As explained before, the entire system consists of several CR clusters. Each cluster is related to a different available capacity. Through an Admission Control Policy, we decide on a cluster to which a CR must be assigned, in order to minimize the objective function, where $R_k$ is replaced by $R_k^*$ for this sub-problem. Moreover, we consider that CRs may have different requirements, and they may modify them depending on the available resources. We consider different levels of requirement for each CR that can differ from user to user. At the beginning, each CR has its preferable requirement.

In the following, the algorithm is described in detail:

- The value of the requested data rate or demand level of the $k^{th}$ CR is defined as $R^*_{k,i}$, with $i = 1,...,I_k$. The number of levels $I_k$ and the values of requested rates may vary from user to user.
- The preference of the $k^{th}$ CR is defined by selecting a value among the possible demand levels $R^*_{k,i}$.
- After having ordered the CR preferable requirements from the lowest to the highest value, we start to serve the CRs.
- At each new request by a CR to enter the system, the available capacity $C^j_{av}$ is calculated for each $j^{th}$ cluster.
- The request of the new CR is subtracted from the expected available capacity of each cluster and, if the amount is a positive value at least in one case, the new CR is allowed to enter the system.
- The CR will be assigned to the cluster that has the maximum value in the previous calculation.
- If, on the other hand, the value of the difference between the available capacity and the new request is a negative number for each cluster, then, the cluster with minimum absolute value of the calculated difference is selected.
- The new CR is asked to decrease its demands to its lower level, by moving to a lower quality coding, in order to enter the cluster.
- If the CR is on its lowest level of requirement, or if the decrease is not enough so that the problem persists, then another user is asked to decrease its demand by one level, among the CRs already assigned to the selected cluster.
- The CR chosen to decrease its demand is the user for which a decrease in its requirement allows to minimize the unused available capacity in the cluster.
- If it is not possible to reduce the CR requirements in the chosen cluster, then the new request is rejected.
- If there is still available capacity in some of the clusters after considering all the CR requests, the CRs belonging to the cluster with available resources are asked to increase their demands.
- The first to be satisfied is the CR whose increasing demand minimizes the unused available capacity.
- When CRs are assigned to the clusters and their final requirements are defined, the resource allocation for power and subcarrier allocation is carried out to satisfy the CR rate requirements as explained in the next section.

#### 4.2.2.2. Resource Allocation inside the cluster

After the CR users have been assigned to a cluster, the subcarriers and the power are selected through the Resource Allocation such that the CR rate requirements are satisfied. In particular, for the allocation of available resources we consider an OFDMA system within a cluster. We refer to $K^j$ as the total number of CRs served in the cluster and $N^j$ as the number of subcarriers in one OFDM symbol for the $j^{th}$ cluster. In the proposed subcarrier and power allocation algorithm, after initializing all the parameters, the procedure consists of $N^j$ iterations. In each iteration, the CR user that is assigned to a cluster first, is given a priority to choose its best available subcarrier. Assuming a fixed transmission power over the entire bandwidth, each subcarrier adds an equal portion of the total power $P_{total} / N^j$ to the CR it has been assigned to. $P_{total}$ is equal to $P_{s_{\max}}$ or $P_s$ depending on whether the PU is idle or active, respectively. The current power of each user $P_k$ is then allocated to its subcarriers by water filling policy as in [35]. After each iteration, the assigned subcarrier is excluded from the set of available subcarriers $S$. The procedure continues for a number of OFDM symbols, satisfying the upper bound of CR transmission time, so that all the available subcarriers are assigned to CRs in order to satisfy their rate requirements. The Admission Control Policy, explained in Section 4.2.2.1, assures that all CRs admitted to $j^{th}$ cluster will meet their requirements. By reallocating the power in each iteration, we ensure that each CR achieves its maximum data rate within its allocated power in order to satisfy its requirement.

In the following, the summary of the algorithm is presented for each OFDM symbol.

Algorithm 1: Resource allocation algorithm inside a cluster

1: Initialization
$c_{k,n} = 0, \forall k, n$
$R_k = 0, \forall k$
$S = 1, 2, ..., N^j,$
$U = 1, 2, ..., K^j.$

2: Subcarrier Allocation
**while** ($S \neq \oslash$ or $U \neq \oslash$):
choose $k$ following the ordered list of CR preferable requirements
$n = argmax_{n \in A} H_{k,n}$
$c_{k,n} = 1$, $S = S - n$,
$R_k$ (updated with water filling policy),
**if** $R_k = R_k^*$ then $U = U - k$.
**end**

#### 4.2.2.3. Information stored in the REM database

The keys points of the proposed RRM system are the opportunities provided by the heterogeneity of the PUs. In particular, the REM information used by the RRM, is summarized as:

- PU Allowed Interference levels (to calculate the available capacities and to adapt the CR transmission power)
- PU Activity patterns (to calculate the available capacities and to adapt the CR transmission time)
- PU bandwidth (to calculate the available capacities and to adapt the CR bandwidth)

- Propagation features, such as propagation factor, (to calculate the CR transmission power)

This information is valid for the geographical area where the CRs operations are applied.

In particular, the PU allowed interference level is used to calculate the CR transmission power $P_s$, when contemporary PU and CRs transmissions are considered. Specifically, CRs assure protection towards PU by lowering the transmission power from $P_{s_{\max}}$ to $P_s$. $P_s$ is calculated by considering the allowed interference level $P_I^j$, in terms of received interference power allowed by $j^{th}$ PU. $P_s$ is calculated by the path-loss propagation model.

$$P_s = P_I^j + P_{L0} + 10\alpha \log_{10}\left(\frac{d}{d_0}\right) \quad (19)$$

where $P_{L0}$ and $\alpha$ are the propagation features stored in the REM. $P_{L0}$ is the path loss at distance $d_0$ (typically 1m) and $\alpha$ is the path loss exponent. We suppose that CR has the capability of calculating the distance $d$ exploiting the location information stored in the REM.

As detailed in D5.1 [2], the allowed interference level $P_I^j$ along with the other PU features, i.e. the bandwidth $B^j$ and the activity index $\phi^j(i)$, that is formulated in [34], are used to calculate the value of available capacities $C_{av}^j$. $C_{av}^j$ are then used for resource management at the CR base station, as explained before.

The proposed RRM design requires specific interactions among the architectural components of the FARAMIR architecture, namely the REM-SA (Storage & Acquisition), the REM Manager and the CR devices, used for reporting measurements towards the REM. The details about the messages exchanged between entities can be found in [36] and in section 3.4.5 of deliverable D2.4 [3].

## 4.2.3. Evaluation methodology

### 4.2.3.1. Simulation Environment

All simulation results have been obtained using MATLAB. The modelled system is composed of several PU types which use OFDM transmission, and a CR centralized network. The CRs, after detecting PUs, send their information to a CR base station that broadcasts the presence of PU types and their features to all CRs for rate adaptation. We consider the following PU standards: 802.11, 802.16e and DVB-T 2K mode. Moreover, we take into account different interference thresholds $P_I^j$ allowed by the PU standards. The PU activity index $\phi^j$, is randomly distributed between 0.1 and 0.4 [31]. The bandwidth $B^j$ for each PU is obtained by $N^j \times \Delta f^j$, where $N^j$ is the FFT size and $\Delta f^j$ is the subcarrier spacing. The wireless channel is modelled as a Rayleigh fading multipath with two rays that are spaced by 4 μs. The power values are equal to −0.4576 dB and −5.2288 dB with constant amplitudes. Perfect knowledge of subchannel gains is assumed at CR receivers.

#### 4.2.3.2. Key Performance Indicators

The performance of the proposed solution is evaluated in terms of available capacity, CRs achieved data rates and CRs satisfaction.

- *Available Capacity:* The capacity $C_{av}^{j}$ available for a cluster of CRs is calculated according to the PU features, as formulated in D5.1 [2]. Specifically, the capacity $C_{av}^{j}$ will be first analyzed by varying the PU allowed interference threshold, then by varying the PU bandwidth, the PU activity index, and finally by considering the combined effect of all the features. In each of the aforementioned cases, we compare the performance of the available capacity by using or not the REM. In particular, we made the assumption that, in case we use the REM, after the detection and classification of heterogeneous PUs we are able to extract the PU features stored in the REM. On the contrary, without using REM, we are not able to recover the value of the PU features, thus we consider to use the minimum value of those features in order to avoid interference towards PUs.
- *CRs achieved data rates and satisfaction:* The performance of the proposed suboptimal algorithm is evaluated in terms of total data rate $\sum_{k=1}^{K^j} R_k$ achieved by the CRs for each cluster, so that the unused available capacity $C_{av}^{j} - \sum_{k=1}^{K^j} R_k$ is computed. Moreover, the satisfaction of CRs is calculated in terms of percentage of non-served CRs, CRs decreasing their data rates, CRs transmitting with their preferable requirements, and CRs increasing their data rates.

### 4.2.4. Results

#### 4.2.4.1. Available Capacity

In the following we analyze the available capacity by varying each PU feature.

- *Allowed Interference Threshold*: Figure 29 shows the behavior of the available capacity $C_{av}^{j}$, normalized to the transmission bandwidth, depending on the various interference thresholds allowed by different PU standards. The interference $P_I^j$ allowed by a PU device receiving CR interference is set equal to 0.9 pW, 9.9 pW and 31.5 pW respectively. These values are consistent with the 802.11, 802.16 and DVB PU standards. The received PU power level is set to the typical value of 100 pW. We set the noise power to the usual value 0.1 pW for a bandwidth of 20 MHz. In this way, the SINR is easily calculated starting from the PU interference thresholds. In particular, the chosen interference thresholds 0.9 pW, 9.9 pW and 31.5 pW that correspond to SINR of a PU device receiving CR interference equal to 20 dB, 10 dB, and 5 dB, respectively. Moreover, the interference threshold values are used to calculate the CR transmission power $P_s$ according to (19), by setting $\alpha$ equal to 5 at a distance $d_{j,n}$ of 10 m. $P_s$ is used to calculate $C_{av}^{j}$ when there are contemporary PU and CR transmissions. Furthermore, the interference $P_I$ that a PU transmission causes to the CR is set equal to 2 pW. When CR does not detect any PU signal, it uses the maximum transmission power $P_{S_{\max}}$ set to 50 mW. To calculate $C_{av}^{j}$, as formulated in D5.1[2], $P_f$ is set to 0.1, $P_d$ is equal to

0.5, $P_{idle}$ and $P_{busy}$ are set to 0.37 and 0.63 respectively. In case the REM is not used, the contribution regarding contemporary PU and CR transmissions is not computed to calculate $C_{av}^{j}$ because it is not possible to recover the interference level allowed by the PUs.

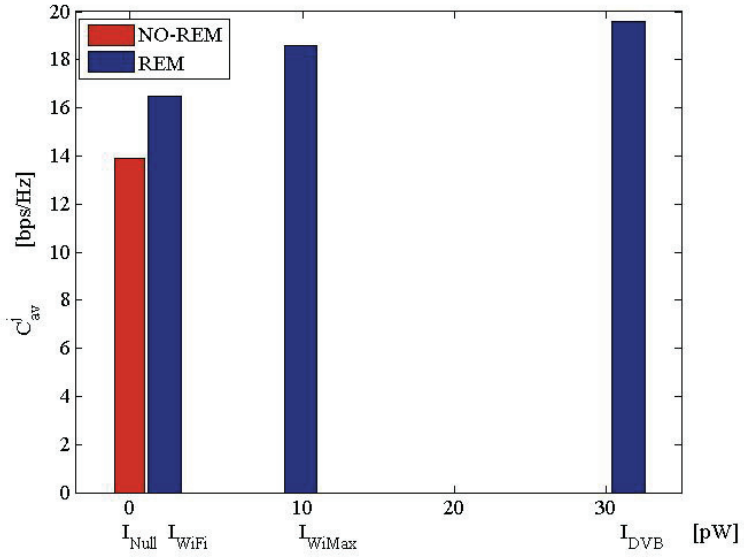


Figure 29: Available capacity for various interference thresholds.

- *Bandwidth:* Figure 30 shows the behaviour of $C_{av}^{j}$, varying the bandwidth $B^{j}$: 5 MHz bandwidth if a 802.16 PU signal has been detected, 8 MHz for DVB PU signal, and 20 MHz for 802.11 PU signal. As shown in Figure 30, the available capacity $C_{av}^{j}$ increases with the bandwidth. In case the REM is not used and, thus, the exact value of the available bandwidth is not obtainable, we set the bandwidth available for CR equal to the minimum value of 5 MHz in order to avoid interference towards each type of PU.

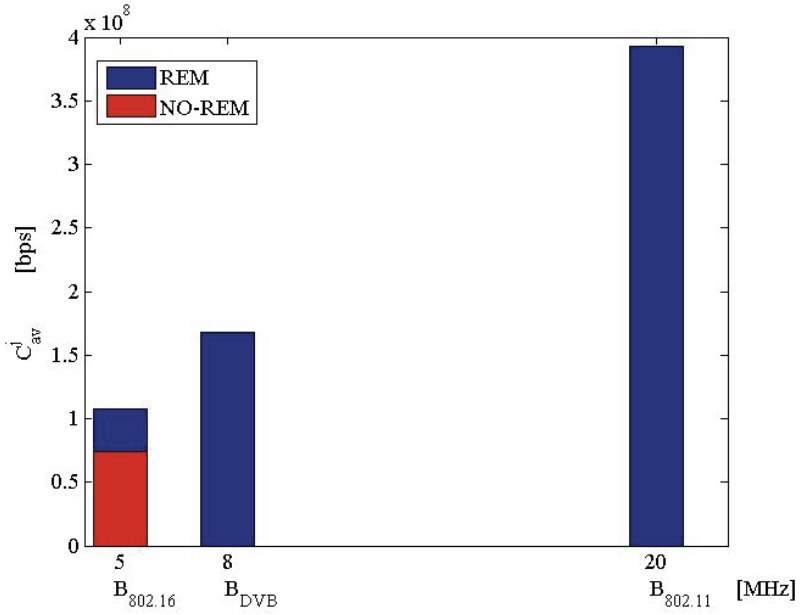


Figure 30: Available capacity for different bandwidths.

- *Activity Index:* The maximum value of transmission time $T_{tx}^{j}$, available for CRs that transmit in the band of the j[th] recognized PU type, is equal to PU idle time $T_{idle}$ when PU has not been detected (case H0), and PU busy time $T_{busy}$ when a PU has been detected (case H1). $T_{idle}$ and $T_{busy}$ depend on the PU activity index $\phi^{j}$. We set the value of $T_{tx}^{\max}$ equal to $T_{idle}$ (case H0), and equal to $T_{busy}$ (case H1) to calculate the available capacity $C_{av}^{j}$ expressed in deliverable D5.1 [2]. Figure 31 shows how the value of the CR available capacity $C_{av}^{j}$ varies depending on the value of $\phi^{j}$. In particular, in case the REM is not used, the sensing time $T_s$ of $\gamma$ in $C_{av}^{j}$, as expressed in D5.1[2], is equal to $T_c+T_p$. $T_c$ is the time used to detect and classify PUs, while $T_p$ is the observation time devoted to extract the activity index $\phi^{j}$. $T_c$ is set equal to 5 OFDM symbol time that, for FFT size of 2048 and guard interval equal to $T_u/4$ with $t_s$ = 0.1 μs, corresponds to 1.28 ms. $T_p$ is set equal to 10 s, as in the simulation in [31]. In case the REM is used, it is possible to reduce the sensing time $T_s$, thus improving $C_{av}^{j}$ as shown in Figure 31. In fact, in this case, we consider that CRs take turn at updating the REM with their sensing information, thus $T_c$ becomes equal to $(T_c+T_p)/N_{CRs}+T_{infoREM}$, where $N_{CRs}$ is the number of CRs involved in updating the REM and $T_{infoREM}$ is the time required to recover the sensing information from the REM. We set $N_{CRs}$ equal to 10 and $T_{infoREM}$ equal to 160 ms, equal to the LTE delay budget. Finally, we consider a bandwidth of 20 MHz and an interference threshold $P_I^{j}$ equal to 31.5 pW. $P_f$ and $P_d$ are set to reasonable values of 0.1 and 0.95 respectively, while $P_{busy}$ is set to [0.63 0.64 0.65 0.66] and $P_{idle}$ is set to [0.37 0.36 0.35 0.34], as in the simulation results in [31].

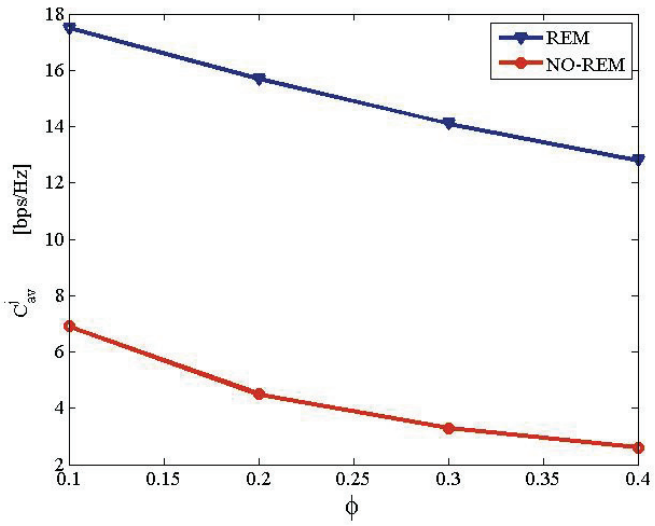


Figure 31: Available capacity as a function of the activity index.

- *Effects of the Combined PU Features:* Figure 32 shows the total effects of the features of heterogeneous PUs on the available capacity $C_{av}^{j}$, which is normalized to the bandwidth. As explained before, $C_{av}^{j}$ varies depending on the PU allowed interference, bandwidth and activity index. As shown in Figure 32, the DVB signal is the PU type that allows the maximum normalized

capacity $C_{av}^{j}$ available for CRs. When the REM is not used, it is not possible to extract the exact value of the features of heterogeneous PUs, thus, the value of the features is set to the minimum value in order to avoid interference towards each type of PU. Specifically, the bandwidth is set equal to 5 MHz, the activity index $\phi^{j}$ is set to 0.4 and a null value is considered for the interference threshold $P_{I}^{j}$ allowed by the PU. In other words, the term that accounts for contemporary PU and CR transmission does not contribute to the calculation of $C_{av}^{j}$ in case the REM is not used.

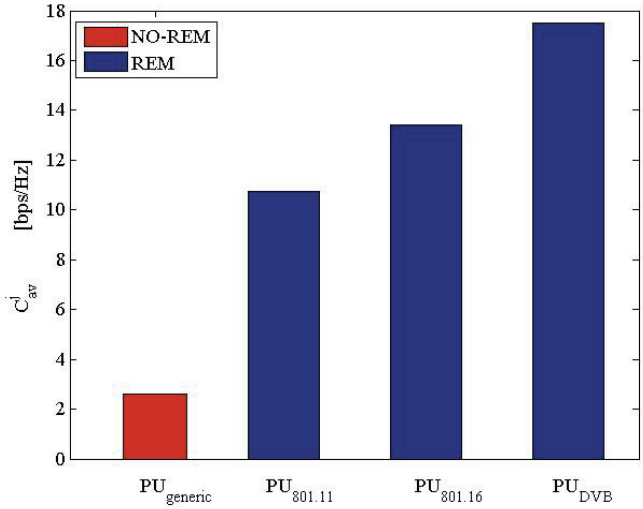


Figure 32: Available capacity for different features of the primary users.

### 4.2.4.2. CRs achieved data rates and satisfaction

Figure 33 compares the available capacity $C_{av}^{j}$ and the CR data rates $\sum_{k=1}^{K^{j}} R_{k}$ achieved in each cluster according to the Cognitive RRM, whose values are normalized as explained before. It is shown that the value of the available capacity $C_{av}^{j}$ of the j[th] cluster varies according to the detected PU type. Specifically, the value of $C_{av}^{1}$, the available capacity for Cluster 1, is higher than $C_{av}^{2}$, the available capacity for Cluster 2. In fact, $C_{av}^{1}$ and $C_{av}^{2}$ are calculated as formulated in D5.1 [2] and their values depend on the features of the detected PU type, 802.16 and UHF TV signal respectively. In Figure 33, we consider two cases:

- CRs with variable data rate requirements (VRR),
- CRs with fixed data rate requirements (NO-VRR).

In Figure 33 we also compare the satisfaction of different CRs with VRR and with NO-VRR. In Figure 33 (a), (b) and (c) we show the normalized available capacities and achieved CR data rates in different cases. In Figure 33 (d), (e) and (f) we show the satisfaction of CRs calculated in terms of percentage of non-served CRs, CRs decreasing their data rates (Dec), CRs transmitting with their preferable requirements (Pref), and CRs increasing their data rates (Inc).

In a low load case, the number of CR requests is much lower than the available resources. The total unused available capacity is 30% of the total available capacity with the VRR algorithm. When NO-VRR algorithm is used, the unused capacity is 98% of the total available capacity. With the VRR, the CRs can increase their data rates, while with the NO-VRR algorithm they can only satisfy their preferences.

In a medium load case, the total unused available capacity is 26% of the total available capacity when the VRR algorithm is used, while it becomes 35% with the NO-VRR. In the latter case, even if more CRs transmit with their preferable requirements, some CRs are not served. With the VRR some CRs decrease their requirements but others increase their data rates, while assuring that everybody is served.

In a high load case, the total unused available capacity is 4% of the total available capacity when the VRR algorithm is used, and the 14% with the NO-VRR algorithm. As expected, less CRs are not served with the VRR than with the NO-VRR.

Figure 34 shows the total unused available capacity normalized to the total available capacity in the low, medium and high load case respectively, using both the VRR and NO-VRR algorithms. Note that the total unused capacity is the function to minimize as formulated in the optimization problem. The VRR algorithm shows better performance than the NO-VRR because it enables a lower value of the total unused capacity.

Simulation results show that the value of the available capacity for CRs varies according to the detected PU types. Moreover, these results show that the overall performance of the network, in terms of the achieved data rate, is improved when variable CR requirements are needed. These improvements are observed by higher achieved data rates, and hence less wasted available capacity and higher satisfaction rate, in terms of percentage of served CRs out of total number of CRs.

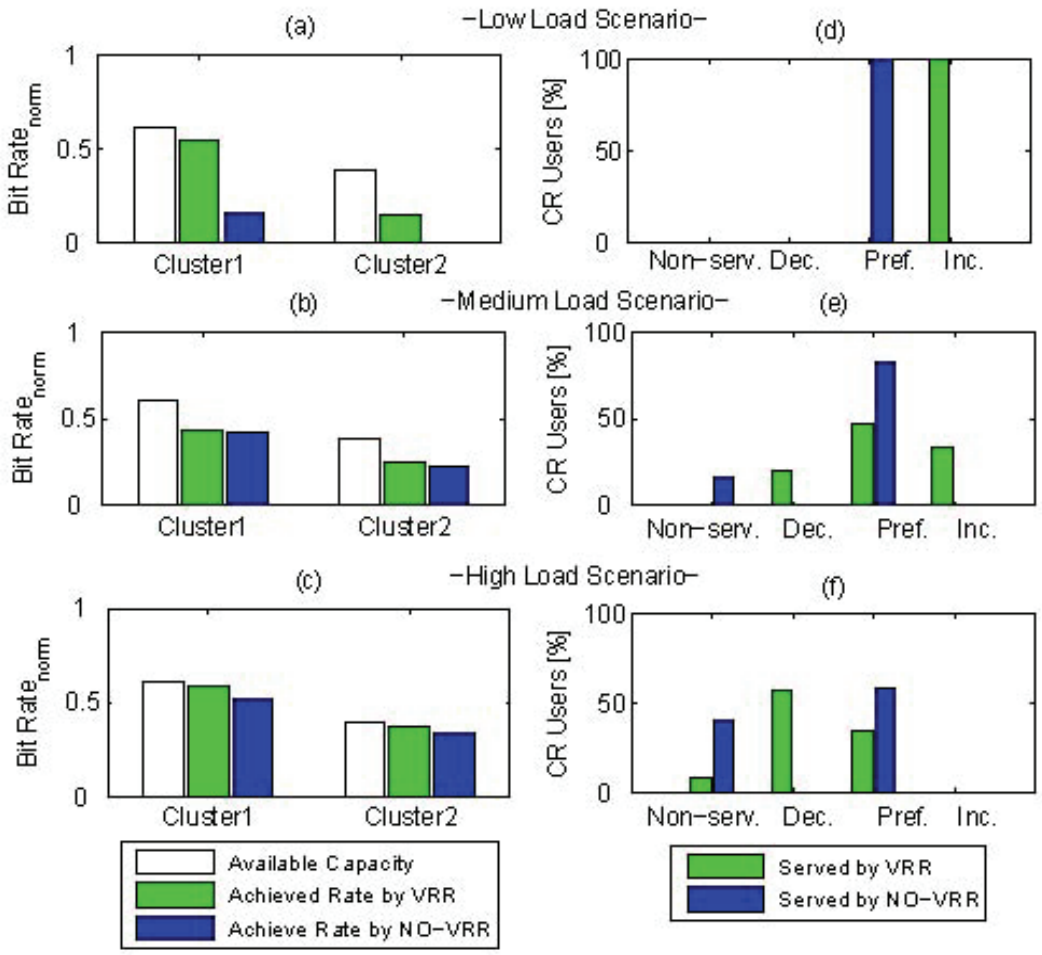


Figure 33: Comparison between available capacity and achieved data rates.

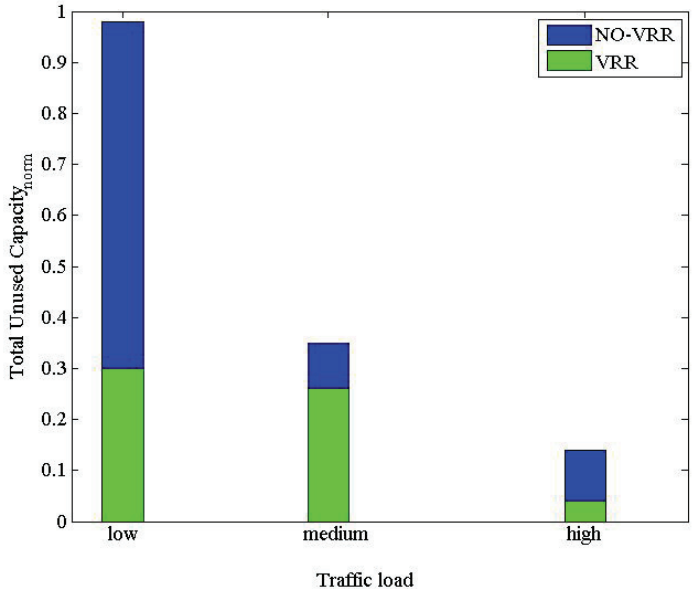


Figure 34: Comparison between total unused capacity.

### 4.2.5. Conclusions

An optimization framework for Cognitive RRM has been developed. The key point of the approach is the exploitation of multiple features of heterogeneous PUs, which are stored in a REM, and variable CR rate requirements for the efficient utilization of spectrum resources. Being the optimal solution unfeasible, a suboptimal solution has been proposed, which satisfies the CRs demands through an efficient and adaptive use of available resources. The procedure has the objective to minimize at each step the difference between the available capacity and the achieved data rates of the CRs. In this way, the number of operations to adjust the CR data rates is reduced, while pursuing the satisfaction of the CR demands and balancing between the number of CRs served and the available capacity.

## 4.3. Spectrum selection based on PU transmission patterns

### 4.3.1. Summary of the optimization problem

This optimization problem focuses on the scenarios where it is assumed that a group of SUs perform opportunistic spectrum access to a set of channels that are left unused by PUs. In particular, the problem pursues a focused exploitation of primary-user statistical patterns capturing intra-channel dependence structures potentially exhibited by primary systems for optimizing the specific task of spectrum selection. In this way, the usage of spectral resources can be improved while trying to avoid as much as possible the need for executing Spectrum Handovers (SpHOs) to vacate a channel when a PU appears. Therefore, the main contributions and advances with respect to the state-of-the art are twofold: (1) To propose the usage of advanced statistics associated to heterogeneous primary-users and retain such characterizations in a REM, (2) To exploit this knowledge in the spectrum selection decision-making process to suitably match multi-service secondary traffic to the observed spectrum opportunities targeting the minimization of the SpHO rate.

Table 12 summarizes the main elements of the considered optimization problem.

Table 12: Optimization problem: Spectrum selection based on PU transmission patterns.

| Spectrum selection based on PU transmission patterns | |
|---|---|
| Scenario(s) of applicability | Scenarios belonging to the group “Non-coordinated Spectrum Access between PUs and SUs” from Deliverable D2.2 [1] |
| General description | This problem targets the optimization of the spectrum selection policy when SUs with different service profiles access opportunistically a set of channels during the inactivity periods of PUs. Selection will be done taking as input the statistical characterization of the PU activity that will be stored in the REM and the SU service profiles. |
| Assumptions | - A set C of channels accessed opportunistically by SUs.<br>- REM contains the statistical characterization of the duration of activity/inactivity periods in the different channels<br>- M different secondary services, each one characterized by a Mean Holding Time.<br>- The SU system is able to detect the arrival of a PU to a given channel and correspondingly trigger a spectrum handover to any of the available channels. |

| | |
|---|---|
| Optimization target | Minimize the rate of spectrum handovers in the scenario |
| Tunable parameters | Spectrum selection policy that determines which channel is assigned to each SU both at session set-up and after a spectrum HO. |
| Input parameters | - Statistical characterization of the PU activity in the different channels stored in REM (see section 4.3.2 for details)<br>- SU traffic characteristics in terms of mean holding time for each service accessing the system. |
| Constraints | A SU can only access a channel while in an OFF period.<br>As soon as the PU starts transmission in a given channel, the SU call in that channel will be handed over to another channel, if available. |
| REM information | Statistical characterization of the PU activity in the different channels, valid for the geographical area and period of time where SU operation is carried out (see section 4.3.2 for details). |

## 4.3.2. Optimization techniques

The problem assumes a set *C* of channels each of bandwidth $B_P$ shared opportunistically by SUs in accordance with PU activity, meaning that only those channels where there are not PU transmissions can be assigned to SUs and that whenever a PU starts the transmission in an occupied channel, the SU must vacate it and perform a SpHO towards another channel, if available.

For each channel $i \in C$, the two discrete random sequences $ON_i$ and $OFF_i$ are introduced to respectively denote the sequences of activity and inactivity periods. At a given discrete time index *j*, $ON_i(j)$ and $OFF_i(j)$ correspond to the duration of the *j-th* activity and inactivity period, respectively.

With respect to SUs, a set of *M* heterogeneous secondary service types is assumed having opportunistic access to the considered channels. Service type *m* is characterised by a certain mean holding time $MHT_m \ \forall m \in \{1..M\}$.

Assuming that the SUs have the capability to make SpHO to switch communication from one channel to another, but that every SpHO will have a cost in terms of signalling requirements and service degradation in terms of latencies for SUs, the target of the optimization will be to find a channel selection policy that minimises the number of required SpHOs. For that purpose, it will make use of statistics of the PU temporal usage patterns that will be stored in the REM. These will be described in the following sub-section 4.3.2.1. Then, the considered selection techniques will be described in sub-section 4.3.2.2.

### 4.3.2.1. Information stored in the REM database

As indicated previously, the optimization problem considered here focuses on exploiting the time dimension information to decide the appropriate channels to allocate a SU communication. This means that the statistics that will be stored in the REM will capture the activity/inactivity periods of the PU behaviour for the different channels. Focusing on the time perspective, some empirical measurements [37] have shown that, in addition to the expected daily/weekly periodicity of

activity (ON) and inactivity (OFF) processes of PUs, some correlation has been in fact observed between consecutive ON/OFF periods depending on the band of interest and the considered traffic conditions. Then, advanced statistics capturing this type of correlation structures can be of interest when performing the spectrum selection decision-making.

Generally speaking, the PU statistics that are stored in the REM can be classified into first-order metrics such as means or conditional probabilities or higher-order metrics such as variances or correlation functions. Some useful statistics characterizing primary activity/inactivity periods are structured in buckets. A bucket includes the ON (alternatively OFF) period durations falling in a given interval. Buckets for the ON periods are numbered as $a \in \{1..\left|B_i^{ON}\right|\}$ so that $B_i^a \in B_i^{ON}$ denotes the *a-th* bucket, $B_i^{ON}$ denotes the set of buckets and |·| denotes the cardinality. The same would be for OFF periods numbered as $b \in \{1..\left|B_i^{OFF}\right|\}$, $B_i^b \in B_i^{OFF}$ denoting the *b*-th bucket and $B_i^{OFF}$ the set of buckets.

Bucket length is assumed to be a fraction $\alpha$ of the average value of the corresponding distribution. This means that, considering for instance $OFF_i$ distributions, $\forall b \in \{1..\left|B_i^{OFF}\right|\text{-}1\}$, bucket $B_i^b$ is defined as $B_i^b = [(b-1).(\alpha.E(OFF_i)), b.(\alpha.E(OFF_i))[$ where $E(OFF_i)$ denotes the average value of OFF period. The last bucket $B_i^{\left|B_i^{OFF}\right|}$ is assumed to be infinite of the form $[(\left|B_i^{OFF}\right|-1).(\alpha.E(OFF_i)), \infty[$.

A wide range of possible statistics of interest could be envisaged in the REM. In particular, for the considered problem, the following metrics are extracted for each channel i∈C:

- Average value of *ON* and *OFF* periods, $E(ON_i)$, $E(OFF_i)$.
- DC (Duty Cycle):

$$DC_i = \frac{E(ON_i)}{E(ON_i) + E(OFF_i)} \tag{20}$$

- The conditional probability of observing a certain duration of the *OFF* period given a certain duration of the last *ON* period was observed. Specifically, $CP^i_{OFF,ON}(B_i^b, B_i^a)$ is defined as the conditional probability of observing $OFF_i$ in $B_i^b \in B_i^{OFF}$ given that the last outcome of $ON_i$ was observed in $B_i^a \in B_i^{ON}$:

$$CP^i_{OFF,ON}(B_i^b, B_i^a) = \Pr\left[ OFF_i(j) \in B_i^b \,/\, ON_i(j) \in B_i^a \right] \tag{21}$$

- The conditional mean of $OFF_i$ given the last outcome of $ON_i$ was observed in bucket $B_i^a \in B_i^{ON}$ defined as follows:

$$E(OFF_i \,/\, ON_i \in B_i^a) = \sum_{B_i^b \in B_i^{OFF}} \hat{B}_i^b \times CP^i_{OFF,ON}(B_i^b, B_i^a) \tag{22}$$

where $\hat{B}_i^b$ is the centre value of bucket $B_i^b$ which is given by . $\hat{B}_i^b = (b-0.5) \times (\alpha \times E(OFF_i))$

- A measure of dependence level between successive ON/OFF periods defined as:

$$DEP_i = \frac{1}{\left|B_i^{ON}\right|} \sum_{B_i^a \in B_i^{ON}} \max_{B_i^b \in B_i^{OFF}} \left( \delta_{a,b} \times CP^i_{OFF,ON}(B_i^b, B_i^a) \right) \quad (23)$$

where $\forall a \in \{1..\left|B_i^{ON}\right|\}$ and $\forall b \in \{1..\left|B_i^{OFF}\right|\}$, $\delta_{a,b}$ is a dependence indicator between $B_i^a$ and $B_i^b$ defined as:

$$\delta_{a,b} = \begin{cases} 1 & if\ CP^i_{OFF,ON}(B_i^b, B_i^a) > pdf^i_{OFF}(B_i^b), \\ 0 & \text{otherwise} \end{cases} \quad (24)$$

Notice that only those buckets $B_i^a$ such that $pdf^i_{ON}(B_i^a) \neq 0$ are considered in $B_i^{ON}$ when calculating $DEP_i$ in Eq. (23). The value of $DEP_i$ will range from 0, corresponding to the case where ON and OFF periods are independent, to 1, corresponding to the case in which the OFF period is totally known from the preceding ON period.

Depending on primary activity, useful knowledge about PUs can be inferred thanks to some of these metrics. Other statistics such as the variances of the ON or OFF period durations could also be used. For instance, in case the variance of the OFF periods duration is equal to 0, a deterministic primary activity pattern can be inferred and e.g. $E(OFF_i)$ provides full estimation of primary OFF periods. Nevertheless, in a more general case of random primary activity, $E(OFF_i)$ may not be the best choice for characterizing OFF periods if there are some patterns involving ON/OFF periods (e.g. dependencies between consecutive ON/OFF periods, two successively observed OFF periods, etc). In this respect, $DEP_i$ can be for instance used to evaluate how dependent consecutive ON/OFF periods are. The observation of a high $DEP_i$ value would indicate that $E(OFF_i / ON_i \in B_i^a)$ would provide a much better estimator of actual OFF periods.

#### 4.3.2.2. Spectrum Selection Techniques

The basic idea of optimizing spectrum selection is to choose the best channel for secondary operation (according to a given criterion). While this problem accepts some mathematical formulation, the dynamism in the radio environment, the heterogeneity in PU types as well as secondary traffic types and the fact that previous spectrum selection decisions condition future selections suggest that a heuristic approximation can be suitable to devise the main principles to follow in this decision-making process. On the other side, one can anticipate that the formulation of a comprehensive and general spectrum selection strategy is complex, since there will not be a single criterion that will result suitable in the wide range of different scenarios and configurations that may arise in practice.

As a basic principle, the knowledge retained in the REM about the PU traffic will be used to estimate the remaining free-time for each of the sensed-as-free channels. In particular, for each idle channel *i* it is assumed that we are keeping track of the duration of the last $ON_i$ period assumed to fall in bucket $B_i^a$ as well as the so-far observed duration of the current $OFF_i$ period ($Idle\_C^i$). The remaining OFF period ($Rem\_T^i$) at a given time instant can be estimated by

subtracting the so-far observed availability time (*Idle_C*$^i$) from an estimation of the actual OFF period given the last observed ON period as follows:

$$\mathrm{Re}\,m\_T^i = E(OFF_i / ON_i \in B_i^a) - Idle\_C^i \quad (25)$$

It is important to point out that a more complex statistic such as $E(OFF_i / ON_i \in B_i^a)$ is considered here in order to formulate a more generic case for an estimator of actual OFF periods. In case that no dependency is observed between consecutive ON/OFF periods (i.e. $DEP_i = 0$), the statistic reduces to $E(OFF_i / ON_i \in B_i^a) = E(OFF_i)$. In turn, as *DEP*$_i$ increases and ON/OFF become more dependent, $E(OFF_i / ON_i \in B_i^a)$ becomes much more accurate than $E(OFF_i)$.

The estimation of the remaining free-time for each of the sensed-as-free channels can be considered in the spectrum selection decision-making process. Letting *i** be the selected channel, the following criteria exploiting differently the statistical metrics provided by the REM are proposed as follows:

- ***Criterion 1:*** This criterion (*Crit*$_1$) makes a straightforward use of the available statistics simply by picking up the channel with the longest availability whenever a channel has to be selected for a SU. It can be formulated as:

$$i^*_{Crit_1} = \arg\max_i \left( \beta_i \times \mathrm{Re}\,m\_T^i \right) \quad (26)$$

  where $\beta_i$ is a compensation factor that should be adjusted for each channel based on the accuracy level in the estimation of OFF periods (*Rem_T*$^i$).
- ***Criterion 2:*** This criterion takes into account the characteristics of the secondary service requesting a channel (in terms of MHT). It tries to choose a channel whose remaining time fits with the MHT of the service. In this way, it intends to prevent that some secondary services use those channels that might be more suitable for other services. It is formulated as:

$$i^*_{Crit_2} = \arg\min_i \left| \beta_i \times \mathrm{Re}\,m\_T^i - MHT_m \right| \quad (27)$$

  Like in the previous case, $\beta_i$ is a compensation factor.

- ***Criterion 3 (Combined Spectrum Selection strategy):*** A suitable spectrum selection criterion depends on a number of aspects such as composition and characteristic of primary users, level of dependence exhibited by primary traffic, secondary service mix, etc. Based on these considerations, and in accordance with a previous analysis of results, the third strategy targets a more efficient exploitation of the spectrum opportunities trying to combine the benefits of previous criteria 1 and 2 based on the existing traffic mix of each service.

  The procedure is detailed in Algorithm 2. The inputs are, on the one hand, the statistical characterisation of the different channels in terms of $E(OFF_i / ON_i \in B_i^a)$ and the dependence level *DEP*$_i$. It is assumed for the sake of simplicity that all channels have the

same dependence level ( $DEP_i = DEP, \forall i \in C$ ). While both these statistics will be obtained from the REM, the algorithm uses, on the other hand, as input the secondary traffic load levels of the different services as well as their characterizations in terms of MHT. For simplicity, the algorithm is detailed only for the case with two different secondary service types.

As detailed by the pseudo-code of Algorithm 2, it is assumed that secondary service types are served in the increasing order of their indices (loop in line 3). For the service at hand (the *m*-th one), the remaining OFF period of each available channel i∈*av_List* (*Rem_T*$^i$) is first estimated by subtracting the so-far observed availability time (*Idle_C*$^i$) from the expected OFF period given the last observed ON period (line 5). Once all *Rem_T*$^i$ are estimated, the list of potential channels for assignments for *serv*$_m$ (*Candidates*) is built differently depending on the dependence level provided by the REM. Specifically, if *DEP* is below a given threshold *DEP*$_{thr}$, the list of candidate channels for assignments to the service type at hand (*serv*$_m$) is built using *Crit*$_1$ (i.e. picking channels that maximize *Rem_T*$^i$) (line 8). Otherwise, *Candidates* is constructed using *Crit*$_2$ (i.e. by channels that best fit *MHT*$_m$) (line10). The threshold *DEP*$_{thr}$ for deciding about the significance of the dependency level at hand is a function (denoted as g) of traffic loads of both service types to capture the fact that the convenience of one or other criterion depends on the specific traffic loads (the motivation for this choice will be illustrated in the results section). Finally, in the very specific case of multiple channels in Candidates, the channel with lowest DC is selected for the service request at hand (line 12).

Algorithm 2: Combined Spectrum Selection Strategy

**1:** $\left\{\mathrm{Re}\, m\_T^i\right\}_{1\le i\le |C|} \leftarrow 0;$

**2:** $candidates \leftarrow \varnothing;$

**3: for** *m*=1 to *2* **do**

**4:** **for** *i*=1 to $|av\_list|$ **do**

**5:** $\mathrm{Re}\, m\_T^i \leftarrow E(OFF_i / ON_i \in B_i^a) - Idle\_C^i;$

**6:** **end for**

**7:** **if** $(DEP < DEP_{thr} = g(\lambda_{s,1} \times MHT_1, \lambda_{s,2} \times MHT_2)$ **then**

**8:** $Candidates \leftarrow \left\{ i \in av\_list / i = i^*_{Crit_1} \right\};$

**9:** **else**

**10:** $Candidates \leftarrow \left\{ i \in av\_list / i = i^*_{Crit_2} \right\};$

**11:** **end if**

**12:** $i^*_{m,\,Crit_3} \leftarrow \arg \min_{j \in Candidates} \left(DC_j\right);$

**13:** **end for**

As for the execution of these strategies, it is assumed that the CR network operates in a centralized way, so that decisions are made by the RRM entity through interactions with the REM Manager entity considered in the FARAMIR architecture [3]. In that respect, the strategy does not need explicit data dissemination mechanisms to provide the REM information to the terminals since

only the resulting RRM allocation decisions need to be delivered. This can be done through the available control channels in the CR system, whose development is out of the scope of this work.

### 4.3.3. Evaluation methodology

The performance evaluation of the different spectrum selection techniques will be performed through system-level simulations using a controllable primary user activity pattern.

In order to account for heterogeneous spectrum opportunities, *K* primary-users using different sub-sets of channels are considered in the simulations. Specifically, $\forall k \in \{1..\mathrm{K}\}$ $C_k$ denotes the set of channels used by the *k-th* PU so that $\bigcup_{k=1}^{K} C_k = C$. Primary traffic is modelled through $\lambda_{p,k}$ and $\mu_{p,k}$ that respectively denote the primary arrival and departure rates of the *k-th* PU operating on all channels $\mathrm{i} \in \mathrm{C}_k$.

As for secondary operation, the *m-th* service type will be denoted by $serv_m$ $\forall m \in \{1..\mathrm{M}\}$. In order to vary secondary traffic loads, the mean holding time of each $serv_m$ ($MHT_m$) will be kept constant while varying the corresponding arrival rate (denoted as $\lambda_{s,m}$).

Considering a periodic sensing every $\triangle T$ seconds, a perfect sensing (free of miss-detections and false alarms) is assumed for the sake of simplicity. In case a PU shows up in any of the opportunistically-accessed channels, the involved SU will be handed-over to another channel if there is any, or will be dropped if there is no channel available.

It is assumed that the statistics stored in the REM have been previously obtained from measurements obtained during a given acquisition time ($acq_{time}$). Correspondingly, the accuracy of these statistics will be related to this time.

For simulation purposes, a controllable primary traffic time series is introduced for each channel i. At a given time index j, the OFF period duration is generated based on the preceding ON period duration $ON_i(j)$ as follows:

$$OFF_i(j) = p \times f(ON_i(j)) + (1-p) \times unif([OFF_i^{\min}, OFF_i^{\max}]) \tag{28}$$

where 0≤p≤1 is a probability that controls how dependent successive ON/OFF periods are, unif[a,b] denotes a uniformly distributed random variable in the range *[a,b]* and the function *f* is defined as:

$$f(x) = OFF_i^{\min} + \frac{(x - ON_i^{\min}) \times (OFF_i^{\max} - OFF_i^{\min})}{(ON_i^{\max} - ON_i^{\min})} \tag{29}$$

With these definitions, it can be shown that $p = DEP_i$.

The main considered Key Performance Indicator (KPI) to illustrate the algorithm performance will be the rate of Spectrum HO procedures, which is an indication of the optimization target pursued by the problem.

As a reference for comparison in which no REM information is used, a selection criterion consisting in a random selection among the idle channels will be performed. It will be denoted as *RandSS*.

Note that this could be a reasonable criterion in case that there would not be a REM supporting the cognitive system and providing knowledge about primary users.

### 4.3.4. Results

This section presents the evaluation of the different techniques. First, the sensitivity of the proposed multi-service spectrum selection criteria to the accuracy level of REM's statistics will be evaluated. Then, a comparative study between performances of the different criteria will be conducted for several primary traffic patterns and different secondary configurations.

#### 4.3.4.1. Impact of accuracy of REM statistics on Spectrum Selection Performance

The sensitivity of the proposed criteria to the reliability of REM data is evaluated by considering the impact of the acquisition time (*acq_time*) used to measure the different activity/inactivity periods and to obtain the different statistics. Clearly, a long value of *acq_time* will be associated with a better accuracy in the REM data. Without lack of generality, the conducted analysis particularly focuses on $Crit_1$ performance in the case of fully-dependent ON/OFF periods ($DEP_i=1$). Furthermore, it is assumed that the distribution of OFF periods follows an exponential distribution with average value $1/\lambda$=60s, just to consider a large variability in the distribution enabling to evaluate the system robustness under relatively bad convergence performances.

Table 13 presents the accuracy in the estimation of the statistic $E(OFF_i / ON_i \in B_i^a)$ in one channel for different values of the acquisition time. The buckets for this statistic are built with $\alpha$=0.1 (i.e. bucket size is $\alpha/\lambda$=6s) and with a total of 31 buckets (see section 4.3.2.1). The accuracy is measured as the error in the obtained statistic with respect to the theoretical value. The same table also indicates, the percentage of buckets that have been observed at least once (i.e. there is at least one sample of the duration of the OFF period that falls within the bucket) during acquisition time. It can be observed how with an acquisition time of 1h only a reduced number of buckets have been observed, and the error in the estimation is quite high. This error reduces as the acquisition time increases.

Table 13: Accuracy in the statistics stored in REM.

| Acquisition Time | Error (%) in the estimation of $E(OFF_i / ON_i \in B_i^a)$ | Percentage of buckets measured (%) |
|---|---|---|
| 1h | 10.06 % | 41.9% |
| 3h | 4.01% | 80.6% |
| 15h | 1.45% | 100% |

In order to see the impact of these accuracy errors over the system performance, Figure 35 plots the resulting spectrum HO rate for different values of $acq_{time}$ and different values of the duty cycle DC. A single secondary service with MHT=60s is considered, and there are 12 channels with an average OFF period of 60s and 4 channels with an average OFF period of 15s. It can be observed in Figure 35 that performances corresponding to $acq_{time}$=3h are almost the same than performances obtained with $acq_{time}$=15h and are also quite similar to those obtained with $acq_{time}$=1h. This reflects

that stable performance results can be achieved even with moderate accuracy levels of $E(OFF_i / ON_i \in B_i^a)$ in the order of 4%. This robustness of the algorithm is justified by the fact that the channel selected by the algorithm is based on the comparison between the estimated OFF period durations for the different channels. Then, even if this estimation contains some moderate errors (as it is the case of the estimation with $acq_{time}$=3h), these errors are not meaningful enough to make the algorithm select a different channel than in the case with the longest $acq_{time}$.

Further examples about the performance of the algorithm depending on the accuracy of the REM measurements can be found in [38]. In this paper, different distributions of the inactivity periods (e.g. uniform and exponential) as well as different dependency levels have been analyzed, reaching similar conclusions as the ones presented in this deliverable.

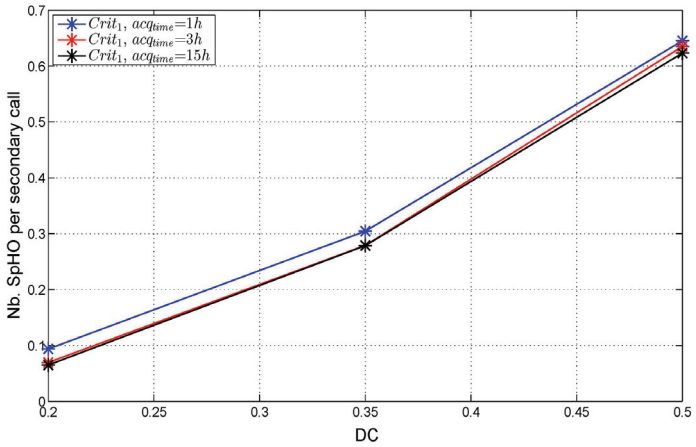


Figure 35: Performance sensitivity to accuracy levels of $E(OFF_i / ON_i \in B_i^a)$

### 4.3.4.2. Comparative Study of Spectrum Selection Criteria Performances

This section aims at getting an insight into the relevance of the proposed spectrum selection criteria as far as multi-service secondary spectrum selection is concerned. The parameters of the case study are described in Table 14. Performances of the proposed criteria will be evaluated for different primary traffic patterns and different secondary service traffic mixes (in terms of the offered load computed as $L_m=\lambda_m \cdot MHT_m$ for service m). The compensation factor $\beta_i$ used by the different criteria is set to $\beta_i$ =0.95, as it has been obtained through previous simulations not shown here for the sake of brevity [39].

Table 14: Simulation parameters of the considered case study.

| | Parameter | Definition | value |
|---|---|---|---|
| **PU parameters** | C | Set of primary channels | {1-16} |
| | K | Number of PUs | 2 |
| | $C_1$ | Set of channels of the 1st PU | {1-4} |
| | $C_2$ | Set of channels of the 2nd PU | {5-16} |
| | $\frac{1}{\lambda_{p,1}}$ | Average OFF period of the 1st PU | 15s |
| | $\frac{1}{\lambda_{p,2}}$ | Average OFF period of the 2nd PU | 60s |
| | $\{DC_k\}_{k\in\{1..2\}} = DC$ | Duty cycle | 0.2 |

| | | | |
|---|---|---|---|
| **SU parameters** | M | Number of secondary service types | 2 |
| | $MHT_1$ | Mean holding time of $serv_1$ | 15s |
| | $MHT_2$ | Mean holding time of $serv_2$ | 60s |
| | $\triangle T$ | Sensing period | 0.1s |

Figure 36 plots performances in terms of SpHO rate for the different criteria as a function of the dependency value *p* for a given set of secondary traffic mixes. For a better visualisation, the figure is split in Figure 36(a) for the extreme traffic loads (i.e. either low load or high load) and Figure 36(b) for the intermediate traffic loads.

Performances of the reference strategy *RandSS* not making use of the REM are given separately in Table 15 for the considered traffic loads since performance is independent of *p*. The first observation is that for all considered traffic loads, the gains that all considered criteria are introducing with respect to the reference scheme are very significant. For the case with independent ON/OFF periods (i.e. *p*=0) the gain (i.e. reduction in terms of SpHO rates) achieved by the proposed strategies using REM ranges from 70% for the high load case up to 98% for the low load case. Furthermore, as *p* increases, the accuracy of $E(OFF_i / ON_i \in B_i^a)$ in estimating the remaining OFF periods duration gets improved and gains rise up to around 100% in some cases.

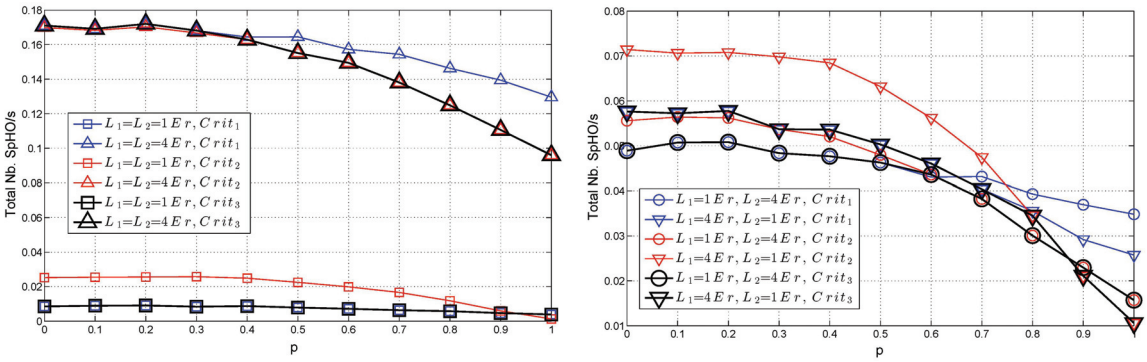


(a) Extreme traffic loads (b) Intermediate traffic loads

Figure 36 : Performance evaluation of the considered spectrum selection criteria.

Table 15: Spectrum selection performances for the reference criterion not using REM.

| | Offered load Service 1 (Erlang) | Offered load Service 2 (Erlang) | Total rate of SpHO/s |
|---|---|---|---|
| Extreme traffic loads | 1 | 1 | 0.66 |
| | 4 | 4 | 0.63 |
| Intermediate traffic loads | 1 | 4 | 1.05 |
| | 4 | 1 | 0.51 |

The analysis of the results in Figure 36 focuses first on the comparison between $Crit_1$ and $Crit_2$ performances. The reasoning is dependent on the secondary traffic load as follows:

- Low traffic loads ($L_1$=$L_2$=*1Er*): Results show that for low traffic loads of both service types (see Figure 36(a)), $Crit_1$ is outperforming $Crit_2$ regardless of the dependence level at hand (p). This is due to that fact that, at such low load conditions, there are often some available channels whose remaining OFF period lengths (*Rem_T*) are longer that the MHT of the

secondary request at hand. The assignment of the largest estimated $Rem\_T^i$ (i.e. $Crit_1$) basically picks the channel with the largest availability among these channels and correspondingly no subsequent SpHO will be experienced. On the contrary, assigning a channel whose $Rem\_T^i$ tightly fits MHT (i.e. $Crit_2$) can result in more SpHOs if the reliability of OFF period estimation in not perfect. Specifically, for low dependence levels (small p), $E(OFF_i / ON_i \in B_i^a)$ is just providing a rough estimation of actual OFF periods. This means that $Crit_2$ can assign $serv_1$ requests to channels whose remaining OFF period ($Rem\_T^i$) was over-estimated and was wrongly supposed to tightly fit $MHT_1$. This increases the number of unnecessary SpHOs compared to $Crit_1$. As the dependence level (p) increases, the estimation reliability is improved, the number of unnecessary SpHOs performed by $Crit_2$ is reduced, and performances of $Crit_1$ and $Crit_2$ get closer.

- High traffic loads ($L_1$=$L_2$=*4Er*): When high traffic loads are considered for both services, (Figure 36(a)), it is observed that $Crit_2$ outperforms $Crit_1$ for all dependency levels (p). At such high traffic loads, it is less likely to find a channel whose remaining OFF period can fit MHT, which makes inevitable the assignment of secondary requests to channels to be switched-off. This means that possible wrong assignments that may be performed by $Crit_2$ due to estimation inaccuracy are not likely to result in unnecessary SpHOs. Nevertheless, the assignment performed by $Crit_2$ tends to assign $C_1$ channels to $serv_1$ and $C_2$ channels to $serv_2$, which results in a better assignment since the channels with the longest OFF period duration are mainly assigned to the service with the longest MHT.
- Intermediate traffic loads ($L_1$=*1Er,* $L_2$=*4Er)* and ( $L_1$=*4 Er,* $L_2$=*1Er*): For intermediate traffic loads and mixes (Figure 36(b)), it is observed that relative performances of $Crit_1$ and $Crit_2$ strongly depend on the value of the dependency level *p*. Specifically, for low values of *p*, $Crit_1$ is performing better while $Crit_2$ is preferable for high dependency levels. This means that there is a threshold at which relative performances are reversed, and this threshold is dependent on the traffic loads. Considering for instance $L_1$=*1Er,* $L_2$=*4Er*, $Crit_1$ is better up to *p*=0.8, while for larger values, $Crit_2$ becomes better.

With respect to the performance of the combined strategy $Crit_3$, it is also presented in Figure 36. Note that the previous discussion to compare $Crit_1$ and $Crit_2$ has led to the conclusion that, depending on the traffic mix, there exists a different value of p for which $Crit_2$ starts to outperform $Crit_1$. This justifies that the dependency threshold $DEP_{thr}$ =g() used by Algorithm 2 in the combined spectrum selection criterion, needs to be set based on the existing traffic mix. In the results presented here, it has been fit based on previous simulations using a polynomial regression model with an overall Root Mean Squared Error (RMSE) of 0.1. With this setting, it can be observed in Figure 36 that the combined strategy efficiently switches between $Crit_1$ and $Crit_2$ for a given secondary traffic mix and the dependence level at hand. As a result, it achieves approximately the best performance among $Crit_1$ and $Crit_2$ for every dependence level.

### 4.3.5. Conclusions

This work has focused on the spectrum selection in to improve CR's operation in a scenario where PUs and SUs coexist without coordination, targeting the reduction of the spectrum handover rate. The following conclusions have been obtained:

- This work has proposed the usage of advanced statistics associated to the temporal activity of PUs that are stored in the REM. Specifically, statistical patterns that capture

among others hidden dependence structures potentially exhibited by primary ON/OFF periods have been formulated and developed. In order to benchmark the utility of such knowledge in a REM, three spectrum selection criteria exploiting differently the formulated patterns have been proposed in a multi- secondary service context. Performance evaluation has shown that, in case a REM supporting the cognitive system and providing knowledge about primary users is available, the proposed criteria can introduce significant gains (in terms of reduction in the rate of spectrum handovers) ranging from 70% to 100% with respect to a reference criterion not making use of the REM.

- The proposed criteria have been evaluated for different accuracy levels of the statistics retained in the REM. Results have shown substantial robustness in terms of performance even if the level of accuracy of the stored statistics is only medium (i.e. in the order of 4%).
- It has been identified that the suitable spectrum selection criterion depends on a number of aspects such as composition and characteristic of primary users, level of dependence exhibited by primary traffic, secondary service mix, etc. In that respect, among the considered selection techniques making use of REM information, the combined strategy that includes in the selection process considerations about the existing secondary user traffic mix provides the best performance. This strategy is able to smartly switch between a selection that purely chooses the channel with the longest availability and a selection that tries to fit the remaining availability time in a channel to the secondary service duration.

## 4.4. Using Geolocation Information for DSA

Dynamic Spectrum Access (DSA) to cellular spectrum is normally avoided, especially because operators would not accept to share their spectrum with their competitors. In addition, spectrum opportunities in this case are more difficult to detect and exploit due to their fast dynamics. However, a more efficient spectrum use is also needed in this block of spectrum and DSA is one way to increase spectrum efficiency. Such approach can be possible in the future especially if spectrum regulation policies become more flexible allowing new spectrum sharing concepts, such as DIMSUMnet [40], to be implemented especially if (1) primary and secondary operators do not provide the same service, (2) the price paid for these spectrum bands by the primary operator is lower than the price of other bands, and (3) a conservative approach towards protecting primary users is adopted by secondary networks. Machine to Machine (M2M) communication and monitoring networks are possible candidates of such secondary networks. Another requirement for such approach to become operational is the presence of a database such as the REM where the needed information for secondary network, such as power bounds, propagation models, primary constraints and locations of base stations. can be found.

### 4.4.1. Summary of the optimization problem

The detection of spectrum opportunities in licensed spectrum of cellular networks is more challenging than in TV white space due to the fast dynamics of the former, namely the requirement for pervasive coverage, the presence of different services with different quality constraints, dynamic traffic patterns, the presence of several neighboring primary transmitters and adaptive primary transmit powers. The first two problems can be normally dealt with by defining suitable interference constraints such as in [19]. The dynamics of primary traffic are taken into account by using fast and cooperative sensing techniques [41]. The problems of multiple transmitters and dynamic transmit power are starting to attract researchers and several

approaches have been presented in the last few years [20][42][43]. These proposals consider either the most difficult case where no information about the power and the location of primary base stations is known [42][43] or the simple case where both location and transmit power are known [20] by the CR or the secondary user. In some countries the locations of cellular base stations can be available for public based on regulatory demand [44]. However, transmit power can change very fast, especially if fast power control or fast scheduling is applied. Therefore, a reasonable assumption in the case of primary cellular network is to consider that the CR knows the positions of primary base stations through a local or regional database as it is suggested by the FCC [45] without knowing their transmit powers. Therefore, we study the possibility of employing a Maximum Likelihood Estimator (MLE) to detect the activity of primary base stations and exploit this information to determine the power with which a cognitive node can transmit knowing its own position and the positions of primary base stations.

In order to explain the proposed approach we consider *M* cognitive radio clusters (C-Clusters) deployed in the coverage area of a cellular network as shown in Figure 37. Each C-Cluster *c* is a set $S_c$ of cooperative Cognitive Nodes (C-Ns) that act also as spectrum monitoring sensors. The locations of the C-Ns follow a probability distribution $f_L$. The primary network involves *N* base stations (P-BSs) that can be either active or idle in a given channel. The activities of these base stations are supposed to be unknown to the C-Ns. In particular, the transmit power $P_l$ of an active primary transmitter *l* is not known. This is realistic assumption since base station activities in cellular networks can have very high dynamics. Therefore, unacceptable signaling traffic will be generated if the activity information is to be sent to the C-Ns in real time.

Without loss of generality, we consider only one channel used by the primary network in our analysis. In the following we denote by Φ the set of all primary base stations and by $\Phi_a$ the set of primary active base stations using the channel of interest. The objective of our proposed DSA approach is to determine the power with which a C-N can transmit, while respecting primary constraints, based on the measured power on the channel of interest and its location. For clarity, we use the following notations: $j \in \{1,2,\cdots,\sum_1^M |S_c|\}$ to denote a cognitive node, and $l \in \{\sum_1^M |S_c| + 1, \sum_1^M |S_c| + 2, \cdots, \sum_1^M |S_c| + N\}$ to denote a primary base station, where $|S_c|$ is the cardinality of set $S_c$. Moreover, index *i* denoting a receiver in a primary cell has the same range of index *l*. In addition, spectrum monitoring sensors are referred to as sensors in the following.

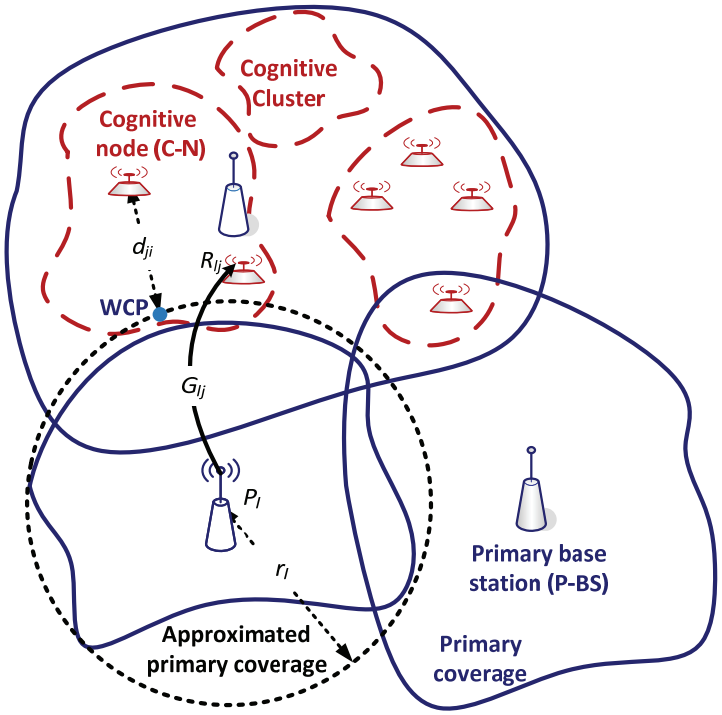


Figure 37: Primary and secondary networks.

As in all cellular networks, a transmitter can be either idle or active with power ranging from $P_{min}$ to $P_{max}$. These bounds are known by the cognitive network since this information is specific for the used technology and defined by standardization bodies. The same restriction is applied on the C-Ns that should transmit using power higher than $P_{th}$ due to hardware constraints. If the computed allowed power is less than $P_{th}$, the C-N cannot transmit at all [7].

The objective of the secondary node is to compute the allowed power with which it can transmit while satisfying primary constraint. In our study we assume that the primary constraint is a limit on the interference probability experienced by any primary receiver $i$ [20][43]. This constraint is defined by

$$\mathbb{P}\{I_i > \iota_{max}\} \leq \varepsilon \tag{30}$$

where $I_i$ is the experienced interference by receiver $i$ due to secondary activity, $\iota_{max}$ is the interference threshold and $\varepsilon$ is the interference probability threshold, defined by the primary network. We also assume that all C-Ns have access to a central database that distributes the frequency bands, and thus only one C-N can transmit at a given channel and time. Although this type of allocation is rather difficult to implement in operational systems, the determination of the transmit power in a multiple secondary transmitter context is still an open problem and several methods are proposed to solve it [15][46]. Hence, we do not consider this problem here, but the model can be easily extended to the general case. By considering this assumption, $I_i$ becomes the result of the transmission of one C-N and can be computed as

$$I_i = P_j G_{ji} \tag{31}$$

where $P_j$ is the secondary transmit power and $G_{ji}$ is the path gain between nodes $i$ and $j$ given by

$$G_{ji} = \frac{k_{sp}}{d_{ji}^{\alpha_{sp}}} \xi_{ji} \tag{32}$$

where $d_{ji}$ is the distance separating the two nodes, $k_{sp}$ and $\alpha_{sp}$ are propagation constants that depend on the type of the nodes, and $\xi_{ji} \sim \ln\mathcal{N}(0, \sigma_{sp}^2)$ is a log-normally distributed random variable representing the shadowing effect.

From (30), (31) and (32), $P_j$ can be written as

$$P_j = \frac{\iota_{\max} d_{ji}^{\alpha_{sp}}}{k_{sp}} e^{\sqrt{2}\sigma_{sp}\mathrm{erf}^{-1}(2\varepsilon-1)} \tag{33}$$

Therefore the computation of $P_j$ requires the knowledge of the distance between the C-N and the closest active primary receiver or at least a lower bound on this distance. If the primary network is active in uplink, $d_{ji}$ can be computed accurately since the position of the receiver (i.e., base station) is known. If the primary network is active in downlink however, only the lower bound of the distance can be estimated since the position of the receiver (i.e., terminal) cannot be known accurately. Hence, we assume that the coverage area of the primary network is known and it is approximated by the disc with radius $r_i$ encompassing the real one (see Figure 37). In this case, the lower bound is computed as the distance between the transmitting C-N and the closest point inside the disc. Here two cases appear: if the C-N is inside the coverage area, the lower bound becomes 0 since the primary receiver can be at any location inside the coverage area. If the C-N is outside the coverage area, the lower bound is the distance between the C-N and the closest point or worst case position (WCP) at the borders of the covering disc [20]. To detect the closest active receiver, the closest active primary cell (i.e., where a base station or a terminal is transmitting) has to be detected first. The main problem in detecting this cell is the presence of multiple simultaneous primary transmitters. In the following, we consider the downlink case and the model can be easily extended to the uplink case. In this case, each sensor $j$ receives power $R_j$, which is the aggregation of the signals received from the active primary base stations

$$\begin{aligned} R_j &= \sum_{l\in\Phi} R_{lj} \\ &= \sum_{l\in\Phi} P_l G_{lj} \end{aligned} \tag{34}$$

where $P_l \in \{0\} \cup [P_{\min}, P_{\max}]$ is the primary transmit power and $G_{lj}$ is the path gain between P-BS l and C-N $j$

$$G_{lj} = \frac{k_{ps}}{d_{lj}^{\alpha_{ps}}} \xi_{lj} \tag{35}$$

One of the difficulties to detect the active P-BSs based on the received power is the presence of the shadowing factor $\xi_{lj} \sim \ln\mathcal{N}(0, \sigma_{ps}^2)$ between P-BSs and C-Ns. In the next section we show how we can detect these base stations using a Maximum Likelihood Estimator (MLE).

### 4.4.2. Optimization techniques

To detect their closest active cells, all C-Ns in each set $S_c$ exchange the measured received signals or send them to a central unit. The probabilistic description of $R_j$ when multiple primary transmitters are active, i.e. $P_l$ is non-zero for multiple values of $l$, has been studied in [42]. In particular, it was shown that the distribution of $R_j$ can be approximated by the log-normal

distribution $\ln\mathcal{N}(\mu_j, \beta_j)$ where $\mu_j$ and $\beta_j$ are defined in [7] as a function of $P_l$, $d_{lj}$, $\sigma_{ps}$, $\alpha_{ps}$ and $k_{ps}$. The log-likelihood computed by cluster $S_c$ from measurements $R_j$ is defined by

$$\ln \mathcal{L}(\mathbf{P}|\mathbf{R}) = \sum_{j \in S_c} \ln \left[ \frac{1}{R_j \sqrt{2\pi\beta_j}} e^{-\frac{\left(\ln R_j - \mu_j\right)}{2\beta_j}} \right] \quad (36)$$

where **P** and **R** are the vectors of the transmit power by the primary base stations and the received powers by the sensors in the cluster $S_c$. Since $\mu_j$ and $\beta_j$ depends on vector **P**, the latter can be estimated using MLE as follows

$$\widehat{\mathbf{P}} = \arg_{\mathbf{P}} \max \ln \mathcal{L}(\mathbf{P}|\mathbf{R}) \quad (37)$$

Finding $\widehat{\mathbf{P}}$ yields a non-convex optimization problem which is difficult to handle analytically, especially for large number of P-BSs. There exist multiple ways to approach this problem numerically. In this work, we apply a numerical approach based on simulated annealing to solve the arising maximum likelihood estimation problem. In [42], simulations were performed based on the simulated annealing technique and the performance of the estimator was investigated as function of various channel parameters (e.g., fading statistics, path loss parameter) and the number of sensors. It was shown that under realistic assumptions for the channel, the sources and the sensors the algorithm succeeds to estimate the transmitters' activity.

In this work, we are interested only in knowing if the P-BS is active or not (i.e. determining set $\Phi_a$) and not in determining $P_l$, which facilitates the decision and reduces the error in the estimation of the closest active P-BS. When set $\Phi_a$ is determined, each C-N determines its closest cell from this set and determines its allowed power based on (33). If the allowed power is higher than $P_{th}$, the C-N can transmit. Otherwise it will stay idle or choose another channel.

### 4.4.3. Evaluation methodology

To study the performance of the proposed approach and analyze its limitations, simulations in Matlab were conducted. We evaluate our approach in a system where the primary network is a cellular network consisting of only macrocells served by base stations at a height of 27m. These P-BSs serve mobile terminals (MTs) with antenna height of 1.5 m. The C-Ns are considered to be IEEE 802.11 kind of access points (i.e., modified access points to enable cognitive features) with antenna height of 3 m. In all simulations we consider the downlink of the primary and secondary networks, i.e., the transmitters are the P-BSs and the C-Ns.

We use the Xia-Bertoni propagation model [21]. This model is chosen since it is able to take into account all types of propagation losses such as the one between base stations and the one between mobiles in addition to usual propagation loss between a base station and a mobile. Given a frequency $f$ in GHz and distance $d_{XY}$ between transmitter $X$ and receiver $Y$, path gain $G_{XY}$ is given by $G_{XY}(d_{XY}) = K_{XY} + B_{XY}\log_{10}(f) + \alpha_{XY} \log10\ (d_{XY})$, where $K_{XY}$, $\beta_{XY}$ and $\alpha_{XY}$ are constants computed using the Xia-Bertoni model as depicted in Table 16.

Table 16: Constants of the propagation model.

| | $\alpha$ | $B$ | $K$ | $\sigma$ |
|---|---|---|---|---|
| C-N ↔ P-BS | -37.6 | -21 | -113.2 | [0.69;3.45] |
| C-N ↔ MT | -40 | -30 | -141.7 | 2.3 |

### 4.4.4. Results

The performance of the system is studied in two scenarios: a simple scenario with two cells and a more realistic scenario where the base station locations are taken from real deployment in Los-Angeles.

#### 4.4.4.1. Scenario with two cells

First, we shall study the performance of the proposed algorithm as function of the number of sensors in a simple scenario with two cells of 1 km radius. For this we consider that $P_{max}$ = 27.4 dBm, $P_{min}$ = 17.4 dBm and $P_{th}$ = 20dBm. Therefore if the C-N determines that the primary transmit power is lower than 17.4 dBm, it will identify the corresponding base station as idle. Regarding the standard deviation of the shadowing between the P-BS and C-N, we use $\sigma_{ps}$ = 1.38 (this corresponds to 6 dB) except for the case where the impact of $\sigma_{ps}$ is studied. Simulations are repeated 200 times for each setting in order to compute the marginal distributions. In the simulations we consider the following three scenarios:

- **Scenario 1**: One base station (denoted cell 1) is active while the second is idle (denoted cell 2). The sensors are distributed uniformly inside one cell.
- **Scenario 2**: The two base stations are active. The sensors are distributed uniformly inside one cell.
- **Scenario 3**: The activity pattern is the same as in scenario 1, but the sensors are distributed uniformly inside the two cells.

By considering that the primary transmit power is 24 dBm, we show in Figure 38 the cumulative distribution functions (CDFs) of the estimated power of the primary base stations, for different numbers of sensors and considering the three scenarios. It should be noted that the lines that do not appear in the figure correspond to the cases where the C-Ns are not allowed to transmit. In scenario 1, the figure shows that with 17 sensors or more this base station is detected to be active in more than 90% of the cases. However, this percentage drops to 60% in case only one sensor is in the active cell and to 40% when the sensor is in the idle cell. This shows the importance of cooperative detection and that the proposed method can protect the primary receivers if the number of sensors is large enough. Furthermore, the figure shows that the inactivity of the idle base station (i.e., spectrum opportunity) can be detected with high accuracy when the sensors are in the idle cell. Even in the case of one sensor, a false detection appears in less than 5% of the studied cases. However, when the sensors are in the active cell the false detection increases to 60% in case we have more than 9 sensors and to more than 95% in case we have only one sensor. This shows how many opportunities can be lost due to the position of the sensors. This is normal due to the high shadowing standard deviation. For example, a sensor situated at the common boundary of two equally sized cells, with both primary transmitters utilizing the same transmit powers, would have to estimate whether one or both transmitters are active based on expected difference in average received power of approximately 3 dB. However, given that the typical

standard deviation of the shadowing component is higher than 3 dB, we see that the differences in the activation patterns are easily overshadowed by the contributions from shadowing in terms of likelihoods. This effect can be eliminated by distributing the sensors over the two cells as it shown in the plots corresponding to scenario 3. Moreover the plots corresponding to scenario 2 show that the sensors can detect the activity of the two cells with high probability. However, the level of the power of the non covering cell is significantly reduced due to the high separating distance. In summary, these results show that the positions of the sensors can have more impact than their number.

In Figure 39, we show the CDF of the allowed secondary transmit power in the three scenarios as a function of the number of sensors when the primary power is 24 dBm. The results show that in most of the cases where the C-Ns are close to the idle base stations the secondary transmit power is relatively high.

In Figure 40, we show the distribution of the estimated allowed power for different values of $\sigma_{ps}$ (i.e., the standard deviation of the shadowing factor between P-BS and C-N) in scenario 1 where the primary power is 24 dBm and there are 17 sensors. The figure shows that the estimated power decreases when $\sigma_{ps}$ increases. Moreover, the miss-detection probability that can be estimated from the left-hand figure (i.e., the probability that the power is higher than 20 dBm) increases with the standard deviation, which reduces the protection of the primary network. However, for a standard deviation of 2, which is a typical value for urban zones, the miss-detection probability is less than 0.05.

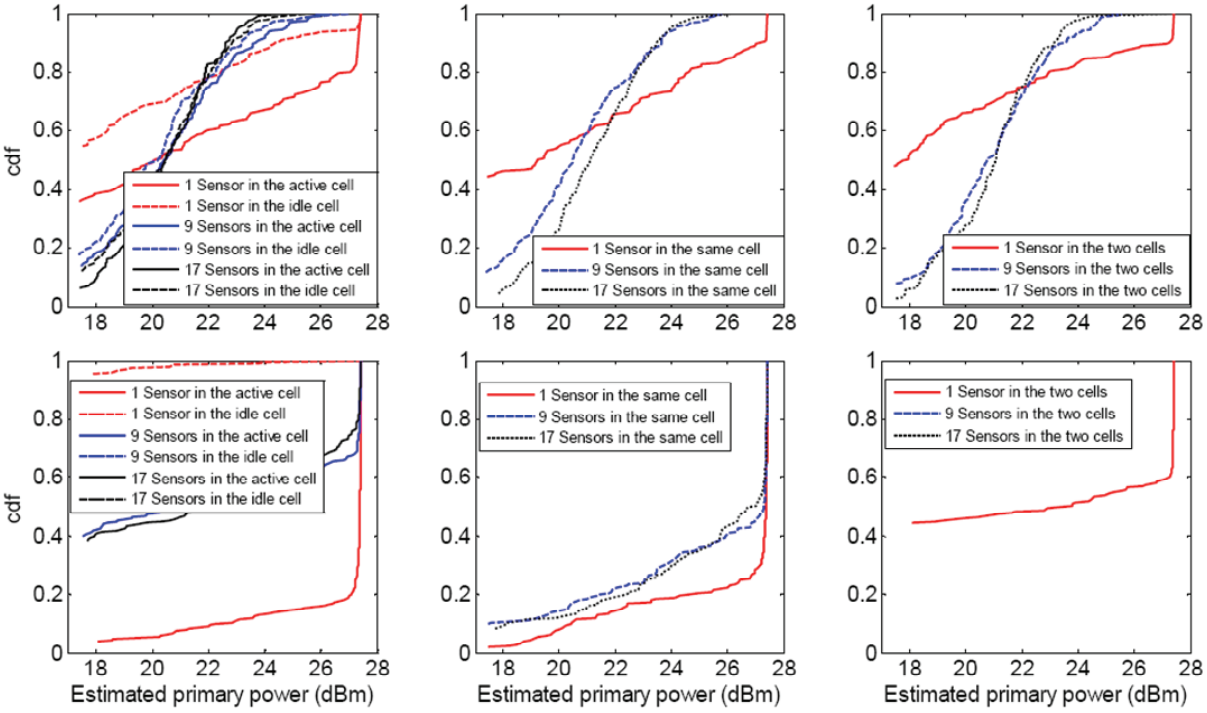


Figure 38: The distribution of the estimated power of primary base stations by secondary network. The first (resp. the second) row reflects the estimated power of cell 1 (resp. cell 2), while the three columns reflect the three simple scenarios. The legend "One sensor in the two cells" in scenario 3 means that the sensor position is uniformly distributed over the two cells [7].

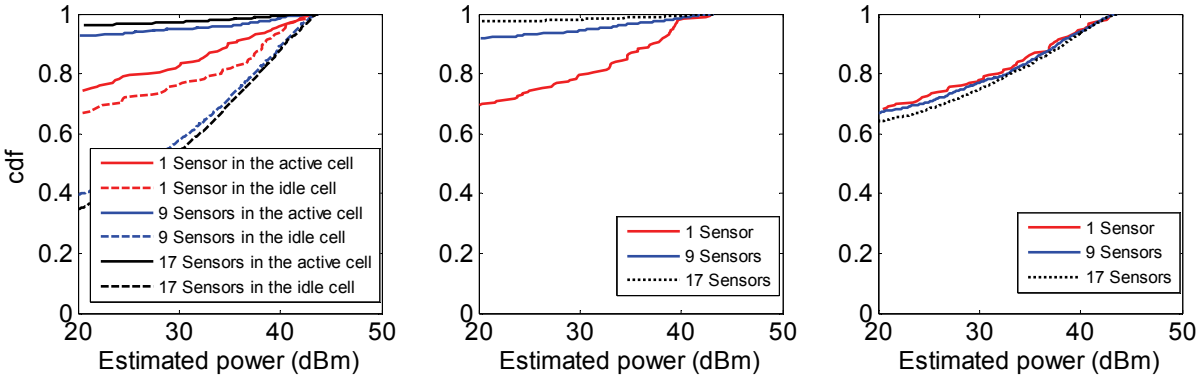


Figure 39: The distribution of the estimated power with which the secondary users can transmit for different numbers of sensors [7].

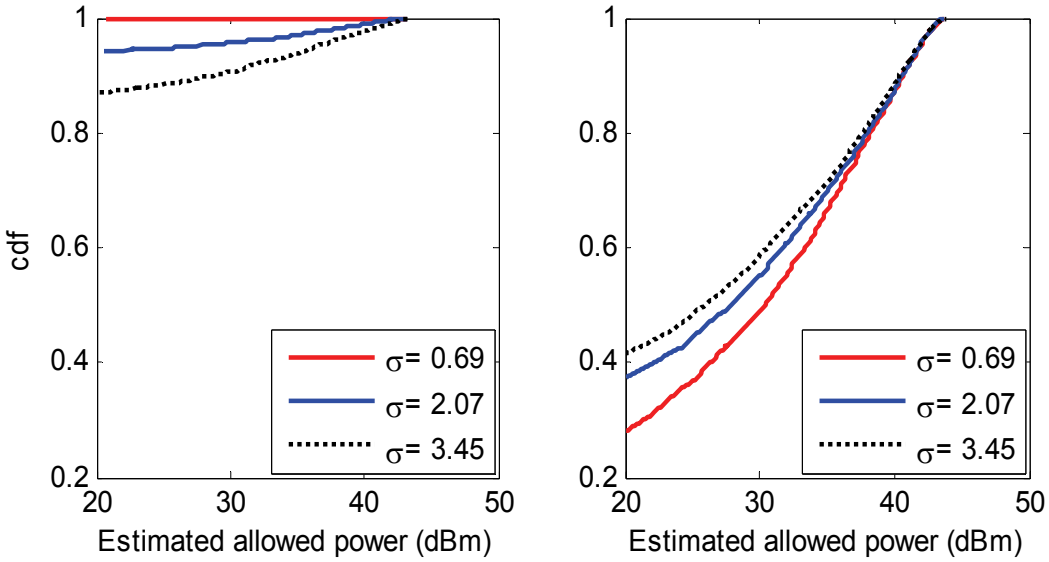


Figure 40: The distribution of the estimated allowed power for different values of $\sigma_{ps}$ in scenario 1 when the sensors are in the active cell (left) and in the idle cell (right) [7].

In order to consider the more general case, we assume now that the C-Ns are distributed inside a cluster that is not centered at the P-BS. Scenario 1 is considered here where the primary power is 24dBm and there are 17 sensors. Figure 41 shows the impact of the position and the size of the cluster on C-N transmit power when the sensors are inside the idle cell. As expected, the power increases as the size of the clusters increases since the sensors are distributed over a larger surface in this case, yielding less correlation in the received signals. Furthermore, the CDF of the power starts at higher values for smaller clusters since the minimum distance separating the C-Ns from the active P-BS is higher than when bigger clusters are used. Moreover, this power increases when the cluster is closer to the idle cell. It can be noted that when the cluster is between the two base stations (i.e., the angle θ is equal to 180°), the secondary opportunities to transmit and the allowed transmit power decrease drastically especially for small clusters (e.g., no transmission is allowed if the cluster radius is less than 0.22 km).

It should be noted that the miss-detection of the active base station does not always yield a harmful interference for primary users since we are considering a protective scheme. In fact, we evaluated the probability of harmful interference by generating one primary receiver in each active cell, where the positions of these receivers are uniformly distributed inside the cell. The results have shown that except from the case of one sensor, the probability of harmful interference was always lower than 0.05.

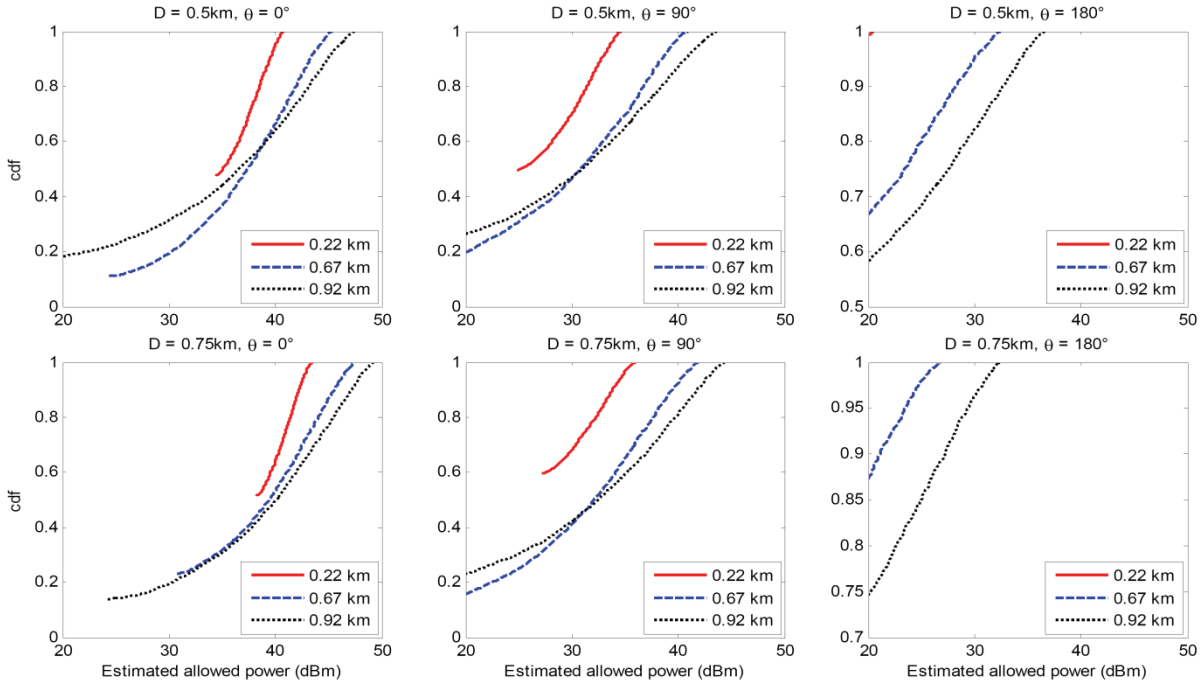


Figure 41: The distribution of the estimated allowed transmit power in scenario 1 for different positions and radii of the S-C (the position and the angle are relative to the idle P-BS and the line joining the two P-BSs) [7].

#### 4.4.4.2. Los Angeles scenario

We shall next study the distribution of the transmit powers for the C-Ns running in a more realistic scenario where the base stations are distributed in a selected area of 400km in Los Angeles city based on the location data from the TMobile network [44]. We consider that three frequency bands are available for the primary network. The distribution of the frequency bands over the base stations is optimized in order to minimize the total received interference in the system, where each base station can be associated to one band. The coverage areas of the base stations are optimized in order to have a full coverage in the studied area. Moreover, we consider that the maximum transmit power of each base station is computed so that users at the border of the coverage area have an SNR higher than 1.5 dB in 95% of the cases. In order to evaluate the proposed method we consider two cells that are using frequency band 1 as shown in Figure 42. These cells have different characteristics in terms of neighboring cells and coverage. Cell 1 has a small coverage area that includes the base stations of other cells, whereas cell 2 has a larger coverage area with no neighboring base stations inside this area. We assume also that the C-Cluster has 17 sensors distributed uniformly inside the cluster. We consider two extreme cases of the cluster radius, specifically 5% and 85% of the radius of the covering cell.

In Figure 43, we show the distribution of the allowed transmit power in frequency band 2 where the two base stations serving the test cells are idle. The algorithm has different behavior in these

two cells when the radius of the cluster changes. The transmit power increases with the increase of the radius in the first cell, whereas it decreases in the second. This is due to the fact that the cluster radius in the second cell becomes very large and the contribution of the other cells becomes more important than the covering cell. Moreover, the estimated power decreases when the center of the cluster is in the middle of the tested cell since the sensor distance to the covering cell becomes higher. It can be noted also that when the radius is 0.38km in cell 1, the C-Ns cannot transmit at all if the center of the cluster is 0.5 km away from the center of cell 1. This is due to the fact that all sensors will be under the coverage of the neighboring coverage cell, which is active in frequency band 2. When the radius of the cluster increases to 1.57 km some C-Ns will be outside this coverage area and are allowed to transmit. We also evaluated the probability of harmful interference in frequency bands 1 and 2 for all cells and it was significantly low due the conservative approach.

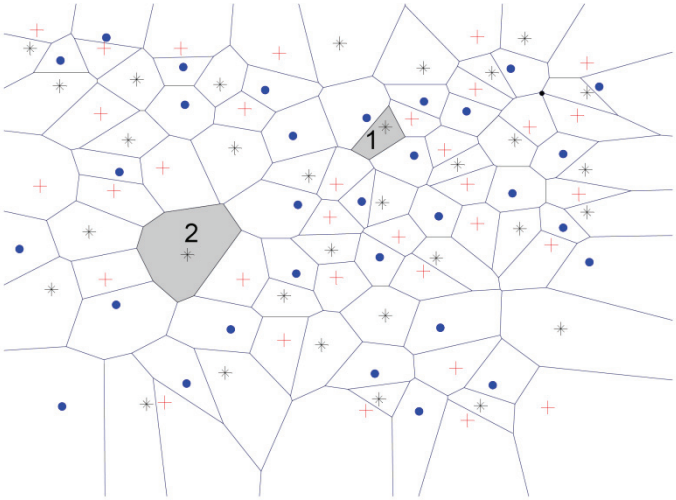


Figure 42: LA scenario where '*', '+' and 'o' refer to cells using frequency bands 1, 2 and 3, respectively. The shaded cells are the cells where the performance of the proposed approach is studied [7].

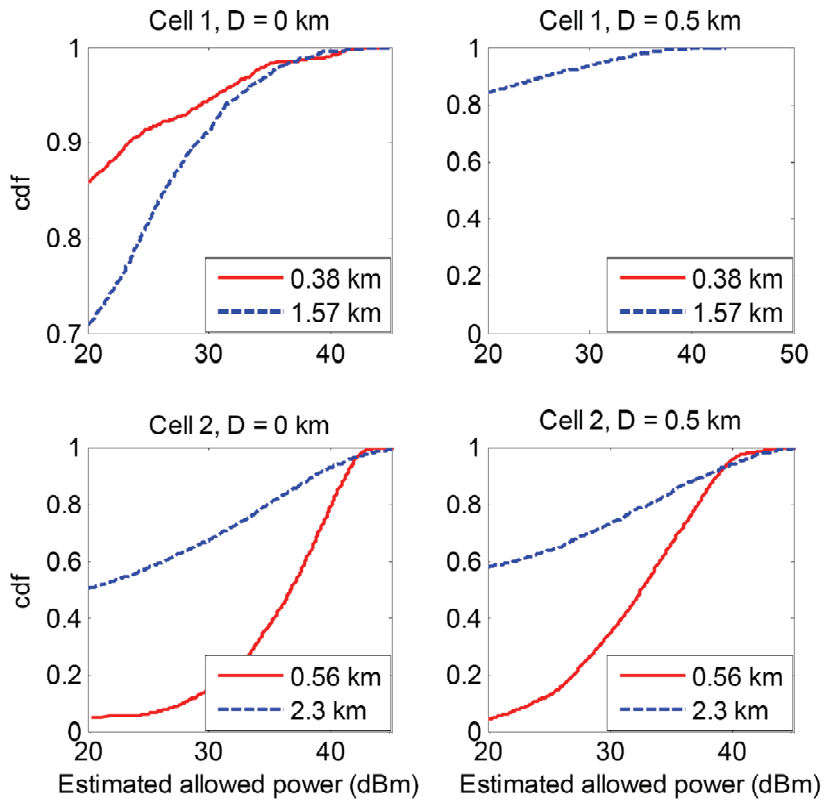


Figure 43: The distribution of the estimated transmit power in the LA scenario when the two base stations are idle for different positions and size of the cluster [7].

### 4.4.5. Conclusions

In this section we have focused on the problem of opportunistic access when the primary network is a cellular network. In order to enable cognitive radio to use cellular frequency bands, we have assumed that the relative positions of primary base stations are known, which is a realistic assumption in some scenarios. This information is used by a maximum likelihood estimator to determine the closest active cell to the cognitive node, which will experience the highest interference due to cognitive node's activity. Then the cognitive node can estimate its allowed transmit power that satisfies primary constraints.

The proposed approach has been evaluated using simulations from which the following conclusions can be drawn:

- IEEE 802.11-like cognitive radio can opportunistically access cellular frequency bands under some constraints and if the cellular network is willing to share its spectrum.
- Even with the assumption of knowing primary base station positions, the detection of spectrum opportunities and the protection of primary users with relatively acceptable probability is only possible under specific constraints. This highlights the fact that without this information, sharing spectrum with cellular networks will be very difficult.
- In order to detect base station activity the sensors should be close to the considered base station. This means that a cluster of sensors should only be interested in detecting the activity of covering cells.

- The position and the distribution of the sensors can be in most cases more important than the number of these sensors. Hence, developing a model that determines the best position distribution of the sensors remains an open problem.

## 4.5. Opportunistic Access Technique using Stochastic Models

As mentioned in Section 4.4, the problem when considering a cellular primary network is the fast dynamics of the primary network and the presence of several primary transmitters. In this case the traditional sensing-based techniques are not any more efficient since (1) these techniques have not been studied with the presence of multiple transmitters and power control and (2) they can be very slow compared to the fast dynamics of the traffic of most cellular networks. To solve the problem of multiple transmitters, some location-based approaches [20][43] were proposed, especially after the adoption of regional database driven techniques by the FCC [45]. Again, these methods will fail to provide good performance in operational networks, especially with primary networks characterized by power control, fast scheduling and short duty cycles, which is unfortunately the case for most cellular networks.

### 4.5.1. Summary of the optimization problem

Due to the limitations of sensing- and location-based techniques, we explore in this section another approach that does not require any sensing or measurement. This will allow secondary networks to overcome the problem of primary fast dynamics and multiple transmitters. Our approach is to exploit the information about primary activity patterns and perform statistical transmission with enough low probability to guarantee primary constraints. Therefore, we use alternating renewal theory [47]-[50] to determine the periods of time where the secondary users can transmit while satisfying statistical primary constraints. Recently, several papers proposed mechanisms based on alternating renewal theory [51][52] to estimate the best channel to transmit or the available time to transmit after detecting a free channel. These methods are based on the sensing-before-transmit concept, which again yields poor performance in case of highly dynamic primary networks. In this section, we develop a general framework based on stochastic opportunistic access with different types of primary constraints without the need for sensing. Then, we study in detail the case where the primary ON/OFF period durations are modeled with exponentially distributed parameters, which is one of the cases encountered in mobile networks [37].

We consider a secondary network that can opportunistically access the licensed spectrum of a primary network under strict constraints guaranteeing the required Quality of Service (QoS) for primary users. Our objective is to find the best secondary activity patterns (i.e., time periods where the secondary node can transmit) over different primary channels leading to the highest possible capacities or lowest transmission delays, while satisfying primary constraints.

The considered primary network comprises *M* base stations using *N* channels. The coverage area of its cells is determined by the region where the required QoS is guaranteed with a specific probability and is usually estimated using planning tools. Each base station has an activity pattern on a given channel that can be different from the activity patterns of other base stations or on other channels. The activity patterns are represented by an alternating renewal process of ON (active) and OFF (idle) periods. The durations of the ON and OFF periods of base station j on channel *k* are assumed to be independent from each other and represented by independent

identically distributed random variables $T_{ON}^{j,k}$ and $T_{OFF}^{j,k}$, respectively. These variables follow general distributions with cumulative distribution functions (CDFs) $F_{j,k}$ and $G_{j,k}$, respectively. This model has been found to be realistic for several legacy systems such as GSM and DECT [37].

In the secondary network side, we consider a network with infrastructure including L stationary nodes (i.e. base stations) and a variable number of mobile terminals associated to the different stationary nodes. We assume that the positions of the secondary base stations with respect to the primary base stations are known, for instance, through regional database as was suggested by the FCC [45]. However, this is not a requirement for the proposed approach that can be also implemented without knowing primary base station locations.

#### 4.5.1.1. Primary constraints

The objective of the proposed approach is to enable secondary users to access licensed spectrum of a legacy cellular network. The latter has normally strict policies on guaranteeing the desired QoS for its users and will not allow any significant degradation of this QoS. Therefore, cellular networks will allow opportunistic access only when they can still control and guarantee such requirements for their users. Hence, several performance metrics can be defined based on the type of network and application. In this study we consider the following metrics without limiting the developed framework that can be extended to take into account other metrics as well:

- $\theta$: Average fraction of time during which a primary transmission is interfered by secondary activity:

$$\theta = \frac{E(T_{\mathrm{ON}}^{j,k} | \text{A secondary is active})}{E(T_{\mathrm{ON}}^{j,k})} \tag{38}$$

  where E($T_{ON}^{j,k}$ ) and E($T_{ON}^{j,k}$|A secondary is active) are the expectation values of the primary ON periods over time for a given cell j and its conditional expectation given that a secondary node is active, respectively. The primary network can be interested that the users in a given cell will only lose data in $\theta \times$ 100% of their transmission time. This is the case for applications that are sensitive to bit error rate such as background download. In this case, the primary network requires that $\theta < \theta_{\mathrm{th}}$ in all cells.

- $\rho$: The ratio between the average number of primary ON periods lost and the average number of the total ON periods. In this case we assume that if an ON period is partially interfered (i.e., only a part of the transmission is interfered) it will be lost, for instance due to the loss of the preamble. Thus, it can be used especially in the case where the ON periods represent whole packets of a user, such as in the case of the uplink of a Wi-Fi network. For this metric the primary network requires that $\rho < \rho_{\mathrm{th}}$.

We define *S* as the set of metrics that the primary operator defines to enable access to its spectrum in an opportunistic way. To estimate these metrics, we consider that a primary receiver *j* is interfered by a secondary node *l* if the latter transmits and the probability that the received interference by *j* due to this transmission is higher than given threshold $\iota_{\mathrm{max}}$ exceeds $\varepsilon$. Formally, we can write this condition as

$$\mathbb{P}\{I_{lj} > \iota_{\mathrm{max}}\} > \varepsilon \tag{39}$$

where $I_{lj}$ is the interference experienced by primary receiver *j* due to the transmission of secondary node *l*. The channels that can be shared by secondary nodes as well as the values of $\iota_{\max}$ and $\varepsilon$ are determined by the primary planning tools [19]. To encourage primary operators to share their spectrum, we assume that any approximation in the computation of the metrics in set S is conservative with respect to primary protection. Therefore, we assume that when a primary is interfered, all data transmitted during the interference time are discarded and considered to be erroneous. Moreover, the coverage area of any base station is considered to be the disc enclosing the real coverage area. By using proper propagation models and shadowing models, this disc can be determined. The same conservative approach is used to determine the coverage area of secondary base stations. In general cellular activity patterns are not stable over time. However, for limited periods of time—in the order of few hours—the activity pattern can be relatively stable. Thus, the primary network can characterize these periods by the most conservative pattern (i.e., the pattern that is the most sensitive to secondary activity).

#### 4.5.1.2. Secondary Transmission Framework

Since no sensing is required in our approach, the secondary node will have a period of transmission ($\bar{T}_{ON}$) followed by a period where it is inactive ($\bar{T}_{OFF}$), where $\bar{T}$ refers to the time of secondary nodes. The sum of these two durations forms the frame of secondary node with duration $\bar{T}$. In general, the frame duration can be either fixed or variable depending on the adopted model. As mentioned before, the objective of the secondary is to maximize its capacity or to minimize the delay by finding the best activity pattern. The capacity can be maximized by maximizing the ratio $\bar{T}_{ON}/\bar{T}$, whereas the delay can be minimized by decreasing the value of $\bar{T}$.

The secondary activity pattern can be determined by either the secondary node or the primary network. In the latter case, the primary will store the allowed computed activity pattern in the REM that can be accesses by the secondary without revealing any information about its activity pattern. This approach is suitable when the primary network is not willing to reveal any information about its activity patterns. In the other case, the primary network has to share its activity patterns that can be stored in the REM. This can be possible in case, for instance, that the secondary is a femtocell network controlled by the same primary operator and where the risks are lower to access the sensitive information of the operator. The activity patterns can be then downloaded by the femtocell to its local REM from the global REM of the macro cells. This mode will allow the secondary node to find better solutions, since in the other mode the pattern is computed in a generic way without taking into account the specific characteristics of each secondary node. In order to enable such type of information exchange we assume that there is a minimum cooperation between primary and secondary networks. This is not only beneficial for secondary networks that will be allowed to use the spectrum but also to primary networks; if the secondary network is owned by the same primary operator (e.g., femtocell case), the operator would be interested in increasing the performance of the whole system, including secondary users. Otherwise, the secondary should pay a price for accessing the primary spectrum, based on the type of required QoS.

Different types of activity patterns can be designed for the secondary network. In general we can divide these patterns into two groups: stochastic and periodic. In stochastic patterns, secondary node *l* will have a policy to be active during a period $\bar{T}_{ON}$ and inactive during a period $\bar{T}_{OFF}$ using channel *k*, which follow specific distributions represented by their CDFs $F_{l,k}$ and $G_{l,k}$. The type of the

distributions and their parameters should be computed using $F_{j,k}$ and $G_{j,k}$ for each possible interfered primary cell *j*. The periodic transmission is a special case of the stochastic transmission, where $\bar{T}_{ON}$ and $\bar{T}_{OFF}$ are constant values. In this study we consider the periodic transmission since (1) it contains less variables and it is easier to find the optimal solutions, and (2) it provides more predictable behavior of the secondary activity. However, it is possible to extend the model presented here to the general case by using the approach developed in [50] for the case of several simultaneous alternating renewal processes.

Secondary transmitters are assumed to be cooperative in terms of scheduling the use of primary channels to guarantee that the primary constraints are preserved; the secondary nodes are only allowed to transmit during the scheduled ON periods. Since the secondary ON and OFF periods on each channel are scheduled on a relatively long time scale (e.g., several minutes or hours), synchronization between the different secondary transmitters is possible. This constraint can be relaxed for distant secondary node clusters, where the interference from one cluster to a given primary receiver is negligible whenever the interference from the other cluster is higher than $\iota_{\max}$.

### 4.5.2. Optimization techniques

The estimation of $\theta$ and $\rho$ can be performed using alternating renewal theory and Laplace-Stieltjes transforms as it is shown in [53]. The ON-OFF periods in wireless communication can follow different types of distributions such as exponential, lognormal, Pareto and Erlang distributions. With the exception of the exponential distribution, it is difficult to derive closed form expressions for $\theta$ and $\rho$. However, numerical evaluation can be done by appropriate extensions of the Cléroux-McConalogue algorithm [54] to evaluate the convolutions. In particular, numerical evaluation of these two metrics have been presented in [49] for Weibull and log-normal distributions.

If *F* and *G* follow exponential distributions with parameters $\lambda$ and $\mu$, we can easily obtain

$$\theta = \frac{\bar{T}_{ON}}{\bar{T}} \tag{40}$$

$$\rho = \frac{\lambda \bar{T}_{ON} + 1}{\lambda \bar{T} + 1} \tag{41}$$

It is interesting to see that $\theta$ is independent of the primary activity and $\rho$ depends only on the distribution of primary ON periods.

The above equations define the relation between the secondary activity pattern and primary performance metrics. For a specific threshold $\theta_{\text{th}}$ of $\theta$, all values of $\bar{T}_{ON}$ and $\bar{T}_{OFF}$ are allowed if they can meet condition (40). This case is suitable especially for real time applications where short delays in transmission are needed since the secondary node can define its transmission periods without any constraints. The maximum achievable $\bar{T}_{ON}/\bar{T}$ is constant and equal to $\theta_{\text{th}}$. However, this is not the case for $\rho$ since the values of the durations should be always positive. Therefore, when considering a threshold $\rho_{\text{th}}$ the secondary transmission period should satisfy the following condition:

$$\bar{T} > \left(\frac{1-\rho_{\text{th}}}{\rho_{\text{th}}}\right)\frac{1}{\lambda} \tag{42}$$

This means that the OFF duration of the secondary node may be much higher than the average duration of the ON periods of the primary. This can be very limiting for the case where the secondary wants to have real time communications such as voice. Moreover, from (41), we can write

$$\frac{\bar{T}_{ON}}{\bar{T}} = \rho_{\text{th}} - \frac{1-\rho_{\text{th}}}{\lambda \bar{T}} \tag{43}$$

which is always lower than the value obtained if the same threshold is used for metric $\theta$. Furthermore, it is an increasing function on $\bar{T}$. Therefore the secondary node should make a tradeoff between increasing its data rate and decreasing delay transmission. An illustrative example of the achievable ratio as a function of $\lambda$ and $\bar{T}$ when $\rho_{\text{th}} = 0.05$ is depicted in Figure 44. In this case if we want to limit $\bar{T}$ to 10ms, the secondary can be active only when $\lambda$ is higher than 10 $\text{ms}^{-1}$, meaning that the average primary ON duration should be lower than 0.1ms.

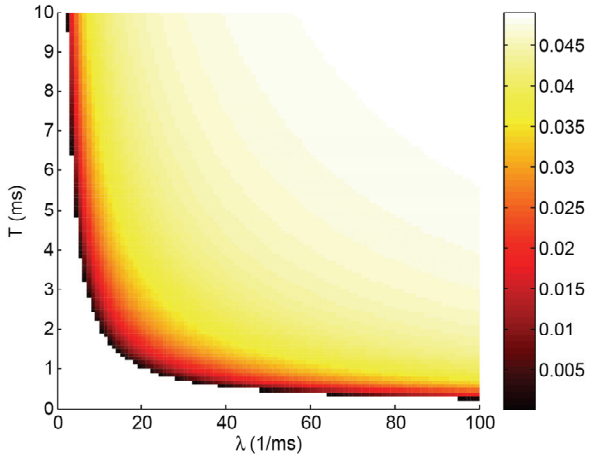


Figure 44: Variation of the ratio $\bar{T}_{ON}/\bar{T}$ as a function of $\lambda$ and $\bar{T}$ when $\rho_{\text{th}} = 0.05$. The white region in the left corner is the zone where the secondary is forbidden to transmit determined using (40) [53].

A primary transmission is interfered by secondary activity if condition (39) is met. Let us consider that the secondary node transmits with fixed power *P* and assume a log-normal distributed shadowing factor with standard deviation $\sigma$. Then, condition (39) can be rewritten as a condition on the distance $d_{sj}$ separating the secondary transmitter s and the primary receiver j: $d_{sj} < d_{\text{th}}$ [20] where

$$d_{\text{th}} = \mathcal{P}_{sj}^{-1}\left[P - \iota_{\text{max}} + \sigma\sqrt{2}\text{erf}^{-1}(1-2\varepsilon)\right] \tag{44}$$

In (44) $\text{erf}^{-1}$ is the inverse of the error function and $\mathcal{P}_{sj}^{-1}$ is the inverse of the distance dependent path loss function.

In order to estimate $d_{sj}$ we need to determine the position of the primary receiver and secondary transmitter. For each transceiver we have two distinct cases. The transceiver can be either a Mobile Terminal (MT) or a Base Station (BS). If it is a BS, then its position is known. Otherwise, the worst case position is considered, which is the closest position to the secondary transmitter (resp. primary receiver) on the circle enclosing the coverage area of the primary (resp. secondary) base station. Hence, we can write

$$d_{sj} = \begin{cases} D_{sj} & \text{if two BSs} \\ \max\{0, D_{sj-}R_s\} & \text{if primary BS and secondary MT} \\ \max\{0, D_{sj-}R_j\} & \text{if primary MT and secondary BS} \\ \max\{0, D_{sj} - R_j - R_s\} & \text{if two MTs} \end{cases} \quad (45)$$

where $R_s$ and $R_j$ are the radii of the circles enclosing the coverage areas of the secondary and primary base stations respectively and $D_j$ is the distance separating the two base stations. Once the distances towards the neighboring cells are computed, condition (44) is verified for all of them. The set of potentially interfered primary cells $\xi$ is then determined as follows:

$$\xi = \{j \in \{1,2,\cdots,M\} | d_{sj} < d_{\text{th}}\} \quad (46)$$

Let us assume that the primary operator wants to have a constraint on $s$ metrics from set $\bar{S} = \{\kappa_i | \kappa_i \in S, i = \{1,2,\cdots,s\}\}$ that can include any of the metrics defined by the primary network. In our approach, the procedure to compute the activity pattern satisfying primary constraints and maximizing $\bar{T}_{ON}/\bar{T}$ is divided into three phases.

The first phase aims at finding the secondary activity pattern corresponding to each potentially interfered cell; for each base station $j$ in set $\xi$, $\bar{T}_{ON}^{(j)}$ and $\bar{T}^{(j)}$ for a given channel $k$ are computed using the alternating renewal theory and the functions $F_{j,k}$ and $G_{j,k}$. The second phase uses the computed values of $\bar{T}_{ON}^{(j)}$ and $\bar{T}^{(j)}$ to reevaluate all metrics $\kappa_i$ for each base station except base station $j$ which was evaluated in the previous phase. The obtained values are denoted $\kappa_i^{(j)}$. In the third phase, the procedure chooses the activity pattern corresponding to cell $j$ determined as follows

$$j = \arg\max_{j \in \xi} \left\{ \frac{\bar{T}_{ON}^{(j)}}{\bar{T}} \middle| \ \kappa_i^{(j)} < \kappa_{i,\text{th}}^{(j)} \ \forall \kappa_i \in \bar{S} \right\} \quad (47)$$

## 4.5.3. Evaluation methodology

In this section we shall evaluate the performance of the proposed technique and compare the results with sensing- and location-based techniques.

We evaluate the three approaches in a simple system of seven hexagonal primary cells, where only the downlink case is considered. Each primary base station is located at the center of the cell and transmitting with a power of 30 dBm in each channel. The primary users of each cell are uniformly distributed inside a disc of radius of 1 km. We consider only one channel in our study and assume that only one primary user can be served on this channel at a given time in each cell. The secondary nodes are considered to be some kind of access points that can be at any place in the network and can transmit with a maximum allowed transmit power of 30 dBm.

We evaluate the different techniques for 100 positions of the secondary nodes distributed in a uniform manner in the zone covering the whole primary system. We assume that the secondary users served by a node are uniformly distributed inside a circle of radius 100m. We also assume that the activities of the primary base stations follow an exponential distribution with the same parameters of ON/OFF periods (i.e., $\lambda$ and $\mu$). Thus, we can define the duty cycle (DC) of a base

station as the proportion of time where the base station is active and is equal to μ/(λ + μ). In the simulations, we use the Xia-Bertoni propagation model [21] that is able to take into account all types of propagation losses, such as the one between base stations and the one between mobiles in addition to usual propagation loss between a base station and a mobile. Given a frequency *f* in GHz and distance $d_{XY}$ between transmitter *X* and receiver *Y*, path gain $G_{XY}$ is given by $G_{XY}(d_{XY}) = \mathcal{P}_{sj}(d_{XY}) = K_{XY} + \beta_{XY}\log_{10}(f) + \alpha_{XY}\log10\ (d_{XY})$, where $K_{XY}$, $\beta_{XY}$ and $\alpha_{XY}$ are constants computed using the Xia-Bertoni model. The obtained propagation constants are collected in Table 17. We also consider a log-normal shadow fading with zero mean and a standard deviation of 7 dB.

Table 17: Constants of the propagation model.

| | $\alpha$ | $B$ | $K$ |
|---|---|---|---|
| Primary BS ↔ Secondary node | 37.6 | 21 | 113.2 |
| Secondary node ↔ Primary terminal | 37.6 | 21 | 122.1 |

The primary metrics are evaluated for each case and compared to the thresholds. For this we assume that a primary cell is interfered when the received interference due to secondary activity is higher than $\iota_{\max}$ = -100 dBm. We also assume that $\varepsilon$, $\rho_{\text{th}}$ and $\theta_{\text{th}}$ are all equal to 0.05. The secondary performance is evaluated in terms of average capacity and allowed transmit power. The capacity is computed as the normalized Shannon capacity in bits/s/Hz, $C = \log_2(1 + \text{SINR})$. The SINR is computed considering only the interference from primary network and noise power. All techniques were evaluated for different values of $\lambda$ and the duty cycle. In our technique, the value of $\bar{T}_{ON}$ is computed from (40) and (41), and the value of $\bar{T}$ has been computed as the minimum value satisfying (42).

Sensing techniques in the presence of multiple transmitters have not been studied heavily. There are some preliminary works in this topic that were proposed in [20][43]. However, these solutions will give lower results in systems with fast power control, fast scheduling, and fast changes in the ON/OFF periods such as the case of mobile networks. Therefore, we consider instead a perfect mechanism but assuming one transmitter in the multi-transmitter case, which gives an upper bound for sensing-based techniques.

Using this assumption, the sensing technique can detect any OFF period where there is no active base station. Therefore, the OFF periods in this case are the intersection of the OFF periods of the seven cells. We assume that the sensing mechanism can detect an aggregate OFF period with a probability $P_d$ = 0.95, which corresponds to the considered $\varepsilon$ in our algorithm. Moreover, we assume that the probability of false alarm is equal to 0.1 as it is normally considered in the existing works.

The location-based technique is a simplified version of the method proposed in [20]. The main idea is to allow the secondary to transmit with a power that will interfere with the closest base station with a probability $\varepsilon$. The technique assumes that the positions of the base stations and the secondary nodes are known. In this case, a secondary node *I* inside the coverage area of an active primary network will not be able to transmit, which is not the case in the proposed approach. To determine the closest active base station, the secondary node compares the received power $S_I$ (i.e., the sum of all received powers from active primary base stations) to a location-specific threshold

$S_{th}(l)$ for each base station $l$. This threshold depends on the known distance $D_{ls}$ between $s$ and $l$ and is defined by

$$S_{\text{th}} = \text{erf}^{-1}(2\varepsilon - 1)\sigma\sqrt{2} + P - \mathcal{P}_{ls}(D_{ls}) \tag{48}$$

Using this threshold, the closest active BS is determined by

$$j = \arg\min_l \{D_{ls} | S_l \leq S_{\text{th}}(l)\} \tag{49}$$

### 4.5.4. Results

We note that all the values of $\rho$ and $\theta$ obtained using the proposed approach were always satisfying the primary conditions. Specifically, in the case of the location- and sensing-based techniques, these values were very low due to the conservative approaches considered.

In the stochastic-based approach, the secondary node transmits with its maximum allowed power during time $\bar{T}_{ON}$, and it stops any transmission during $\bar{T}_{OFF}$. Since the transmission schedule only depends on $\lambda$ as can be seen from (41), the average transmit power over time is always the same for the same value of $\lambda$. Figure 45 shows that it is also an increasing function of this parameter. This is normal because $\bar{T}_{ON}/\bar{T}$ is an increasing function of $\lambda$ as can be seen from (43).

In Figure 46 and Figure 47, we show the distributions of the transmit powers as function of the primary duty cycle, when the location- and sensing-based techniques are used, respectively. The figures show that compared to the stochastic technique the transmit powers are very low especially for high duty cycles. It should be noted that when the location-based technique is used, 12% of the secondary nodes are not allowed to transmit at all. This is the case when the secondary is at the boundary of coverage zones of two or more cells and thus the common OFF periods of the covering base stations are rare for high values of the duty cycle. Moreover, this percentage becomes 97% when the sensing-based technique is used, since the appearance of common OFF periods between the seven cells is very rare for high duty cycle. In fact, according to [48], the probability of having an OFF period in one base station after long time is $\lambda/(\lambda + \mu)$ which is $1 - DC$, where DC is the duty cycle. Therefore, for 7 cells and a duty cycle of 0.9 the probability of having OFF period in the 7 cells simultaneously is $10^{-7}$.

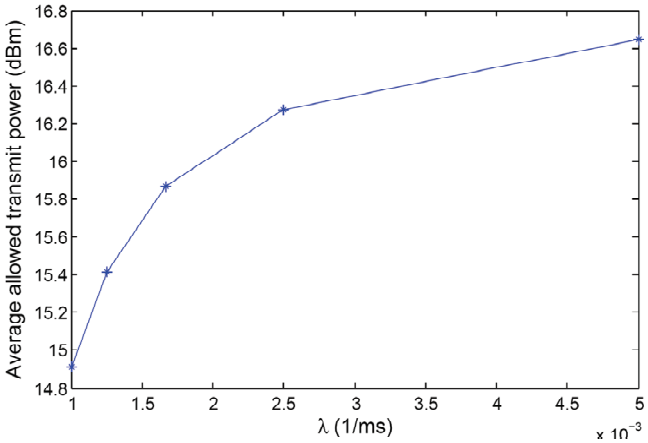


Figure 45: The average allowed power as a function of $\lambda$ when the secondary uses the stochastic-based method [53].

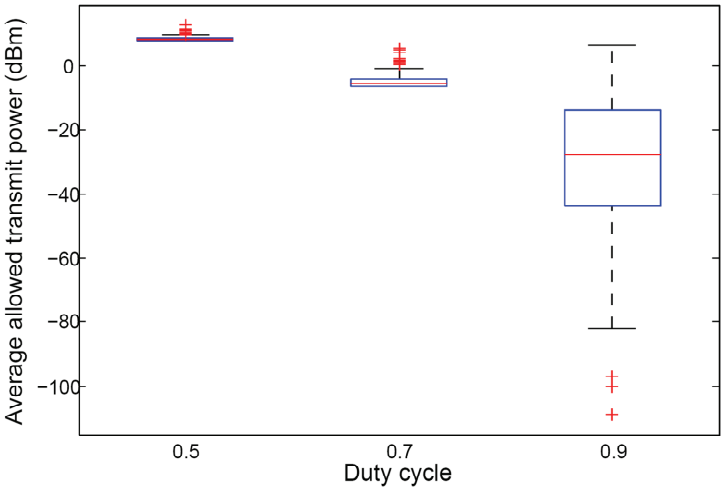


Figure 46: The average allowed power as a function of the duty cycle when the secondary uses the location-based method for $\lambda = 0.005$ ms$^{-1}$ [53].

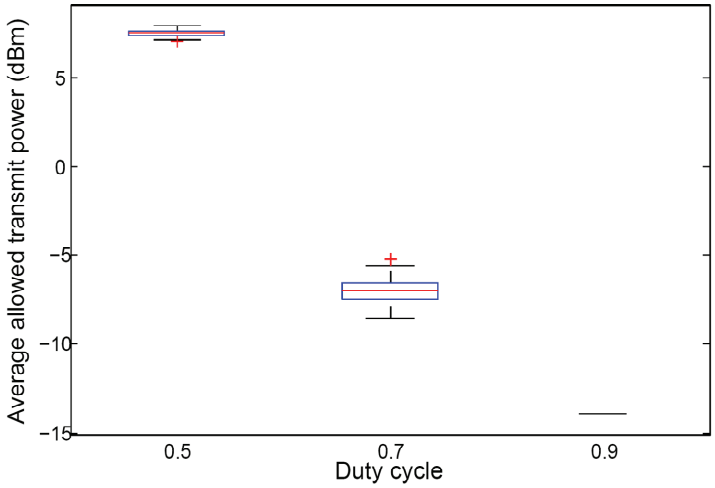


Figure 47: The average allowed power as a function of the duty cycle when the secondary uses the sensing-based method for $\lambda = 0.005$ ms$^{-1}$ [53].

We shall now study the impact of primary activity on the performance of the secondary users. Figure 48 shows the distribution of the capacity as a function of the primary duty cycle and for two values of $\lambda$. Although the average transmit power of the stochastic-based technique is very high compared to the other two, the average capacity is relatively low in comparison, especially for low duty cycles. This is due to the fact that in the proposed method, the transmission time is always fixed to the same small value, and the instantaneous capacity is logarithmic function with respect to the transmit power. The figure shows that both sensing-based and location-based techniques lead to relatively high capacities ranging from 2 to 30 bits/s/Hz when the duty cycle is lower than 0.5. These capacities decrease drastically with the increase in the duty cycle and especially for the sensing-based technique that does not allow any transmission when the duty cycle is higher than 0.5. On the contrary, the stochastic-based approach has a rather stable performance for a given value of $\lambda$ since it does not depend on μ. Even for a duty cycle of 0.9, this technique allows transmission with median capacity around 0.5 bits/s/Hz. The decrease in capacity with respect to the duty cycle is due to the interference generated by the primary network. This leads to a decrease in the instantaneous capacity.

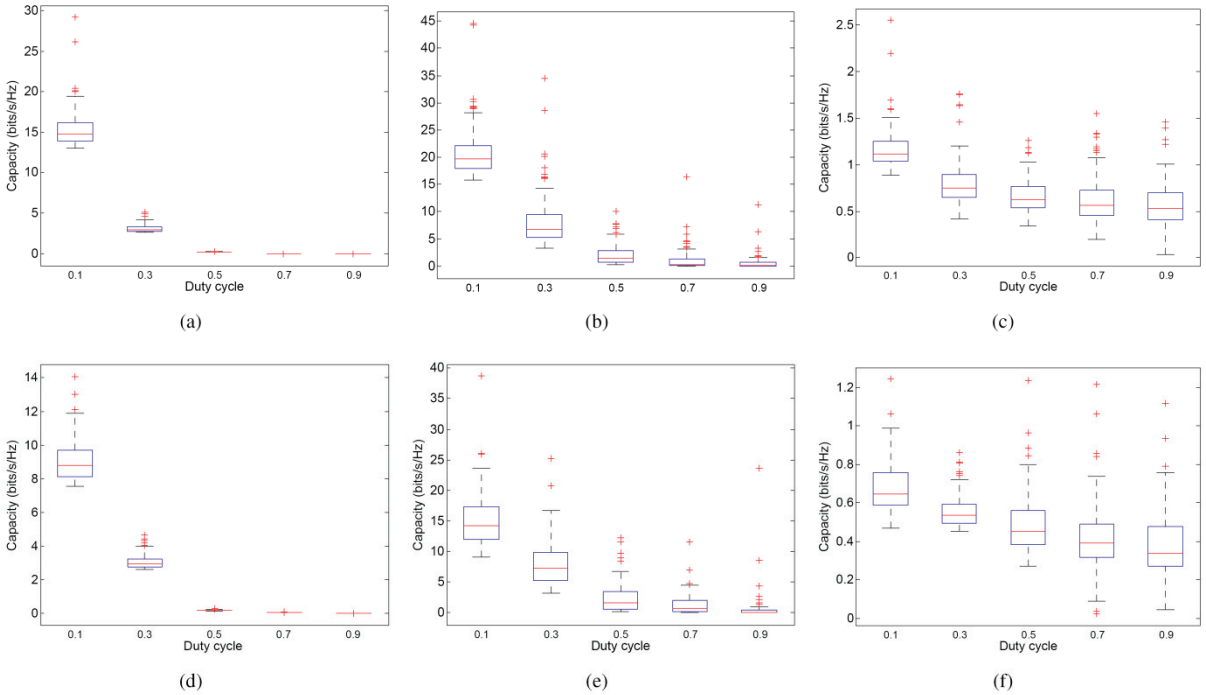


Figure 48: The capacity distribution as a function of the duty cycle for different values of $\lambda$ when using (a,d) sensing-based, (b,e) location-based and (c,f) stochastic-based techniques. The first row gives the distributions for $\lambda = 0.005$ while the second row for $\lambda = 0.001$ [53].

It should be noted that the reference techniques are optimal in the sense of detecting all primary opportunities. However, in practice this is not true and the achieved capacity will decrease depending on the dynamics of the primary network. This is not the case with the stochastic-based method that, even though it gives low capacity, is able to enable transmission even in the case of high primary activity.

### 4.5.5. Conclusions

In this section, we have explored a new approach for dynamic spectrum access based on stochastic models. Although the proposed approach does not yield a high capacity, it is suitable especially if the primary activity patterns are very fast where traditional DSA techniques based on sensing and localization fail to allow any transmission. One advantage of the developed approach is its robustness against the fast activity of the primary networks. In contrary to other DSA techniques, it allows a predictable and controllable quality of service. This can be suitable for several applications that do not require high data rate but are more sensitive to jitter and delay.

The results show that the proposed approach cannot perform as well as optimal sensing- and location-based techniques for low duty cycles of primary networks. However, we believe that such techniques are very difficult to implement and stochastic-based approaches can be a good candidate for dynamic spectrum access problems. Furthermore, the new approach reduces power consumption since it does not require sensing. This work is only a first step to explore stochastic-based approaches that can be improved further by considering other statistical aspects of the primary network.

## 4.6. Hidden node detection and avoidance

There are two main ways in which we consider that the REM approach can be beneficial for hidden node detection and avoidance, firstly by being agnostic and independent of the underlying radio technologies (such as modulation scheme, bandwidth and frequency etc.), and secondly by allowing compensation for uncertainty in signal transmitter power or received signal strength measurement accuracies. These benefits support the goal of predicting hidden nodes with sufficient confidence in existing and future radio deployments.

The hidden node problem is a classic issue with radio systems, sharing the same spectral resources, resulting in significant performance degradation. The reason for the degradation is due to the fact that an interfering node (or node pair) may be unaware that they are causing interference to another transmission, which is normally an essential prerequisite for radio coexistence etiquettes. For instance, to give a concrete example, a Zigbee sensor network node may degrade the performance of a WiFi network (sharing the same channel) considerably without being aware it is doing so and so will continue to operate on the same channel and cause interference. Therefore, it is important when considering spectrum sharing for the hidden node problem to be addressed. Two ways of overcoming this problem are possible, firstly, by proactive prediction of the hidden node occurrence or likely occurrences and secondly by reactive detection, and notification or indication, of the interference caused by the hidden nodes. Both approaches have implications, for proactive prediction the issue is to do with how reliably and what overhead is involved in making predictions and in the case of reactive approaches the issue is how much interference (and degradation) can be sustained before the culprit is identified and agreement on a universally supported indication mechanism.

Scenarios that are difficult for hidden node prediction and detection are mobile or indoor scenarios in which shadowing and other fading phenomena make it hard to determine if a hidden node problem is likely or does exist due to the dynamic nature of measurements. This problem is made harder by consideration of cognitive radio techniques which opportunistically utilize different RAT and frequency bands and hence do not exhibit predictable characteristics. To solve this problem requires measurements of the various radio signals and interference. The hypothesis that we consider with this approach is that intelligently combining many measurements and using REM prediction approaches can assist resource management based on hidden node detection and avoidance.

The REM approach that we consider exploits Measurement Capable Device (MCD) measurements in order to make predictions about the radio environment. Many REM approaches utilise an absolute location reference (i.e. measurements correlated with absolute geographic location using GPS [63]). In our approach the MCD measurements are either taken at fixed points (i.e. static MCD) or the location reference of the MCD is assumed to be possible by exploiting the presence of sufficient static (or fixed) MCD or MCD with known relative location references.

### 4.6.1. Summary of the optimization problem

#### 4.6.1.1. Hidden node problem

A typical way of avoiding the hidden node problem is to utilize request to send / clear to send handshakes before each transmission and deferring the transmission when a hidden node is

active. However, such an approach is not possible in multi-RAT scenarios in which the interferer is not transmitting using the same technology as the potential hidden node, and the same occurs in scenarios where a hidden node may be a PU that shares the same spectrum as a SU. It is also undesirable to utilise these countermeasures as they introduce a high overhead and indeterminate latency. An alternative approach is not to predict or prevent the hidden node occurrences but to detect or predict based on the impact it has on performance. However, such a reactive approach is not possible when one of the node pairs (i.e. the interferer) is not aware that a problem exists (i.e. this pair is still able to continue without significant impact). Therefore, it becomes much more important to predict these occurrences prior to any significant interference. Hence this optimization is concerned with using REM to detect potential hidden nodes and then to initiate an appropriate channel reallocation to avoid the interference that would otherwise be caused.

The first step is to define the meaning of a hidden node in terms of a constraint policy (as defined within the ULLA specification [59]). The definition of a hidden node can be derived as in:

```
IF    {channel(0) = channel(1)} AND
      {rxsignallessmargin(0) < rxsignalstrength(1)} AND
      {timestamp(0) = timestamp(1)} AND
      {rxsignalstrength(2) < THRESHOLD} THEN EXCLUDE
```

In the above policy the necessary constraints are specified in order to avoid (i.e. exclude) hidden nodes. There are four conditions that first determine whether the wanted (0) and interference (1) signals measurements under comparison are made on the same channel, then whether the signal strength of a potential interferer (1) at the receiver position is within a specified margin of the wanted signal (0), which would result in unacceptable interference. Next the time of the two measurements must be within the same epoch, which can be specified according to the temporal resolution required. The final constraint predicts whether the potential interferer (hidden node) can detect the wanted signal based on a sensing threshold. This is determined by signal strength (2), which is the interference signal strength that would be received at the wanted signal transmitter position (i.e. such that the transmitter is unable to detect the interferer given the specified sensing *THRESHOLD*).

The hidden node in this derivation assumes that the signal strength sensing level (detection threshold) given by value of *THRESHOLD* is known, and optionally also configurable, using the assisted resource management approach. When signals are below this level it is assumed that it is not possible for the interference signal to be detected and hence a hidden node is possible. Therefore, the process of using REM to predict the occurrence of hidden nodes and to avoid hidden nodes is given in Figure 49. The first step in the process is for MCDs to measure the signal levels and load on the available channels. The second step is the selection based on a combination of the signal level and load and estimation revised resulting load given assumptions about channel reallocations. Next the REM prediction is used to estimate the localization of the wanted and interference signal sources and hence to make a prediction about the resulting interference signal strength (2) received at the known wanted signal receiver positions. Then the hidden nodes (terminals) are determined in the network using this context information based on the REM prediction. The hidden node policy rule is then evaluated against the terminals with their corresponding hypothetically selected channels.

On detection of a hidden node condition (i.e. policy criteria match) the relevant channel "virtual hand over" (VHO) is initiated, in order to select an alternative channel, and the whole process repeated. In this manner the number of hidden nodes is reduced until none exists or the maximum number of iterations is reached and the channel load is evenly distributed. In most frequency re-use schemes and cognitive radio scenarios there are a fixed number of channels (resources) available and this has an impact on the VHO scheme. It is assumed that there is at least one alternative that can be selected for each node.

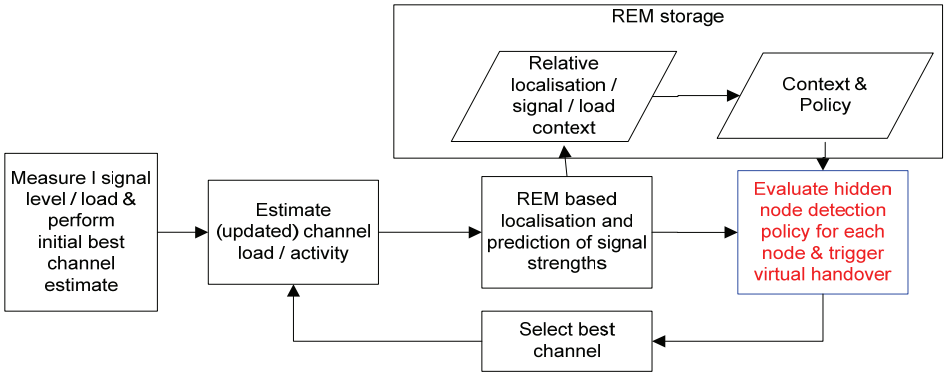


Figure 49: Iterative hidden node avoidance algorithm.

### 4.6.1.2. REM based prediction

The individual measurements taken by MCDs are combined by REM to make predictions about the likely interference. The first step is to utilize relative signal references to eliminate uncertainty (i.e. lack of knowledge) about the transmitter power level and therefore localize the potential interfering transmitters with respect to the MCDs. The next step is to generate the REM model to estimate radio interference level at the intended receiver location. Then the REM results can be used within resource management processes such as configuration optimization, handover triggering or channel assignment by predicting the hidden nodes.

For localization, the relative values are based on the ratio of signal strength received from two reference signals rather than their absolute numeric values. For instance, the ratio of a signal received by one MCD to another received from a different MCD. The REM processing that is required to determine the relative path-loss (i.e. coordinates in signal space) of the transmitter with respect to the MCDs (or vice versa) is then given by the geometric calculation in Figure 50.

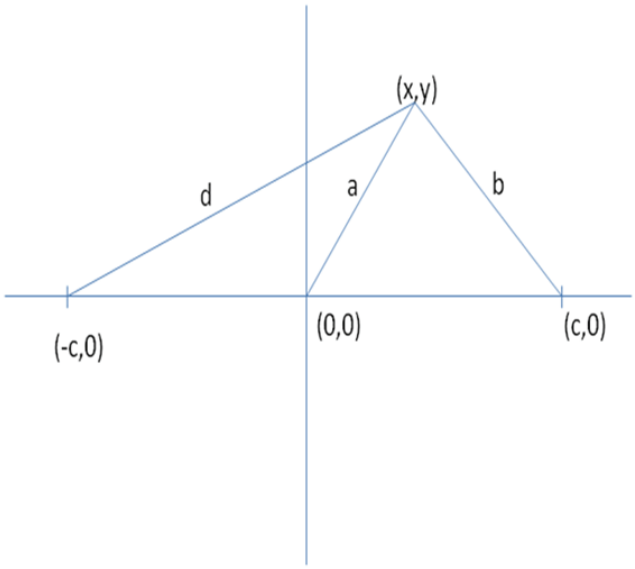


$$a = \sqrt{x^2 + y^2}$$
$$b = \sqrt{y^2 + (c - x)^2}$$
Assuming $b = a.r$
$$r^2 = \frac{y^2 + (c - x)^2}{y^2 + x^2}$$
$$r^2(y^2 + x^2) = y^2 + c^2 - 2cx + x^2$$
$$y = \pm\sqrt{\frac{c^2 - 2cx}{r^2 - 1} - x^2}$$
$$d = \sqrt{y^2 + (c + x)^2}$$
Assuming $d = a.s$
$$s^2 = \frac{y^2 + (c + x)^2}{y^2 + x^2}$$
$$y = \pm\sqrt{\frac{c^2 + 2cx}{s^2 - 1} - x^2}$$
$$x = \frac{c(s^2 - r^2)}{2(r^2 + s^2 - 2)}$$

Figure 50: Relative signal space geometric calculation of coordinates (x,y).

The analysis in Figure 50 shows that the exact signal related coordinates (in two dimensions) can be easily computed from relative signal strengths (i.e. no knowledge of transmitter power assumed) received by three MCDs arranged in a linear manner with equal separation (c). The ambiguity in the y dimension can be resolved by a single extra orthogonal measurement to determine which side of the MCDs the transmitter lies. For non-linear arrangement (i.e. MCDs are not grid aligned) the computation becomes harder but is still possible. Also, a generalization to a three dimensional mapping can occur with at least one (and ideally two) additional orthogonal measurement points. Applying the same equation as above (with additional z2 term) resolves the one dimensional coordinate (i.e. x position) and providing the receiving antenna has consistent gain versus the angle / elevation of arrival, the orthogonal measurements will enable resolution of y and z coordinates.

The REM can now make use of the relative transmitter signal coordinates (x,y) in order to estimate path loss and hence performance or interference levels regardless of RAT and power level as they have been normalized into the relative signal (path-loss) space. Next the coordinates (x,y) of the potential interferer and potential victim are used together with the absolute signal strength measured to estimate rxsignallessmargin(0), rxsignalstrength(1) and rxsignalstrength(2) to determine whether a hidden node condition exists.

### 4.6.2. Performance evaluation methodology

In order to assess the performance of a REM based approach to predicting and avoiding hidden nodes we first have to make assumptions about the deployment and topology. The key factor affecting the performance of REM is the shadowing and multi-path fading characteristics of the radio environment. Therefore, to determine the impact that this has on prediction performance we consider the detection of hidden nodes in the presence of these propagation anomalies. It is possible to eliminate or at least reduce the effects of multi-path fading by considering averaging of measurements over longer timescales and over different channels/sub-channels (if possible), therefore shadow fading is of most interest for evaluation purposes. The deployment layout that

we consider for the evaluation is based on five hundred random nodes within a symmetrical grid of thirty six MCD with twenty units of separation (i.e. c=20). The REM uses the MCD measurements corresponding to each transmitter in order to predict the potential occurrence of hidden nodes within the deployment. The REM predictions are then used to initiate a virtual handover (i.e. reconfiguration) to another channel in order to avoid the hidden node condition.

### 4.6.3. Results

The results that we obtained are firstly to estimate the node localization prediction error and secondly the performance of the hidden node avoidance algorithm. The prediction errors are summarized in Figure 51 and are obtained with the randomly placed obstructions. Each obstruction is on average 5 units long (uniformly distributed between 0 and 10) and are either horizontally (x axis) or vertically (y axis) aligned and cause a shadowing attenuation of 5dB. Two cases are considered, the no obstruction case considers the situation in which there is a direct line of sight between the potential hidden node and the nearest MCD and the obstruction case is when at least one obstruction exists. The other assumptions that are made within this first comparison are that all the radio devices transmit power levels are the same and constant and the MCD signal strength measurement precision is to within 1dB. Clearly if dynamic power control techniques were to be used this would also impact on the accuracy of the REM prediction, but if the measurement epoch is sufficiently chosen this is not an issue.

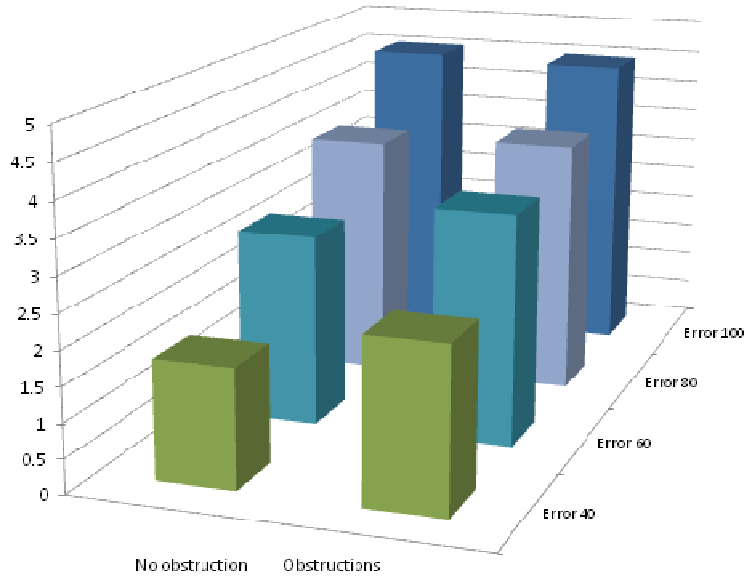


Figure 51: REM Localization Prediction Errors (with different # randomly placed obstructions).

The results in Figure 51 suggest that as more obstructions are placed in the environment (i.e. increased shadowing and probability of no line of sights existing) then the error in localization increases (as expected), from around 1.5 units to 4.5 units. At higher densities the difference between localization prediction errors observed for obstruction and no obstruction cases is much smaller. This indicates that the impact of shadowing for the nearest MCD to the potential hidden node (and victim node) becomes successively less important as the obstruction density increases.

Next we consider the evaluation of the avoidance algorithm in the presence of obstructions. Again two cases are considered, with the first case assuming that ten separate channels are available, and hence there is a good probability of selecting a non-interfering channel. In this case the obstruction density and the signal strength margin using in the algorithm is varied. The second case considers that only two channels are available, and in this case the obstruction density and the signal strength *THRESHOLD* is varied.

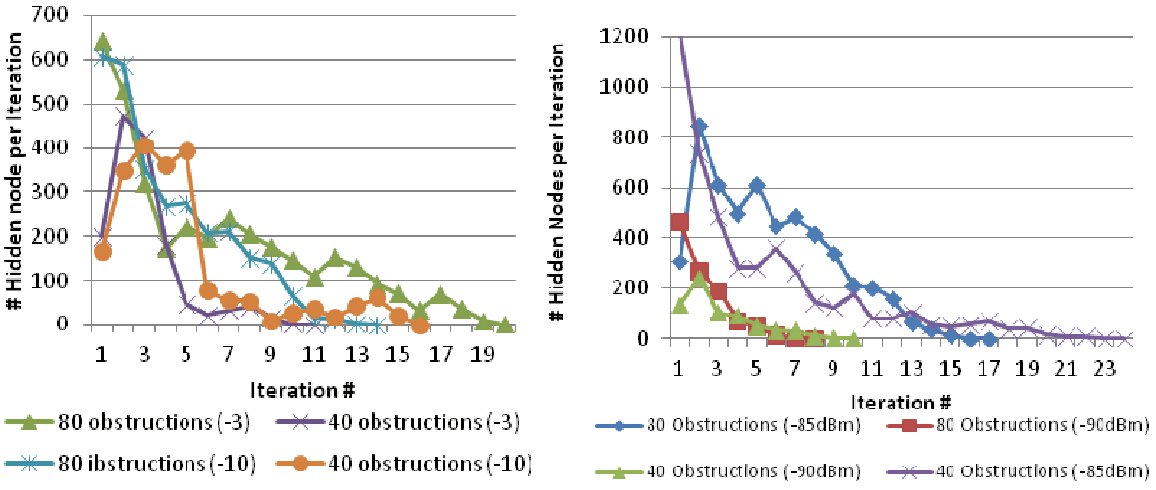


(a) (b)

Figure 52: Hidden Node Policy matches per Iteration for Different Obstruction Density (a) Ten Orthogonal Channels and Varying Margin in dB (b) Two Shared Channels and Varying Threshold.

Figure 52 shows the overall convergence performance of the hidden node detection and avoidance algorithm. It illustrates that when the sensing threshold is at an appropriate level the convergence occurs after 10 or 20 iterations (for 40 and 80 obstructions respectively), and for a higher threshold more iterations are required, but potentially higher overall performance/throughput can be achieved. Another observation is that the signal margin has an impact on convergence and a higher margin affects the initial convergence differently for high and low obstruction densities. In the low density case the convergence takes longer for large margin (i.e. 10dB compared with the 3dB case), but for high density the trend is reversed. This can be explained by the fact that at low obstruction densities there are unlikely to be as many cases with high shadowing and hence fewer matches in general but there are also more nodes with no shadowing impact at all. The other important observation is that most triggers are associated with a few "problem" nodes that occur in clusters near to the obstructions and where the distance between hidden node and victim node is greatest. In the second case the results indicate the implication of increasing the *THRESHOLD,* which is to significantly increase the occurrence of hidden node conditions and the convergence time of the algorithm. Therefore, a trade-off exists to select appropriate *THRESHOLD* values that maximize the overall performance considering both the time taken for hidden node detection and the impact on system throughput.

The REM approach to hidden node detection and avoidance can be deployed within several scenarios as illustrated in Figure 53. For instance, for multi-RAT deployments (such as WiFi / femtocell resource sharing scenarios as in [60]) the REM can be deployed within the Joint Radio Resource Management (JRRM) function on the network side or the IEEE 1900.4 Network Reconfiguration Manager (NRM) entity on the network side as described in [62]. When the REM is

deployed within network-side entities (i.e. JRRM-N or NRM) there are several existing interfaces for providing the MCD measurement as well as terminal and network context interface supported by the existing standards. Technology independent standards such as IEEE1900.4 and IEEE 1900.6 are most general and support RAT agnostic measurements data reporting (i.e. channel related measurements). However, the interface for supporting VHO triggers is less clearly defined. For instance, within the IEEE 802.21 standard a media independent candidate query request / response and event messages are defined (see [63]), and in IEEE 1900.4 there is a facility for changing channels. Therefore, it is expected that for most purposes these existing standards will be sufficient for supporting the deployment of JRRM functions that use REM based hidden node prediction / avoidance.

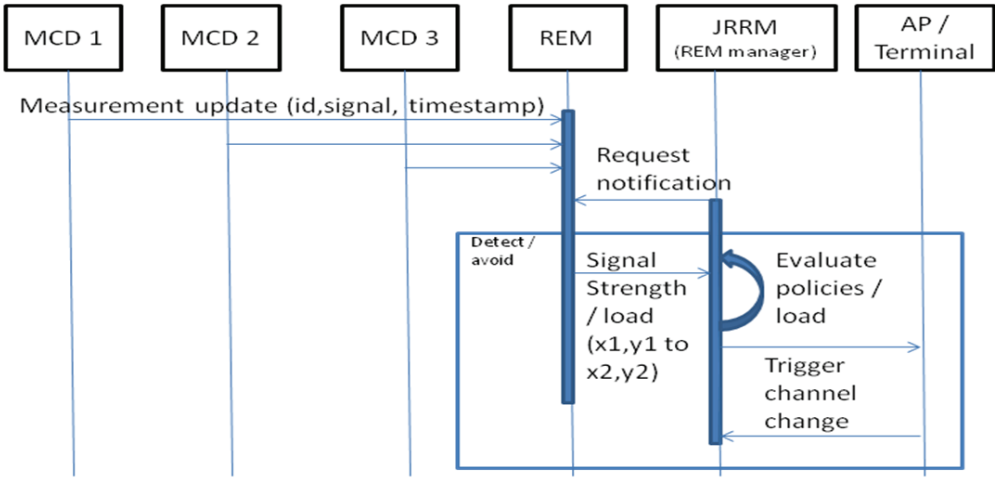


Figure 53: Deployment of REM base Detection / Avoidance Algorithm.

### 4.6.4. Conclusions

The use of REM for measurement based prediction for detection and avoidance of hidden nodes has a high potential value in radio network optimization as the performance degradation that occurs can be severe. It is especially disruptive when deterministic or bounded latency and reliability are required within opportunistic, multi-RAT or cognitive radio deployment environments. The evaluation that has been performed on the REM prediction approach illustrates the ability to compensate for unknown transmitter power and propagation anomalies such as shadow fading. The impact that this has on predictions can be significant even with relatively few obstructions and using low cost commercial measurement devices. Therefore, it is essential that the REM prediction approaches exploit the ability to combine measurements made using different references in an intelligent manner. Doing so not only improves the ability of REM to make interference predictions, but can do so without the need for MCDs to take any excessive additional or more complex measurements (which would otherwise incur extra complexity and power consumption). Also, augmenting the MCD based signal strength measurements with infrastructure based angle or arrival or time difference of arrival techniques could be an interesting and beneficial in extension not only for locating transmitter nodes, but also for locating obstructions. Therefore, when fast convergence is required combining these different techniques could prove to be highly beneficial.

Further work is necessary to apply the REM prediction approach to other interference related problems such as dynamic channel selection and coexistence scenarios, for which similar conclusions can be expected. It is also for a thorough performance evaluation to be conducted on a real system deployment to validate the assumptions made.

# 5. Optimization techniques in Ad hoc Networks scenario

This chapter covers a scenario characterized by a number of ad hoc networks coexisting in the same area and sharing the same spectrum. The general objective is to guarantee to all networks that try to access the spectrum the satisfaction of their requirements on minimum capacity. Given the decentralized nature of the ad hoc networks, an adequate mechanism is needed to disseminate the information captured by the different Measurement Capable Devices (MCD) and to build the Local and Global REMs. This protocol will be presented in section 5.1 since it will be used by the following optimization techniques that will be detailed in the subsequent sections:

- Section 5.2 focuses on the channel assignment problem in highly mobile autonomous ad hoc networks that experience fast changes in the interference conditions and thus they may require frequent reallocation processes. The main issue here is to ensure a fast convergence of the developed solutions and to minimize channel changes.
- Section 5.3 will focus on how to maximize the global capacity of ad hoc networks in which multiple flows need to be transmitted through point-to-point links. The main objective is to perform a resource allocation to the different flows that optimizes the spectrum efficiency.
- Section 5.4 will consider a number of mobile ad hoc networks that share the spectrum with primary networks. The considered problem targets the correct reception of data to all users in the network without interfering with the primary system.

## 5.1. REM population protocol

The architecture developed for REM integration in ad hoc networks (presented in [3]) foresees a two level REM, where a local REM (L-REM) collects data at each network level and a global REM (G-REM) puts together data from all networks in the area and combines them with global statistics and a priori knowledge of radio environment profile.

In each network a node is elected NH (Network Head) and covers, among other functionalities, the role of L-REM of the network. To register the network at G-REM level and to report and retrieve information on the radio environmental profile, we assume the existence of a low data rate dedicated signaling channel.

To populate the L-REM of each network and to control the measurements of the MCDs of the network, a specific protocol is developed.

### 5.1.1. MAC Frame

The messages that carry the information exchanged between nodes of each network are transmitted through a TDMA scheme. Different kinds of slots are characterized at MAC level and they are organized in a MAC frame.

Three kinds of slot are identified:

1. **Beacon slots**: used by the NH to initialize the network, to transmit resource allocation information to users and to transmit L-REM orders to MCDs;

2. **Random Access (RA) Slots**: used by the nodes of the network to indicate their presence, to discover their neighbors, to send resource requests to the NH and to report measurements to the L-REM;

3. **Data slots**: used to transmit user data and to perform measurement operations.

Each MAC frame starts with a beacon slot, followed by a certain number of RA slots and data slots. The total duration of the MAC frame depends to the number of users of each network: more users in the network require more RA slots and so a longer MAC frame duration.


Figure 54: MAC frame structure.

In the first two types of slots, the signaling messages that allow the construction and the update of the L-REM are exchanged as explained in the following paragraph.

### 5.1.2. Local REM population protocol

The following protocol aims at the construction of L-REM of each network and at its population through measurements of nodes.

Periodically the NH broadcasts a beacon message setting a specific field that identifies itself as the L-REM of the network. In the same way, users with measurement capabilities take advantage of hello messages (periodically sent during RA slots to maintain the network topology) to manifest their presence and their measurement capabilities (i.e. class of the node) to the NH. The reception of hello messages from MCDs permits to the NH to feed a database with an entry for each node of the network. Since that, when sending a beacon message, the NH includes in it L-REM orders on measurement activities. More specifically, it details during which data slots each MCD has to perform measurements and on which channels. MCDs can then report measurement results and SINR level of received transmission in the following MAC frame, through hello messages.

This protocol has been conceived for L-REM population in ad hoc networks and it underlies all the solutions to the optimization problems presented in the following paragraphs.

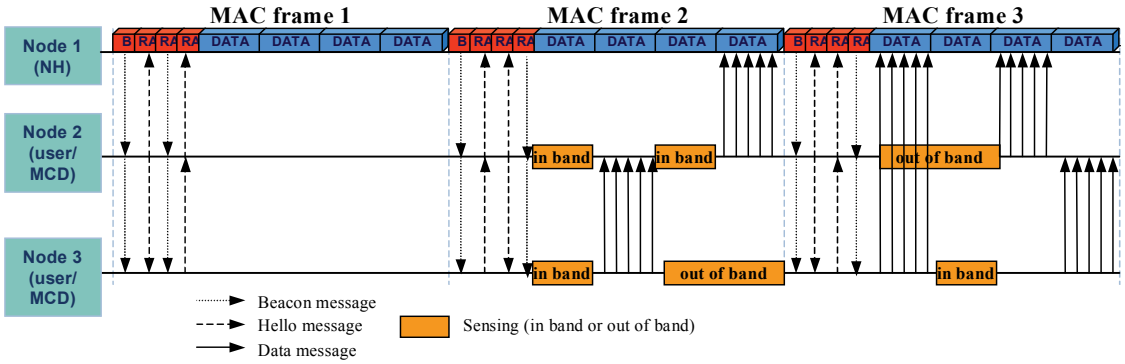


Figure 55: Example of exchange of messages among NH and MCDs to populate L-REM. In this case the traffic in the network foresees several point-to-point links, but the procedure is similar in case of broadcast transmissions from NH.

## 5.2. Fast reactive autonomous networks

### 5.2.1. Summary of the optimization problem

This optimization solution is conceived for the case of highly mobile autonomous networks, where the interference conditions can change in short time and so a resource reallocation process can be necessary quite often. In this case it is of primary importance the reallocation time necessary to arrive at a stable solution when interference conditions change: it is clear that if the reallocation process requires too much time, the solution obtained may not be interesting anymore due to further environmental changes due to mobility. Table 18 summarizes the main aspects of this optimization problem.

Table 18: Optimization problem: Fast reactive autonomous networks.

| Fast reactive autonomous networks | |
|---|---|
| Scenario(s) of applicability | Several mobile secondary networks. |
| Assumptions | • Each network has a central unit (NH) that manages the resource allocation inside the network<br>• In each network there is a channel dedicated to exchange signaling messages among the users<br>• In each network only a unit (that corresponds to the NH) transmits user data<br>• The transmission is broadcasted to all users of the network |
| Optimization target | • Guarantee to each network their requirements in terms of SINR<br>• Avoid signaling among different networks<br>• Minimize the convergence time when conditions change<br>• Minimize channel changes when looking for a new solution |
| Input from sensing and REM | • Position of other networks and channels in use<br>• Propagation model in the area<br>• Interference level on each channel |
| Metrics | • Time to converge on a new stable solution<br>• Number of channel changes before arriving to convergence<br>• Loss of user data while searching the solution<br>• Average SINR of networks<br>• Average NH transmitting power |

### 5.2.2. Optimization techniques

In the following paragraphs several optimization strategies are proposed that can be used in this scenario.

#### 5.2.2.1. GADIA

The GADIA algorithm presented in [55] is a technique that can permit to solve the channel allocation problem considered here under specific assumptions. In this algorithm it is assumed that the distances between clusters (that correspond, in our scenario, to networks) are much larger than the cluster size. In that case any node in cluster i will have the same jamming effect to any node of cluster j as illustrated in Figure 56.

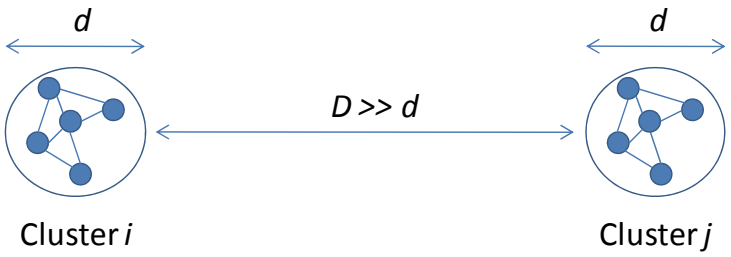


Figure 56: Geometry assumption for the GADIA algorithm.

The GADIA algorithm is a greedy algorithm that is operated at each cluster and that selects the frequency channel for which the cluster experiments the least interference:

Algorithm 3: GADIA algorithm

At each cluster $j$
For $c = 1, N_c$
- measure interference level perceived in the cluster on channel $c \rightarrow I_j^c$
End
Take channel $c_{\text{op}}(j) = \arg\min_{c \in \{1,\ldots,N_c\}} I_j^c$

The interference level is retrieved from L-REM that obtains it through sensing operation.

One of limitations of the GADIA algorithm comes from the geometrical assumption discussed below: when two clusters are close to each other, the GADIA algorithm is no longer applicable. For instance in Figure 57, when cluster 1 and 2 are close together, interference between node i and node u may be much larger than between node j and node v.

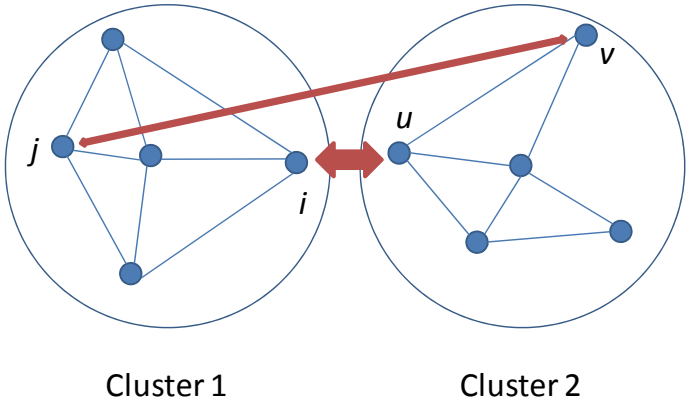


Figure 57: Interference level between nodes of different clusters varies when the clusters are close.

We thus propose to extend the GADIA algorithm to the case where clusters can be close to each other. In order to account for the various possible interference levels, we estimate the interference at all nodes and take the maximum interference in order to protect all the links. Then we select the channel that leads to the minimal maximum interference, as described in the following algorithm:

Algorithm 4: EGADIA: Extension of GADIA algorithm to account for close clusters

At each cluster $j$
  For $c = 1, N_c$
    - measure interference level perceived at each node $k$ on channel $c \rightarrow \{I_{j,k}^c\}_{k=1,K_j}$
    - compute $I_j^c = \sup_{k=1,K_j} I_{j,k}^c$
  End
  Take channel $c_{\text{op}}(j) = \arg\min_{c\in\{1,\ldots,N_c\}} I_j^c$

### 5.2.2.2. Channel and Power Selection Algorithm (CPSA) for Neighbor Protection

In this paragraph we propose a distributed strategy to allocate resources to each network that allows networks to act autonomously choosing channel and power to satisfy their communication needs, but, at the same time, avoiding excessive interference on neighbors.

To proceed to select the best channel and to determine the best power to use on it, the NH of the network needs to obtain information from local and global REM about the propagation model to neighbor networks, the level of interference on each of them and the maximum interference tolerable by neighbors.

According to this information the NH computes the maximum power available on each channel ($P_{AV}$). This power level is the maximum power that a user of the network can use on the corresponding channel without generating harmful interference on neighbor networks. The knowledge of propagation model in the area permits to compute it using the following formula:

$$P_{AVi,j} = \min_u P_{AVi,j,u} = \min_u \frac{I_{TH_u} - P_{noise}}{\alpha_{j,u}(d_{u,j}, h_{i,j,u})} \tag{50}$$

where $I_{TH_u}$ is the maximum interference accepted by network *u* users and $\alpha_{j,u}$ is the attenuation between the networks *j* and *u* that depends on their distance and on the coefficient of channel *i*.

Once computed the maximum available power on each channel, the Cognitive Resource Manager (CRM) proceeds to rank the channels according to the following Utility Function (UF):

$$UF_{ij} = \frac{P_{AVi,j}\alpha_j(r_j, h_i)}{I_{TOT,i}} \tag{51}$$

where $\alpha_j$ is the attenuation value expected for communications inside the network between NH and farthest user, and $I_{TOT,i}$ is the total interference detected on channel *i*.

Furthermore, before to select a channel, the following condition related to the minimum capacity constraint is tested for each channel:

$$P_{AVi,j}\mu_2 \geq P_{\min}\mu_1 \tag{52}$$

Where $\mu_2 < 1$ is a protection margin to reduce the risk of harmful interference on neighbours due to inaccurate estimation of the channel, $P_{\min}$ is the minimum transmission power that NH has to

employ to fulfill the SINR constraint at user in worst conditions and $\mu_1 > 1$ is a margin to protect the transmission. These two protection margins are parameters that can be tuned according to REM accuracy in order to always fulfill system requirements. For example, if REM accuracy is low, protection margin $\mu_2$ can be reduced, while, in case of REM providing high precision information, it can be close to 1. The consequent drawback, when reducing $\mu_2$ to counterweight REM low accuracy, will be a longer time to find an acceptable configuration.

Once the channels have been ranked following the utility function, the NH selects the channel with highest utility function for which condition (52) is satisfied.

If there are no channels that satisfy the minimum capacity requirement, then a random channel is selected and the NH transmits on it at full power. In this way a maximum of users will receive the transmission of the NH. Moreover, if NH uses a power higher than the power available on the channel, some neighbor network will be affected by interference and so it will free the channel and look for a different one.

Otherwise, once the channel has been selected, we propose two different strategies to select the power to use on the channel:

a. **CPSA min**: NH selects to transmit the $P_{\min}$ corrected by the protection margin $\mu_1$;

b. **CPSA fast**: NH selects to transmit the $P_{AV}$ corrected by the protection margin $\mu_2$.

The first strategy aims at reduction of overall power consumption, but this implies a reduction of average SINR of networks and can need a longer time to converge.

The second strategy, on the other side, aims at fast convergence and can determine a higher power consumption of transmitting nodes.

Algorithm 5: CPSA

Check SINR and Pav_of channel in use
**If** (SINR < $SINR_{min}$)
  **If** (condition (53) cannot be fulfilled adapting power in use)
    Rank channels according to (51)
    **If** ((52) can be respected on best channel)
      Select best channel
      **CPSA min**
      Use min $P_{min}$*$\mu_2$ on channel
      **CPSA fast**
      Use min $P_{av}$*$\mu_1$ on channel
    **Else**
      Select random channel
      Use $P_{max}$ on channel

Once the channel is selected, the NH keeps checking if the SINR on it is still acceptable and if $P_{AVi,j}$ has changed. If necessary it can proceed to adapt its power respecting the following constraint

$$P_{AVi,j} \geq P_{used} \geq P_{\min}\mu_1 \quad (53)$$

If it doesn't exist a $P_{used}$ that respects this constraint, NH starts a selection process looking for a new channel.

#### 5.2.2.3. Genetic algorithms

In addition to the previously described techniques we also propose a strategy based on genetic algorithms. With respect to previous approaches, here the choice of channel allocation is centralized at G-REM level, limiting the independence of each network.

Genetic algorithms are inspired by Darwin's theory about evolution: solutions to a problem evolve. The algorithm starts with a set of solutions (represented by chromosomes) called population. Chromosomes from one population are taken and used to form a new population that we hope better than the old one. Chromosomes that are chosen to form new chromosomes are called offsprings and are selected according to their fitness: the more suitable they are, the more chances they have to reproduce. The evaluation of the solution is done using a fitness function that has to be maximized. This process is repeated until some condition is satisfied (for example a solution that leads to a value of the objective function greater than a threshold or a predetermined number of populations).

In our scenario we can conceive an optimization strategy based on genetic algorithms. The existence, in the ad hoc architecture proposed in [3], of a central unit (G-REM) that collects information from all networks permits to apply this centralized approach. The drawback is that networks should renounce to their autonomy in radio resource allocation, delegating the choice of channel and power to use to the G-REM.

To build the allocation strategy we start from the technique based on genetic algorithms presented in [56].

We define a fitness function (FF) based on global SINR of the proposed solution, given by the sum SINR of the users in worst conditions in each network. Moreover we take into account the minimum SINR constraint that leads to the following fitness function:

$$FF = \sum_{i=1}^{N} SINR_i - \frac{1}{\tau_i} \tag{54}$$

where

$$\tau_i = \begin{cases} 0.001 & if \quad SINR_i - SINR_{\min} < 0.001 \\ SINR_i - SINR_{\min} & elsewhere \end{cases} \tag{55}$$

Here below the procedure of the proposed Genetic Algorithm (GA) is synthesized:

Algorithm 6: Genetic Algorithm

```
Initialize chromosomes
Rank chromosomes according to their FF
While (Best FF < fixed threshold)
        Select offsprings
        Apply mutations and crossover
        Generate new population
        Rank chromosomes according to their FF
Select the chromosome with best FF as solution
```

### 5.2.3. Evaluation methodology

To evaluate the performance of the proposed solution, we built a simulation modelling an area of 100Km$^2$ in which several networks coexist.

Each network is modelled as a variable number of users that are included in a circumference of maximum radius of three kilometres. Each network includes a node (NH) that leads the network and that is in charge to take decisions in terms of radio resource allocation.

We assume that the different networks are homogeneous and that they share the same resource allocation strategy and use the same waveform.

Each network has a constraint on SINR to guarantee communications: specifically a SINR threshold ($SINR_{min}$) is defined in reception and corresponds to the SINR that permits to each user of the network to correctly receive the periodic transmission of NH. Moreover NH has a maximum transmission power that it cannot exceed.

We run the simulation for each of the previously described optimization techniques in order to compare their performance. For GA centralized approach, we run the algorithm starting with a population of 100 and 1000 chromosomes.

The comparison is done using the following key metrics identified for this scenario:

- **Convergence time**: talking about mobile networks the time necessary to arrive to an acceptable global configuration (i.e. each network has a channel that allows respecting the $SINR_{min}$ constraint) is a key parameter. If the time to adapt the allocation of resources to the networks is too long, interference conditions can have changed and the configuration found could be not anymore acceptable. For distributed methods, convergence time is computed in terms of number of MAC frames from the beginning of measurement operations of networks and the time when all networks are in acceptable conditions.

- **Channel changes**: the number of times that each network has to change channel before to arrive to an acceptable configuration is another important metric that has to be evaluated. The action to change a channel implies a partial reconfiguration of the network, which can generate problems in keeping in place the network topology. Hence it is important to reduce channel changes.

- **Lost traffic**: the traffic of the network that is not received by all the users with at least the minimum expected SINR. It corresponds to the number of MAC frames during which at least a user does not receive NH transmissions.

- **SINR**: average SINR of networks. Even if in this scenario the focus is not in maximizing data transmission, but in guaranteeing a minimum SINR to each user, the average SINR is a good way to have a comparison on potential capacity of the networks.

- **Power**: average power used by NHs to transmit to users of their networks once a stable configuration is reached.

- **Not valid configuration percentage**: percentage of cases in which the algorithm leads to a repartition of resources that is not acceptable. This can be a consequence of the fact that the algorithm is not able to find a configuration that guarantees the minimum required SINR to all networks in the area or that it requires too much time to find it.

Two scenarios of simulation are foreseen:

- In the first simulation scenario we want to evaluate reactivity of networks in an interference situation. To do it we deploy several networks in the same area all using the same starting channel and we evaluate how the different resource reallocation strategies lead to a stable configuration.

- The second simulation scenario starts in the same way than the first one: several networks in the same area with the same starting channel. Then, one network starts to move randomly in the area, while all the other networks keep the same position. Through this scenario we can evaluate the performance over a longer time period of the different techniques.

### 5.2.4. Results

#### 5.2.4.1. First scenario

To test the different techniques in different conditions we vary the number of networks coexisting in the same 100km$^2$ area from 20 to 55. The number of channels among which the networks can select to communicate is set to 8.

Notice that the simulation area is quite large so not all networks in the area are significantly impacted by interference generated by a network. We fix the number of networks from 20 to 55 considering coexistence of 20 networks as a quite easy problem to solve and coexistence of 55 networks as a tricky one.

We generate 10000 realizations of topology for 20, 25, 30, 35, 40, 45, 50 and 55 networks and we run the different strategies previously explained on all these realizations. For GA, only SINR, power and percentage of not valid configurations are considered as metrics. This is due to the fact that, being a centralized solution, it always requires the same amount of time to find a new configuration (time necessary to collect and report the information to G-REM and to communicate the decisions to all nodes) independently to the number of networks considered (assuming an adequate computation power at G-REM). Similarly the number of lost messages and of channel changes depends only on the interference levels in starting configuration.

Figure 58 represents the number of MAC frames, averaged over the 10000 realizations, that algorithms need to find an acceptable configuration. Notice that the new configuration is considered accepted only when measurements confirm the acceptable SINR level on the channel in use, so even if no changes are needed, at least one MAC frame is necessary to consider valid the configuration in use.

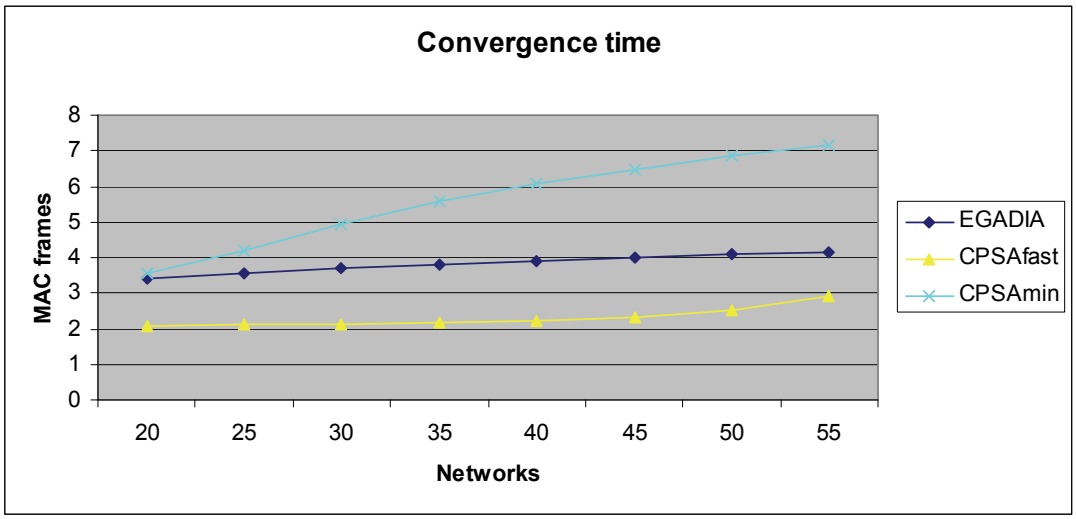


Figure 58: Average convergence time expressed in number of MAC frames.

The graph shows that convergence time in easy situation is quite long for EGADIA, but it does not increase a lot with complexity, following a linear trend. Behavior is worst when looking at CPSA min: in easy situation convergence time is relatively high and increasing complexity convergence time increases as well, with a steeper trend than EGADIA. Best performance in the range considered in our simulations is provided by CPSA fast that is faster in easy conditions and keep better performance even in more complex scenarios. On the other side it has an exponential trend when increasing the number of networks that can penalize this solution for tricky scenarios.

If we look at behavior of different allocation strategies in terms of average channel changes (Figure 59), we will see similar trends, but different results. Due to the fact that in EGADIA the action of a network is only slightly dependent on the total number of networks, we are not surprised to evidence an almost constant number of channel changes when increasing the number of networks. Nevertheless this value is quite high with respect to the values showed by CPSA min and CPSA fast in easy conditions.

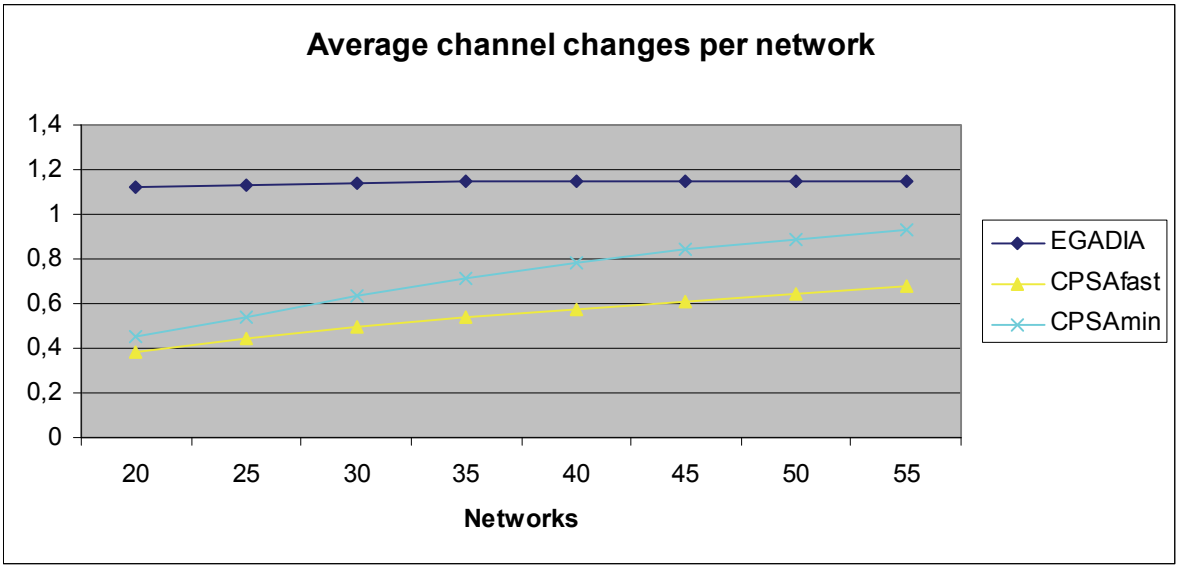


Figure 59: Average channel changes per network.

On the other hand CPSA min and CPSA fast starting values are quite close and their curves increase when the number of network increases. Nevertheless CPSA min presents a steeper trend revealing, once again, worst performance with respect to CPSA fast.

Similar results are provided by analysis of lost traffic (see Figure 60). Here again EGADIA strategy is the worst one, followed by CPSA min and CPSA fast that has very good performance.

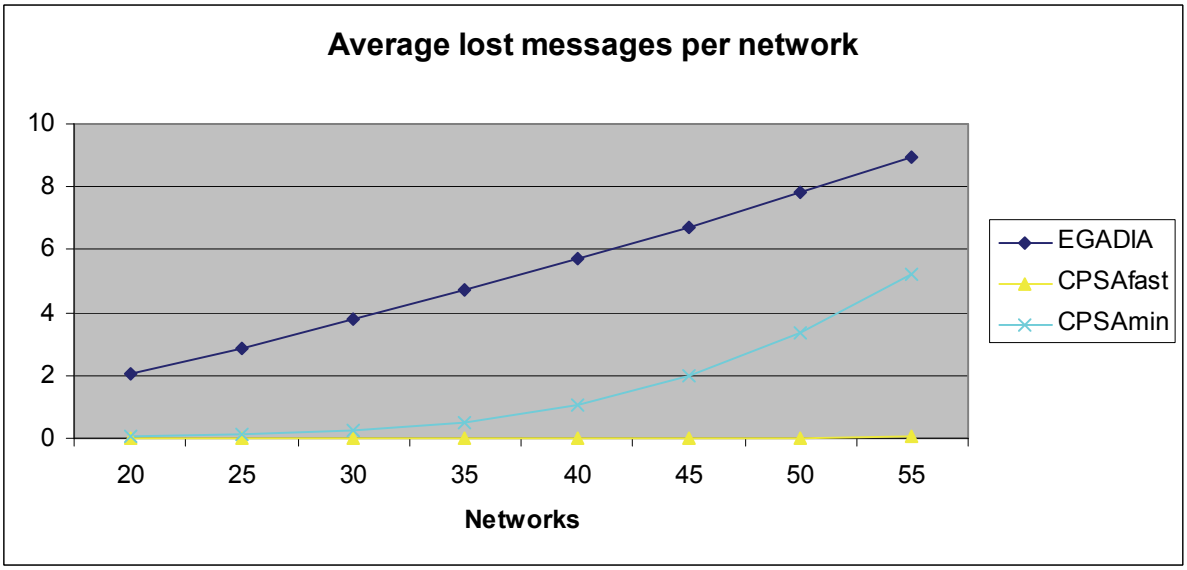


Figure 60: Average lost traffic per network.

However, if we look at average minimum SINR per network (Figure 61), we obtain opposite results. In this case EGADIA has the best performance especially in low complexity case. As expected CPSA min has the worst performance and CPSA fast is worst than EGADIA, but the two curves come closer when increasing complexity. Genetic algorithms both with 100 and 1000 starting chromosomes show almost the same trend than CPSA fast confirming the close to optimal performance of CPSA approach in terms of SINR.

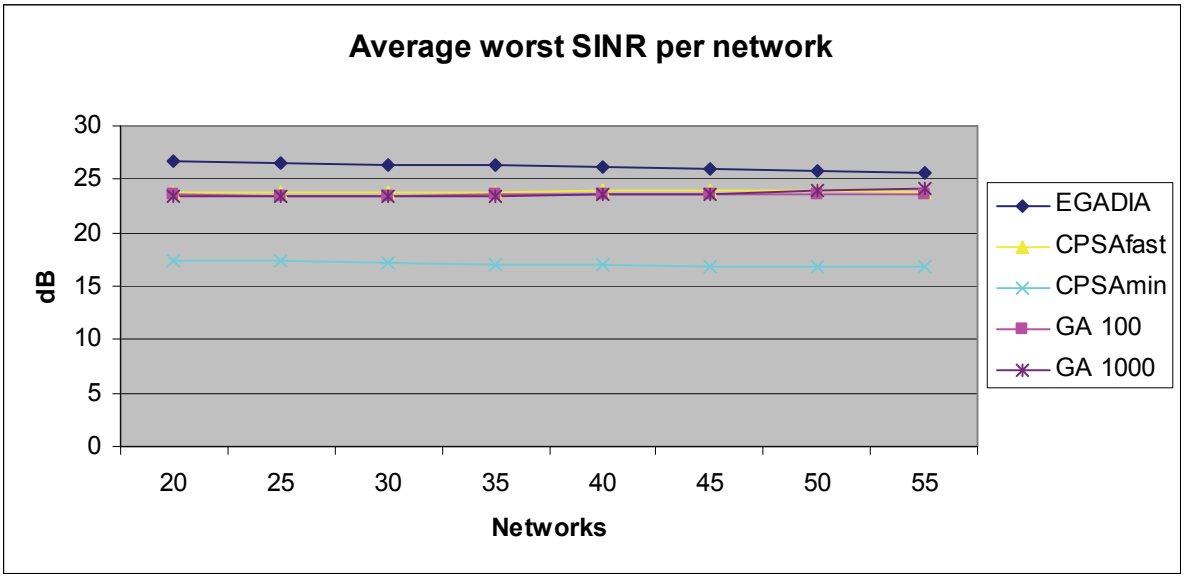


Figure 61: Average minimum SINR per network.

Nevertheless the previous result is paid in terms of power consumption as shown in Figure 62. While EGADIA always use maximum power, CPSA min approach allows to strongly reducing energy consumption in transmission. Moreover, CPSA fast reduces the power consumption with respect to EGADIA, but the two curves are not so far and get closer increasing complexity. GA central approach, instead, allows having a very good SINR level keeping the power consumption low.

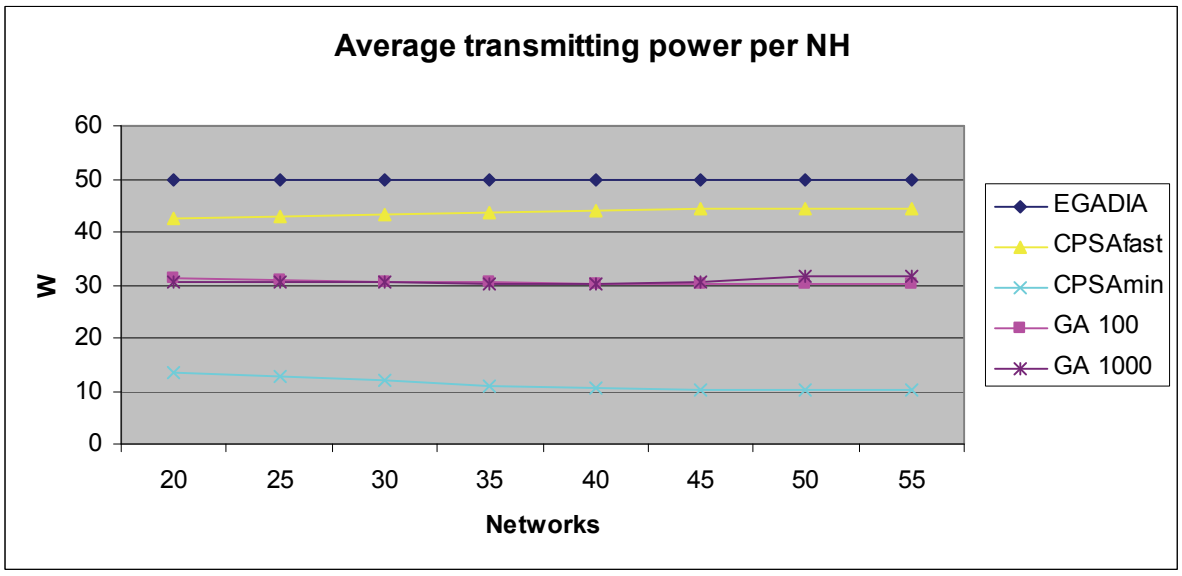


Figure 62: Average transmitting power employed by the NH of each network.

Finally it is important to notice that EGADIA, even if providing best average SINR, does not provide any warranty on worst SINR of each network. Figure 63 shows the number of cases in which the solution obtained does not guarantee the minimum required SINR to all networks in the area at the end of the reallocation process or after a fixed maximum time (set to 100 MAC frames). The graphic clearly confirms that EGADIA strategy does not guarantee minimum SINR to all networks, nevertheless it can be used in low complexity conditions.

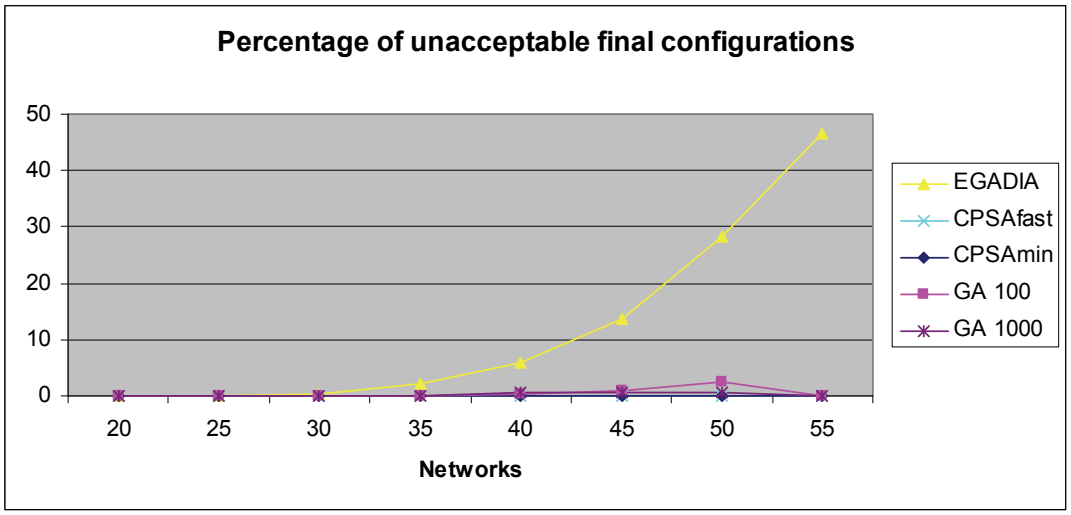


Figure 63: Percentage of unacceptable configurations after reallocation process (or after 100 MAC frames) computed over the 10000 realizations of the topology for the different numbers of networks in the area.

### 5.2.4.2. Second scenario

In this scenario we put 54 networks in the area in fixed positions and we add a network that moves randomly in the area (see Figure 64). We model the movement of the network in a discrete way: we trace a grid in the area composed by squares with side of 1 Km and we assume that the network moves from one point of the grid to another adjacent one every 120 MAC frames. We also assume that the nodes of the network keep their reciprocal positions when moving.

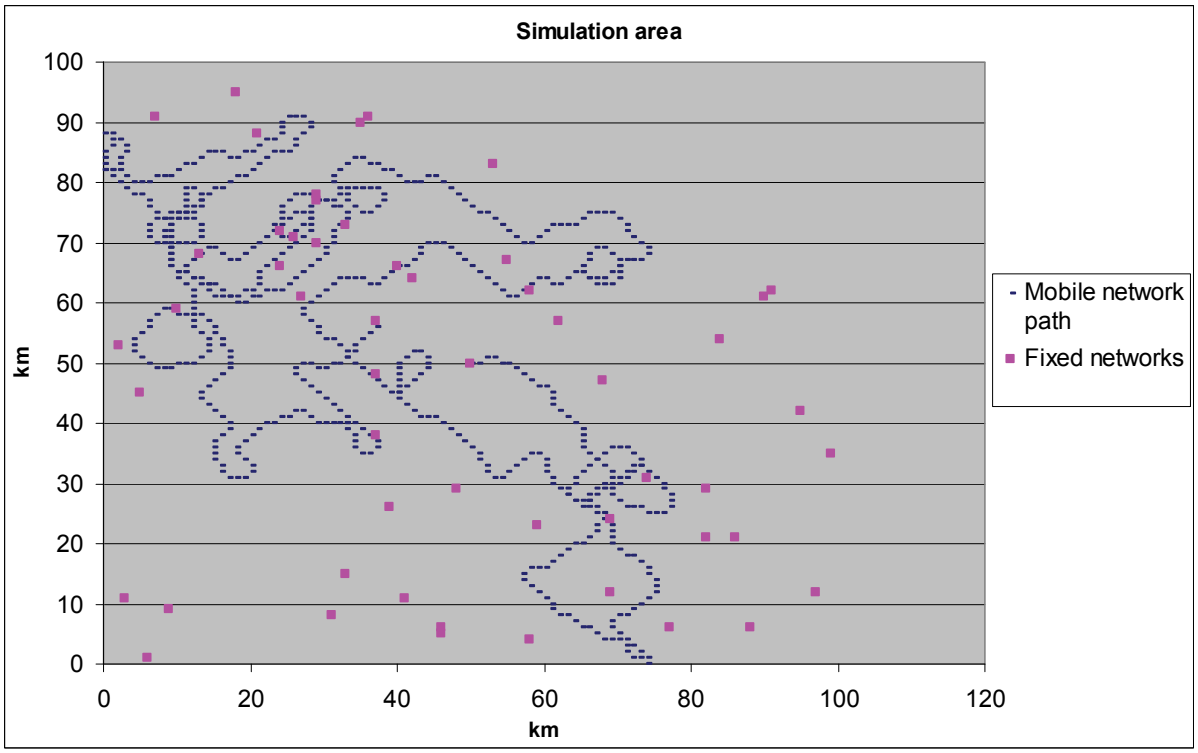


Figure 64: Positions of the 54 fixed networks in the area and path of the mobile network starting from position (50,50).

For this scenario we run EGADIA algorithm and CPSA both with minimum power and fast reaction approach. The metrics considered to evaluate performance of different algorithms are the same than the ones used in first scenario: lost traffic, number of channel changes, average SINR and average transmission power. Moreover we check, as for first scenario, the consistency of solution obtained using EGADIA and the number of cases in which CPSA does not find an acceptable configuration in the fixed time.

In the following table the average results of the three methods are reported.

Table 19: Average performance of algorithms in second scenario simulation.

| | EGADIA | CPSA fast | CPSA min |
|---|---|---|---|
| **Unacceptable configurations** | 8 | 0 | 0 |
| **Average SINR** | 26,426 | 24,054 | 16,576 |
| **Average Power** | 50,000 | 35,848 | 7,349 |
| **Average channel changes** | 0,371 | 0,075 | 0,178 |
| **Convergence time (in MAC frames)** | 1,160 | 1,035 | 1,054 |
| **Lost transmissions** | 0,719 | 0,005 | 0,630 |

The average results on the entire simulation confirm what was observed in the first simulation scenario. In particular EGADIA has the best performance in terms of SINR, CPSA min is the best one in terms of power consumption and CPSA fast is really close to EGADIA in terms of SINR and has the best performance when looking at lost transmissions. More in general CPSA approaches are faster to converge and require less channel changes, but do not reach EGADIA results in terms of SINR.

Figure 65 and Figure 66 show the average transmitting power and SINR of each network all along the simulation. The two graphs confirm the results showed in the previous table, but they also evidence a behavior that was not possible to see looking only at the average values. The CPSA min shows a very regular trend both in terms of SINR and of power used, while the other two algorithms, especially CPSA fast, evidence a more fluctuating trend.

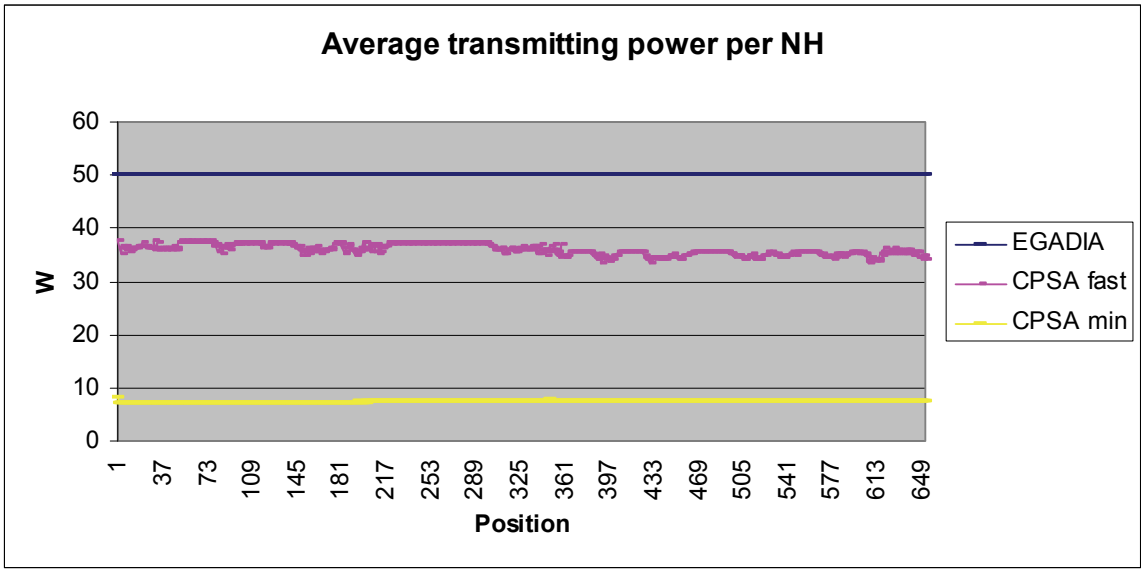


Figure 65: Average transmitting power employed by the NH of each network.

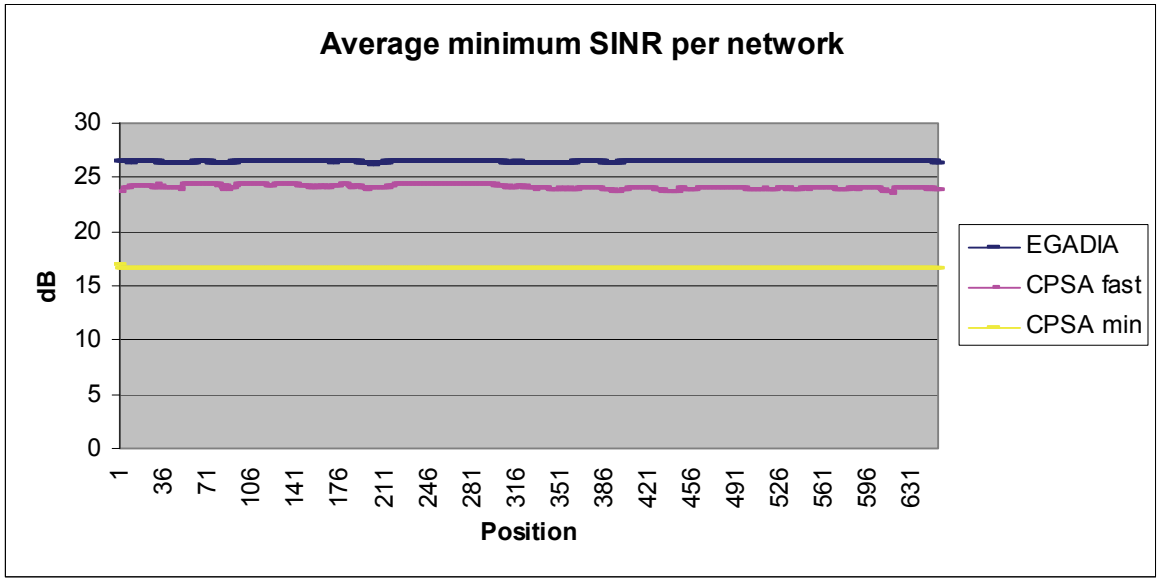


Figure 66: Average minimum SINR per network.

The analysis of convergence time and of channel changes all along the simulation permits to add further elements to the evaluation of the algorithms as it is possible to see in Figure 67 and Figure 68. The figures show that CPSA min has higher peaks with respect to the two other algorithms. This means that it suffers tricky situations (as around position 350), when it requires more time and more attempts to converge. In addition we can notice that CPSA fast is really reactive, never requiring more than three MAC frames to converge.

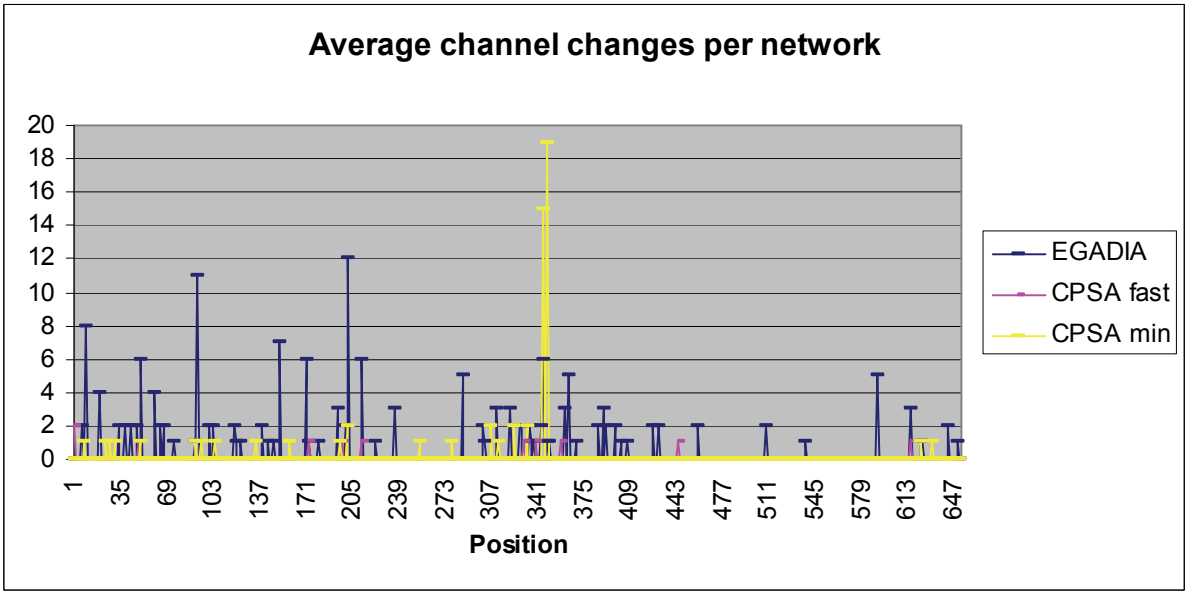


Figure 67: Average channel changes per network.

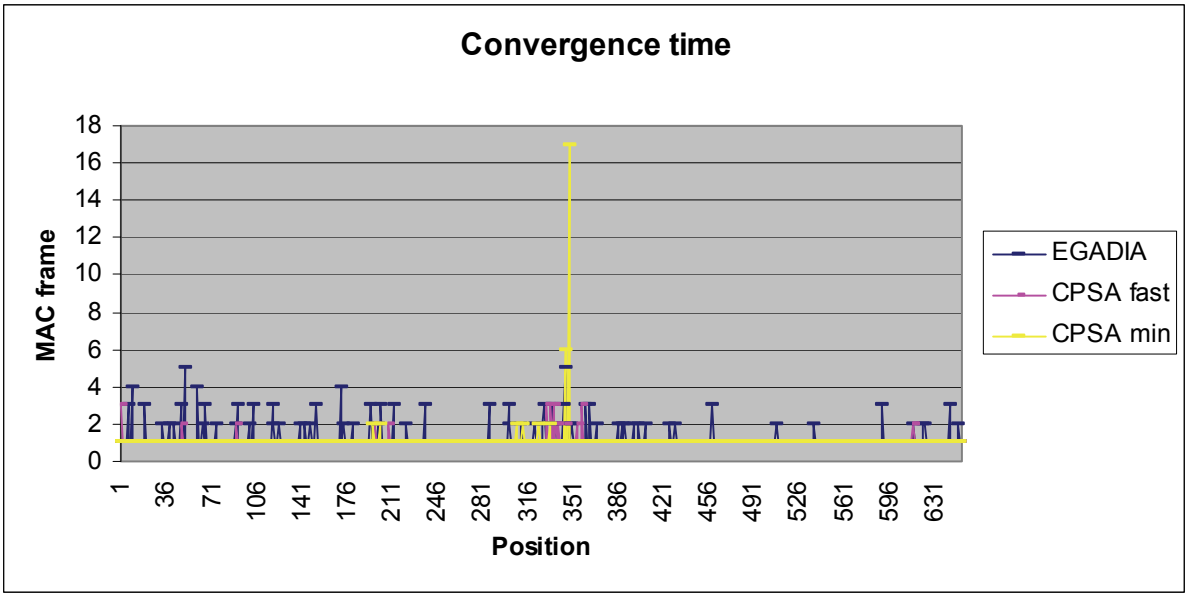


Figure 68: Average convergence time expressed in number of MAC frames.

### 5.2.5. Conclusions

In this paragraph we presented several RRM strategies (both adapted from the literature and brand new ones) to solve the problem of coexistence of autonomous networks. According to the different metrics analyzed, we identified the most performing ones and we highlighted the strength points and the drawbacks of each of the proposed strategies. Taking into account the specificities of the optimization problem (i.e., fixed data rate requirement and fast convergence), CPSA fast is the radio resource management strategy that seems to fit better.

## 5.3. Networks with high data rate point-to-point links

### 5.3.1. Summary of the optimization problem

In this scenario the focus is on maximize the global capacity of networks in which several flows of data have to be transmitted among users through point-to-point links. The main objective is to select for each network an appropriate channel that allows assigning resources to all flows of data optimizing spectrum efficiency. Table 20 summarizes the main features of the considered problem.

Table 20: Optimization problem: Networks with high data rate point-to-point links.

| Networks with high data rate point-to-point links | |
|---|---|
| Problem title | Networks with high data rate point-to-point links |
| Scenario | Several mobile ad hoc networks with high data rate requirements. |
| Assumptions | • Each network has a central unit (NH) that manages the resource allocation inside the network<br>• In each network a certain number of point-to-point communications have to be satisfied. Different communication links inside a network require different resources.<br>• OFDM transmissions |

| | |
|---|---|
| Optimization target | • Maximize the capacity of each network<br>• Reduce loss of messages |
| Input from sensing and REM | • Position of other networks<br>• Propagation model in the area<br>• Interference level on each channel<br>• Channel profile |
| Metrics | • Throughput of networks<br>• Loss of user data |

## 5.3.2. Optimization techniques

### 5.3.2.1. SEGADIA

For the optimization problem presented in section 5.2 we proposed an evolution of GADIA algorithm that takes into account the real topology of each network relaxing the simplification of networks considered as points. Simulation results shown in previous paragraph evidence another weakness of EGADIA algorithm: when looking for the best channel from interference point of view, the algorithm does not evaluate if the channel guarantees a good reception level to all users.

In previous optimization problem, where only broadcast traffic was considered, this could lead to the loss for some users of broadcasted messages, but in case of point-to-point links requiring high data-rate it will lead to loss of transmitted data and to a waste of allocated resources.

We propose to extend the previous algorithm (EGADIA) in order to take into account the point-to-point link quality inside each cluster with respect to the interference from the other clusters. From the interference measured at each node we compute the SINR of the links used in the cluster assuming that we know at L-REM level the averaged channel gain for these links and that we transmit at the maximum authorized power. Then we count the number of links for which the SINR is above a given target SINR and we finally chose the channel that gets the maximum number of SINR constraints satisfied. If there are several channels that maximize the number of links that can be satisfied, the channel is randomly selected among them. The new algorithm is described in the following:

Algorithm 7: SEGADIA: Extension of EGADIA to take into account intra cluster SINR constraints

At each cluster $j$
  For $c = 1, N_c$
    - measure interference level perceived at each node $k$ on channel $c \rightarrow \{I^c_{j,k}\}_{k=1,K_j}$
    - compute SINR for the different links $(u,v) \in \mathcal{L} \rightarrow \Gamma^c_{(u,v)} = \frac{P^c_{\max}\mathbb{E}|h_{u,v}|^2}{I^c_{j,v}+N_0}$
    - compute $\Gamma^c = \sum_{(u,v)\in\mathcal{L}} 1_{\left\{\Gamma^c_{(u,v)} > \Gamma^{\mathrm{T}}_{(u,v)}\right\}}$
  End
  Take channel $c_{\mathrm{op}} = \arg\max_{c\in\{1,\ldots,N_c\}} \Gamma^c$

Once the channel has been selected, the NH assigns specific time and frequency slots to different links, according to their capacity needs and following a TDMA/OFDMA strategy.

For this scenario we use a different approach to the channel with respect to what it was described at the beginning of the chapter. More specifically a frequency dimension is considered in addition to the time dimension applying, for data transmission, a TDMA/OFDMA strategy.

We then modify the MAC frame previously described dividing the channel in time and frequency slots whose intersection defines several Resource Blocks (RBs). The NH attributes these RBs to the different data links. The new frame is depicted in Figure 69.

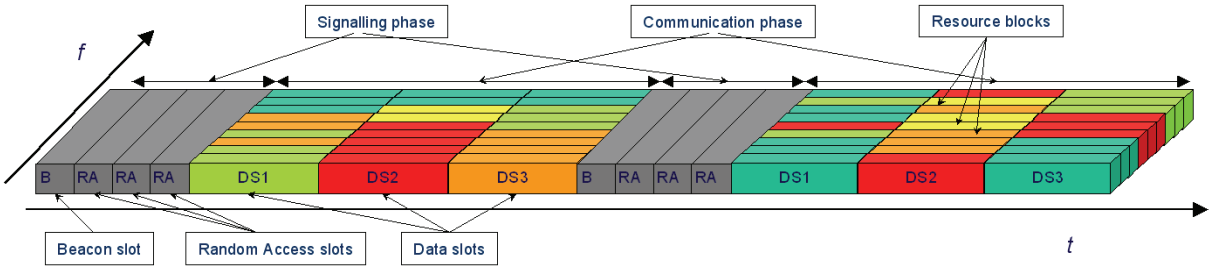


Figure 69: TDMA/OFDMA MAC frame.

According to the REM information available at NH level two different radio resource allocation strategies are proposed:

- **Frequency Selective Allocation (FSA)**, if the channel profile is well known;
- **Interleaved Allocation (IA)**, otherwise.

The FSA strategy takes advantage of the knowledge provided by the REM of the channel profile and attributes resource blocks to data links according to the channel profile in order to maximize the global throughput and to guarantee to each link, which has been selected by SEGADIA algorithm, to be satisfied. Figure 70 shows an example of how resource blocks are allocated using FSA strategy.

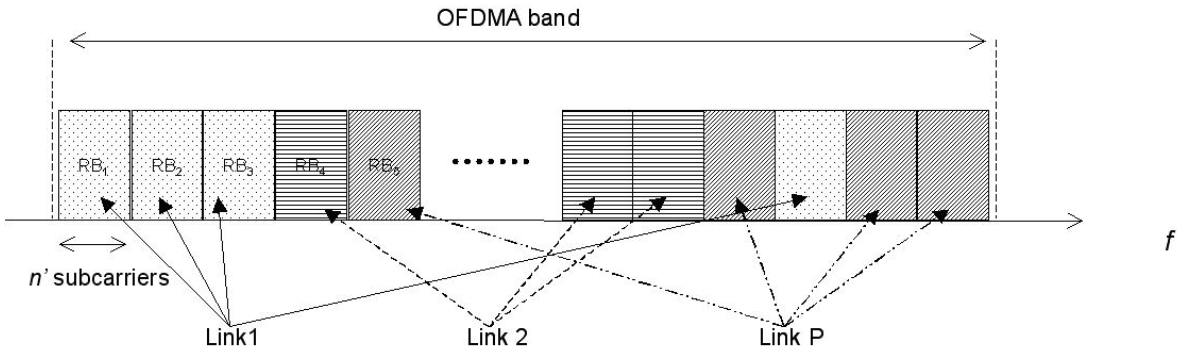


Figure 70: Frequency selective allocation of Resource Blocks.

On the other hand, the IA strategy attributes resource blocks to data links alternating the different links to have more frequency diversity as in the example of Figure 71.

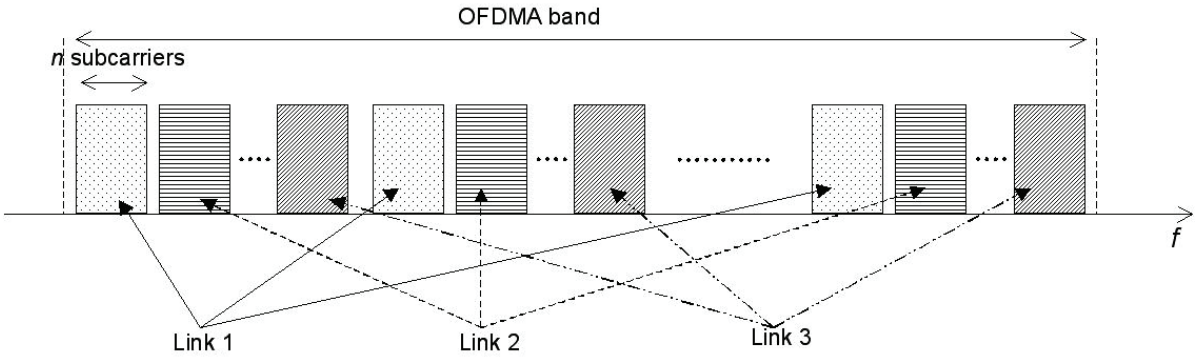


Figure 71: Interleaved allocation of Resource Blocks.

In addition to the resource blocks to use, the users that have data to transmit receive an indication on maximum available power. This value can correspond to the maximum transmitting power of the network or to a value imposed by the G-REM that follows some specific power reduction policy. Using these data each user will select the best modulation and coding scheme that it can use to maximize capacity, staying under the level of maximum available power as shown in Figure 72.

### 5.3.3. Evaluation methodology

The objective of our simulations is twofold: on one side we want to evaluate the performance of the proposed evolution to GADIA algorithm and, on the other side, we want to validate the capabilities of proposed intra-network resource allocation strategies to increase the global throughput.

For the first purpose we use a simulation scenario similar to the first one used for the previous optimization problem (see section 5.2.3). The difference is that now, instead of broadcast traffic, we model, in each network, three point to point links among different users at different distances.

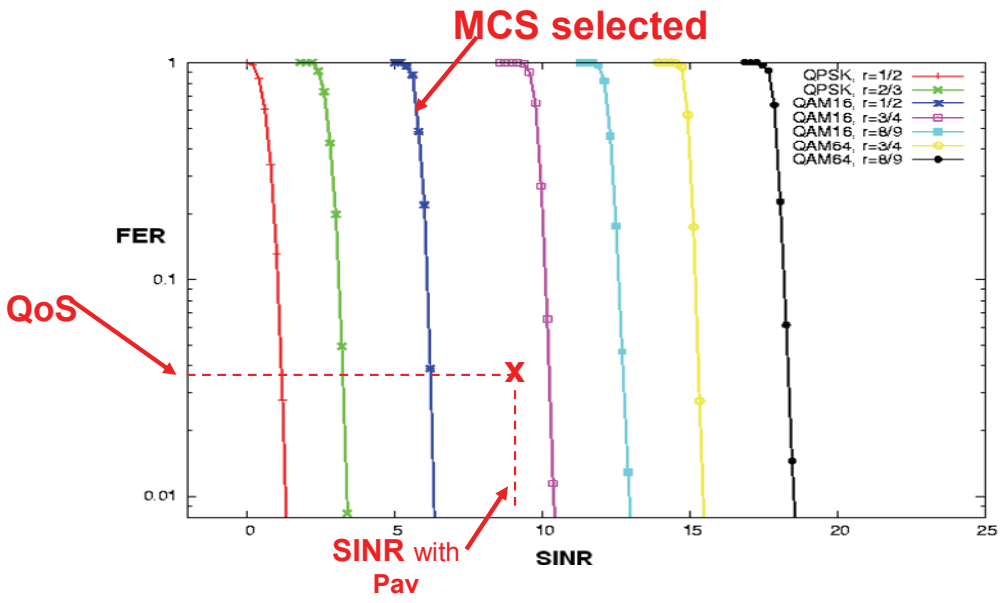


Figure 72: Selection of the best MCS.

The key metric that we consider is the number of links that cannot be satisfied after the channel reallocation process. In addition, we also evaluate the convergence time required and the average SINR on the links. The comparison is done between SEGADIA algorithm and the previously presented GADIA evolution (EGADIA).

To evaluate the second part of the problem, the intra-network resource allocation phase, we build a simulation with ten networks sharing the same channel, each of them with ten nodes in static conditions (i.e., mobility is not simulated). We model an urban channel with 3 taps and we assume the channel constant during the simulation.

The key metric retained is the percentage of loss messages when increasing the traffic needs (i.e., more data to transmit among users).

We compare the two allocation strategies previously described (FSA and IA) with a simple OFDM use of data slots (without any frequency selective allocation) both with and without adaptation of MCS.

### 5.3.4. Results

For the first simulation scenario, in the following figures (Figure 73, Figure 74 and Figure 75) a comparison between EGADIA and SEGADIA is done in terms of percentage of links not satisfied at the end of the reallocation process, average SINR of the links, and convergence time.

As we can see in the figures, SEGADIA algorithm is faster to converge and, above all, it satisfies more links than EGADIA. The price to pay is a reduction of overall SINR.

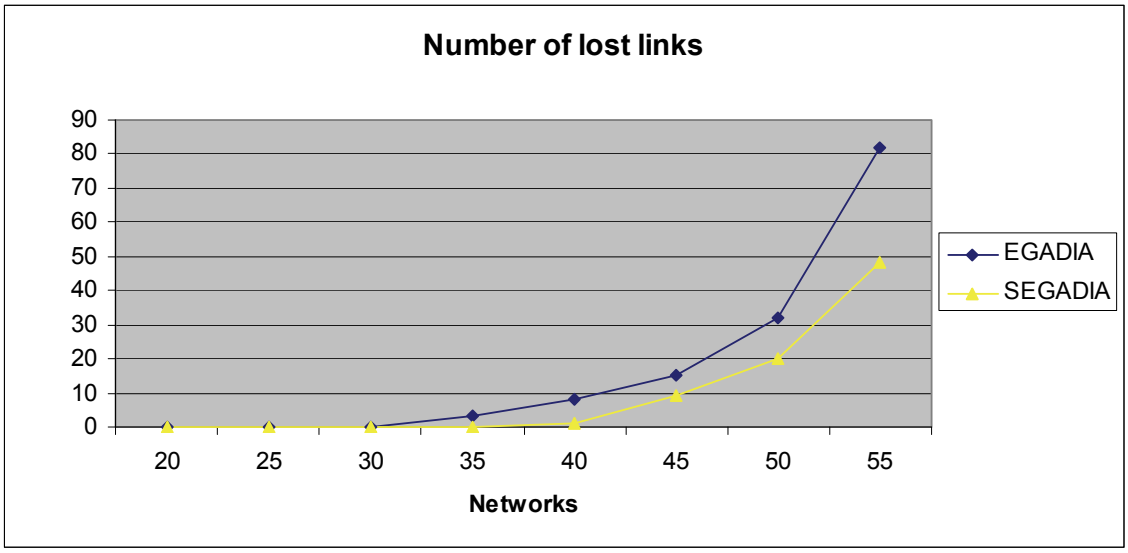


Figure 73: Number of links not satisfied at the end of reallocation process.

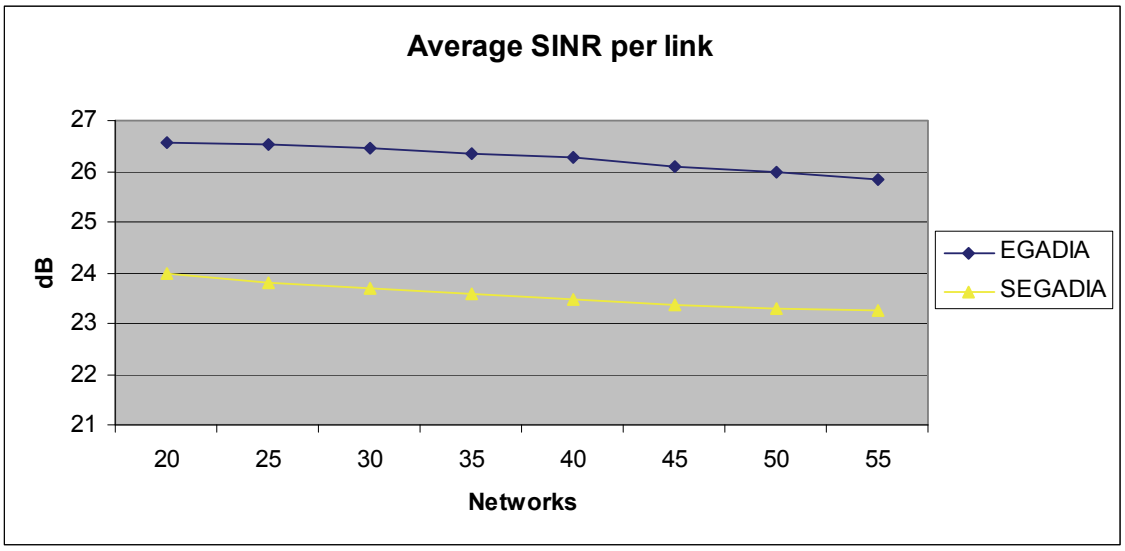


Figure 74: Average SINR per link.

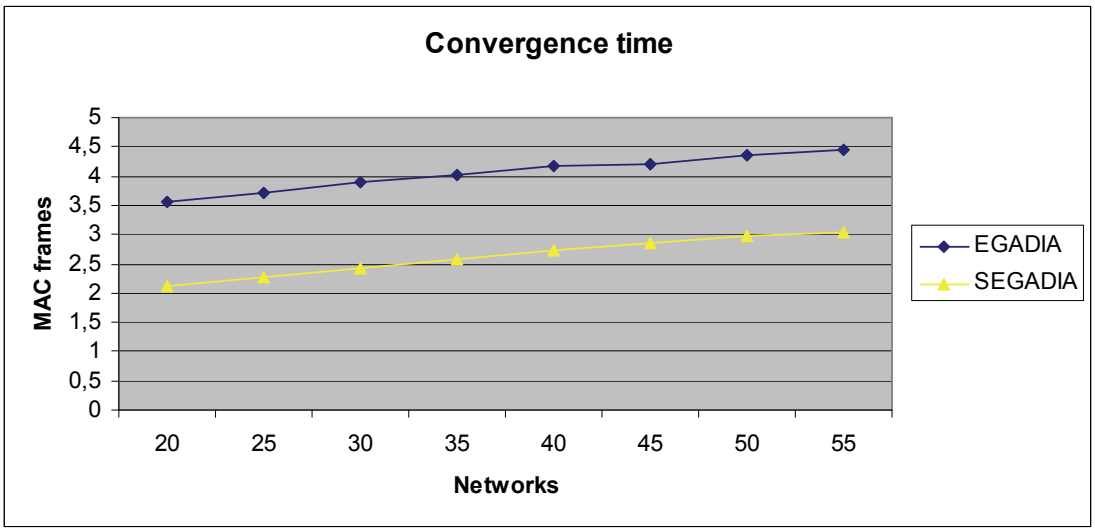


Figure 75: Average convergence time expressed in number of MAC frames.

For the simulation scenario to evaluate intra-network resource allocation algorithms, simulation results are shown in Figure 76, where the percentage of lost messages in the networks, when increasing the traffic requests of users, is depicted. It is clear from the figure that the exploitation of frequency dimension boosts the performance of the system. Moreover the increased awareness of the radio environment and of the expected channel allows reducing to almost zero the loss of user data.

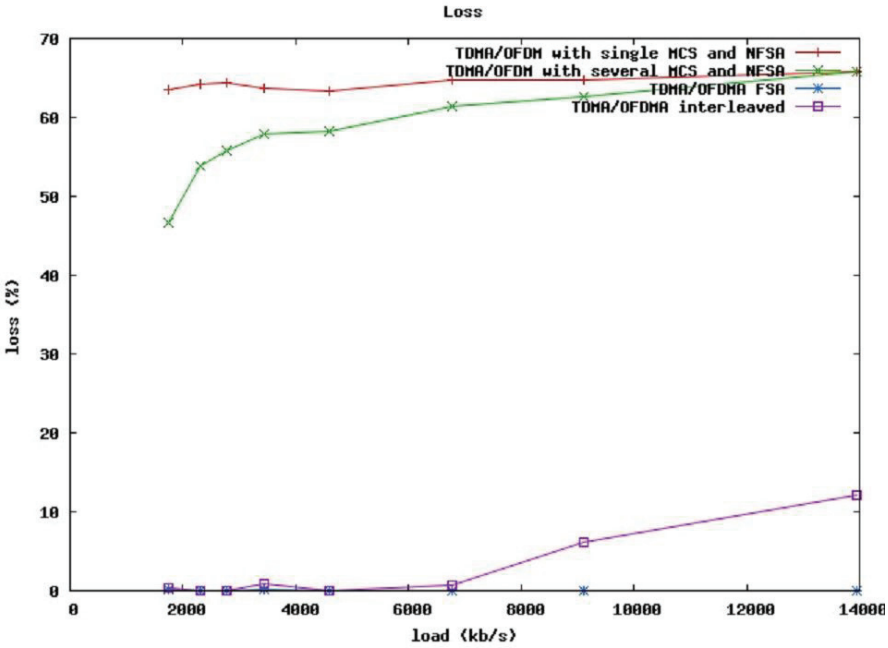


Figure 76: Percentage of loss traffic when increasing the traffic load.

### 5.3.5. Conclusions

In this chapter we propose a further evolution to GADIA algorithm (SEGADIA) that allows taking into account SINR constraints and point-to-point transmissions. In simulations we compared it with EGADIA algorithm evidencing a better capability of SEGADIA to satisfy links with only a slight penalization in terms of average SINR.

Furthermore we propose two intra-network radio resource allocation strategies that permit to each network to attribute resources to the active data links both in case of rich and poor information obtained by REM. Notice that these techniques do not depend on the channel selection strategy deployed, they only need as inputs the selected channel and the maximum available power. This means that instead of SEGADIA also other channel selection algorithms (e.g., CPSA) can be used before to apply these intra-network radio resource allocation strategies.

## 5.4. Mobile networks in primary environment

### 5.4.1. Summary of the optimization problem

In this approach the focus is to guarantee to all users of a network the reception of data broadcasted by NH, without interfering with primary systems that can be present periodically in the area. Table 21 summarizes the main features of the considered problem.

Table 21: Mobile networks in primary environment.

| Mobile networks in primary environment | |
|---|---|
| Problem title | Mobile networks in primary environment |
| Scenario | Several mobile secondary networks coordinating to access the spectrum. Presence of primary system(s). |
| Assumptions | • In each network only a unit (that corresponds to the NH) transmits user data<br>• The transmission is broadcasted to all users of the network |
| Optimization target | • Avoid interference on primary system(s)<br>• Guarantee to each network its requirements in terms of minimum capacity |
| Input from sensing and REM | • Identification of primary systems<br>• Interference level on each channel |
| Metrics | • Interference on primary transmissions<br>• Worst SINR per network<br>• Average transmitting power at NH<br>• Number of channel changes before to arrive to convergence<br>• Loss of user data per secondary network |

## 5.4.2. Optimization techniques

### 5.4.2.1. Dynamic Channel Allocation Algorithm

In [57] a distributed technique to solve channel allocation problem in mobile ad hoc networks is proposed. The approach assumes the existence of a common signaling channel that connects all networks involved, through which they can exchange decision data.

According to [57], each network periodically checks if channel in use is still available. If the channel is not available anymore, the network acts autonomously selecting a channel that guarantees minimum SINR requirement and that presents the minimum interference level. Only in the case that a channel satisfying these criteria does not exist, the network uses the common signaling channel to coordinate with other networks. Basically the network that cannot find an available channel broadcasts to all other networks a change channel request containing the identification of the chosen channel, in order to induce someone else to select a new channel.

When a network receives a change channel request concerning the channel in use it starts a timer to expire after a random amount of time. If, before timeout, it receives a change channel response broadcasted by another network, it can ignore the change channel request previously received because another network has already considered it. Otherwise, when the timer expires, it broadcasts to neighbor networks a change channel response, it frees the occupied channel and it starts a new channel selection procedure.

Algorithm 8: Dynamic Channel Allocation Algorithm

```
Check SINR of channel in use and timer (if started)
If (SINR < SINRmin || timeout)
        If (timeout)
                Broadcast change channel response message to other networks
        Analyze interference information on channels
        Available channels = channels for which SINR > SINRmin
        If (n° of available channels > 0)
                Select channel with min interference
        Else
                Select a random channel
                Broadcast change request message to other networks
Else If (change request received)
        Start timer
Else If (change channel response received)
        Reset timer
Else
        Keep channel
```

Taking advantage of the increased awareness of radio environment provided by REM-based architecture, we can improve the previously described algorithm relaxing the constraint of signaling channel among networks and the delays generated by timers. Moreover it is now possible to identify primary systems and other external interferers avoiding to impact or be impacted by their transmissions.

In the first step of this new channel selection procedure, the NH evaluates the interference information collected in L-REM to identify the channels that guarantee the satisfaction of the minimum SINR requirement of the user of the network in worst conditions. The following action of the NH is to discard all channels where primary presence is detected. If one or more channels satisfy the SINR criterion and are not used by a primary system in the neighborhoods, the NH selects the channel with the lowest interference level to transmit.

However, if it is not possible to find a free channel (i.e. interference level low enough and no primary system detected), the NH randomly selects a channel on which the primary system is not active in its neighborhoods and switches on it even if the minimum capacity level cannot be guaranteed. The NH then reports its choice to the G-REM with an alert about the need for another network to change channel.

The G-REM should always have a visibility on channels in use by each network in order to quickly solve conflicting situation. In particular when a primary system is detected on a channel it has to immediately inform networks that are using the channel and are in the interference area of primary, to look for a new one. Moreover G-REM has to help networks when they are not able to find an available channel sending an order to free a channel to a conflicting network.

Algorithm 9: REM-Aided Dynamic Channel Allocation Algorithm

**NH actions**
Check SINR of channel in use
**If** (SINR > SINRmin && no order to free channel received && no primary detected)
  Keep channel
**Else**
  **If** (primary detected in neighborhoods)
    Send alert to G-REM
  Available channels = channels for which SINR > SINRmin && no primary presence
  **If** (n° of available channels > 0)
    Select channel with min interference
  **Else**
    Select a random channel that is not used by a neighbor primary system
    Report choice to G-REM asking to free channel

**G-REM actions**
**If** (request to free channel received)
  Randomly select a network using the channel in interference area
  Send order to free channel to the network
**Else if** (Primary detected on a channel)
    Send order to free channel to all networks that use it in interference range of primary

### 5.4.3. Evaluation methodology

To test the proposed REM extension and to evaluate its behavior with respect to the Dynamic Channel Allocation Algorithm (DCAA) previously introduced, we modeled the area and the networks as for "fast reactive autonomous networks" scenario (section 5.2), putting several networks with different dimensions in a 100 $Km^2$ area.

In addition to the previously described model, we add the presence of a primary system that can start to use some of the channels shared by secondary networks. The primary is modeled as several emitters that can switch on at different moments. They all have fixed transmitting power and each of them covers several users distant at most 3Km from the emitter.

The most important metric to be considered is the percentage of the traffic of primary systems impacted by the interference generated by the secondary networks. In addition, we also evaluate the lost traffic, the channel changes, the average SINR and the transmitting power at secondary networks.

### 5.4.4. Results

As for "fast reactive autonomous networks" scenario, we vary the number of secondary networks from 20 to 55 and we set the number of available channels to 8.

At the beginning only secondary networks are active in the area. After a period corresponding to 20 MAC frames, one primary emitter switches on and starts to transmit on a channel. As consequence it generates interference on secondary networks and it is affected by secondary transmissions on the channel. After that, each 20 MAC frames a new primary emitter, located at a

different point, starts transmissions on a different channel. We keep adding emitters up to five primary emitters in the simulated area and we observe the behavior of secondary networks.

The simulation is done over 10000 realizations of topology for 20, 25, 30, 35, 40, 45, 50 and 55 secondary networks. For each realization the simulation lasts 120 MAC frames.

In Figure 77 it is represented the averaged percentage of primary transmissions affected by secondary interferences.

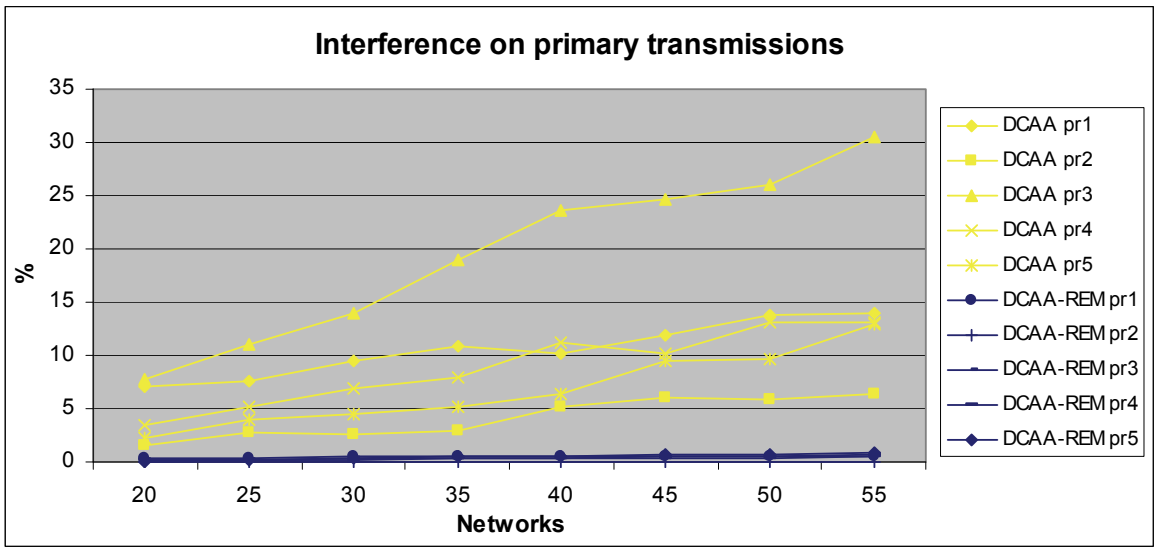


Figure 77: Percentage of primary transmissions affected by interference generated by secondary networks.

The REM extension of the algorithm clearly improves the performance strongly reducing the impact of secondary transmissions on primary systems.

The residual impact on primary system depends on the time necessary to detect the presence of primary system on the channel. For the results presented in previous figure, the simulation was done assuming that primary system is detected through sensing. Following this assumption, at least one MAC frame is necessary between the detection of primary by MCDs and the action of G-REM, because the information should be transmitted to L-REM and reported to G-REM. So during this MAC frame the generation of interference to the primary system cannot be avoided. On the other hand, if we assume that G-REM is in contact with the primary system and, then, that it can directly know when a primary emitter switches on, we can strongly reduce the impact on primary system arriving to a percentage of affection in primary communications close to zero as it is shown in Figure 78.

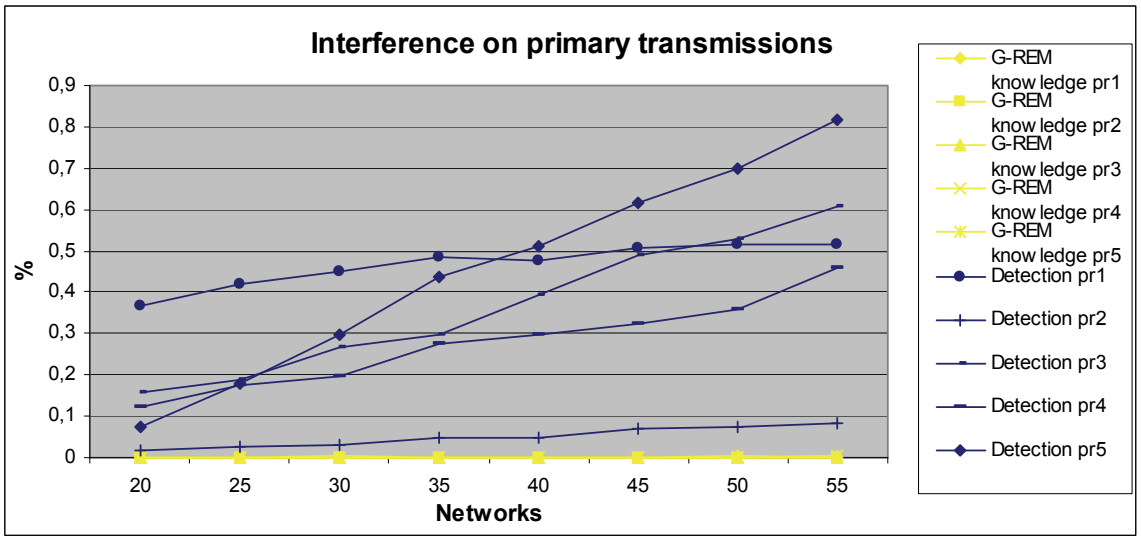


Figure 78: Percentage of primary transmissions affected by interference generated by secondary networks.

The price to pay to avoid impacting the primary system is a degradation of secondary system performance. More specifically, excluding the channels used by a close primary system, the secondary networks require more channel changes to converge to a satisfying configuration and their transmissions can be strongly impacted.

In the following two figures a comparison is done between the two algorithms in terms of channel changes and lost traffic at secondary networks.

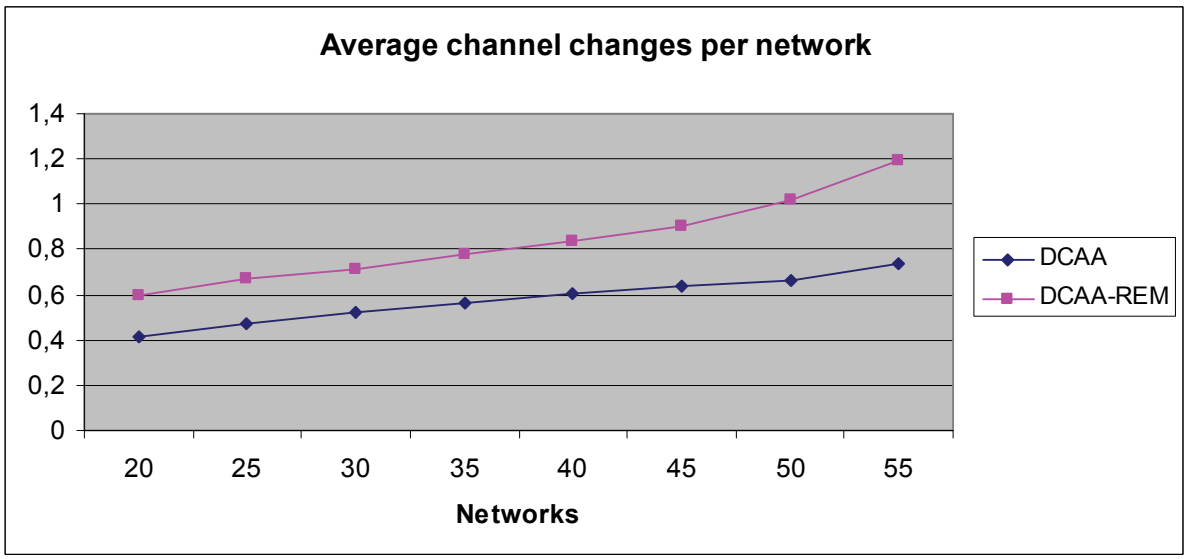


Figure 79: Average channel changes per network.

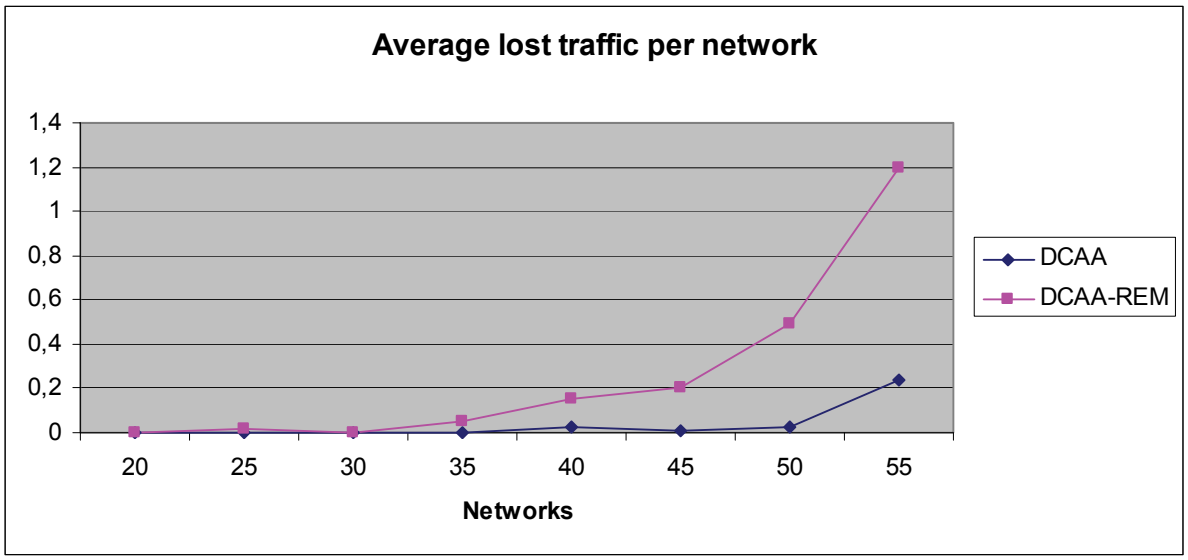


Figure 80: Average lost traffic per network.

As expected the price to pay to protect the primary system, is the reduction of performance at secondary networks both in terms of channel changes when reconfiguring the channels in use and in terms of lost traffic at secondary networks.

Finally, in Figure 81, we compare the average SINR per secondary network obtained by the two techniques when the five primary emitters are transmitting.

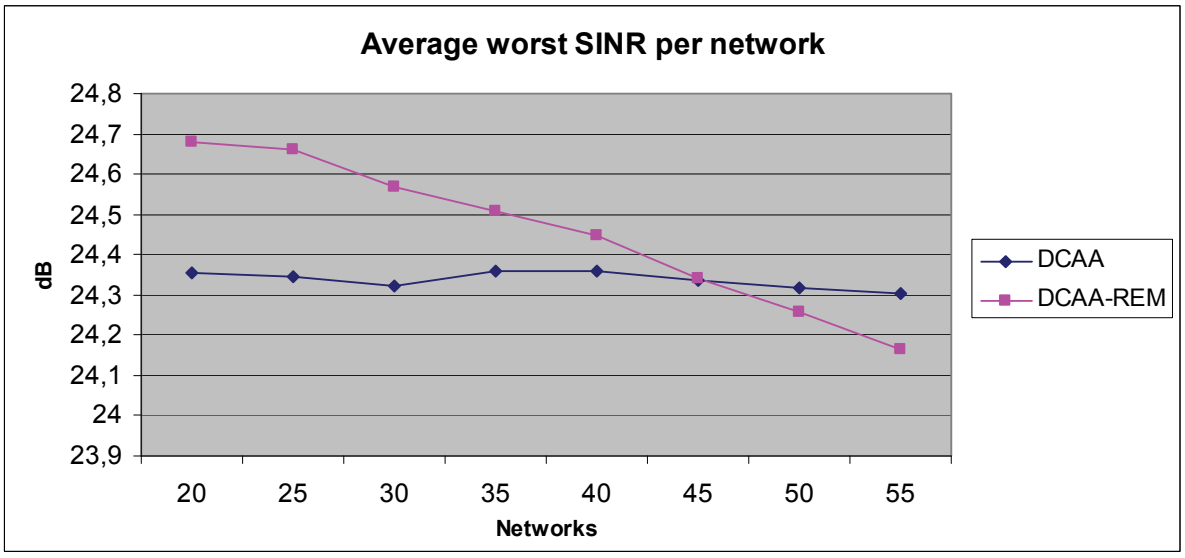


Figure 81: Average minimum SINR per network.

For this metric, the result is quite surprising. In fact the DCAA-REM strategy overcomes DCAA performance in low complexity scenario, while it becomes worst increasing the complexity.

This can be explained by taking into account the fact that in DCAA the interferences of primary emitters are considered in the same way than interferences of secondary networks; hence, when a primary appears, a secondary network does not necessarily change the channel in use, suffering for its interference. On the other side, DCAA-REM will leave the channel and look for a better one.

This allows DCAA-REM to improve performance when better channels are available (as in easy conditions), but the reduced range of available channels will penalize more and more the performance of the network when increasing complexity.

### 5.4.5. Conclusions

In this paragraph we present an algorithm retrieved from the literature that fits well with the problem of resource allocation at secondary networks. Furthermore we propose a REM-based evolution that allows taking into account the possible presence of active primary systems in the area. The simulation results show that the proposed evolution permits to protect much better the primary system paying a not so heavy price in terms of secondary performance, except when considering very dense scenarios.

# 6. Conclusions

This deliverable has presented the performance evaluation of a number of RRM optimization problems relevant to the different scenarios identified in FARAMIR, with the aim of showing the relevance of applying measurement-based information stored in REM. The document has been organized according to the different groups of scenarios of applicability for the considered techniques. For each group, the different optimization problems and corresponding techniques and performance evaluation are presented. In the following, the main obtained conclusions are summarised.

- Intra-operator spectrum management scenarios: The optimization problems in this group of scenarios have dealt with the resource allocation in a OFDMA network, in relation to power and frequency assignment:
    - The power control for co-channel OFDMA networks composed of macrocells and femtocells has been considered first. It adjusts the transmit power by femtocells to ensure the required level of protection from interference to the macrocell users. Results show that the use of stored context information in REM increases the effectiveness of the PC algorithm to protect the macrocell users. A version of the REM-based PC without the knowledge of the shadowing term was also proposed and compared to the previous algorithms. The estimation of the shadowing term with the use of a back-off term, based on the standard deviation, was shown to protect the MUE almost as good as the ideal case, at the expense of a lower femtocell transmission power level that may lead to smaller femtocell coverage.
    - A second problem considered in this scenario has exploited the frequency dimension to mitigate the interference between macrocells and femtocells by means of DFFR and DSA strategies. Proposed approach considers the delay-resistance and low signaling overhead requirement. In particular, the proposed DFFR decides an exclusive part of the resources to be used for femtocells dynamically based on the number of outage users interfered by the macro BS. At the same time, by using the proposed DSA, the interference from the femto BS to macro users can be effectively reduced. It is shown that the overall system throughput can be significantly improved with the proposed approach.
    - The coexistence between PUs and SUs has been addressed in this scenario from the perspective of a primary cellular operator that performs a channel allocation with the target to ensure the QoS of its users while at the same time leaving unused spectrum for secondary sharing. In particular a planning tool has been developed to estimate the number of channels that an OFDMA-based primary system must reserve for exclusive use in order to keep its quality of service requirements. By computing the probability of PUs to face interference above the system-dependent tolerable threshold, upper boundaries of the overall system performance have been provided. With the proposed reservation scheme it is possible that a significant amount of spectrum remains available for secondary sharing, thus contributing to improving efficiency in spectrum use.

- LTE TVWS scenario: The optimization problem considered in this scenario addresses also the spectrum and power optimization for a cellular network composed of multiple femtocells operating with LTE. As a difference from the scenarios in the previous group, the available TVWS frequencies are used for the resource allocation to femtocells. In this case, a two step spectrum and power optimization scheme based on central coordination and simulated annealing is proposed and evaluated. A REM manager is used to collect reports from involved HeNBs and carry out simulated annealing process and then control the maximum transmission power of HeNBs in a centralized manner. When inter-HeNB interface (e.g. a X2 interface) is available, the optimization method can also be implemented in a distributed way. Results in a LTE downlink indoor network configuration reveal that the proposed scheme improves worst case user terminal throughput when the number of HeNBs is bigger than the available TV channels, so it can be used as an effective method for interference coordination in dense urban deployments.

- Scenarios with non-coordinated spectrum access between PUs and SUs: The optimization problems in this general type of scenarios address the way how a secondary network shares the spectrum of a primary network without any coordination among the two. For that purpose, the information stored in the REM database about the PU features and environmental characteristics is used. Proposed strategies deal with exploiting the spatial and/or the temporal utilisation of the spectrum allocated to the PUs, as summarised in the following:
    - Out-of-band or cognitive femtocells have been considered in which a femtocell network is deployed making use of the spectrum left available by a number of primary networks. The framework aims to minimize the spectral footprint of the cognitive femtocells through the bandwidth-power product metric, incorporating the protection to PUs and the limitations of CR users. Results reveal that the proposed framework improves the utilization of spectrum by striking a balance between the consumed power and bandwidth and allows for further spectral opportunities compared to a resource allocation based on waterfilling.
    - The exploitation of heterogeneity in the different PU types has also been analyzed to propose a RRM control mechanism that regulates the sharing of the total capacity among CRs with variable data rate requirements. The proposed procedure has the objective to minimize at each step the difference between the available capacity left by the different PUs and the achieved data rates of the CRs. The proposed technique is subdivided into an admission control and a resource allocation based on the information about PU features stored in the REM. This allows having a better knowledge about the available capacity that can be used by CRs and correspondingly improving their performance.
    - Focusing on the exploitation of the temporal activity of PUs, the use of advanced statistics stored in the REM has been proposed as a means to develop spectrum selection criteria with the target of reducing the spectrum handover rate. Performance evaluation has shown that, in case a REM supporting the cognitive system and providing knowledge about primary users is available, the proposed criteria can introduce significant gains (in terms of reduction in the rate of spectrum handovers) ranging from 70% to 100% with respect to a reference

criterion not making use of the REM. Results have shown substantial robustness in terms of performance even if the level of accuracy of the stored statistics is only medium (i.e. in the order of 4%). It has also been identified that the suitable spectrum selection criterion depends on a number of aspects such as composition and characteristic of PUs, secondary service mix, etc. In that respect, among the considered REM-based techniques, the strategy with the best performance includes in the selection process considerations about the existing SU traffic mix to smartly switch between a selection that purely chooses the channel with the longest availability and a selection that tries to fit the remaining availability time in a channel to the secondary service duration.

- The problem of opportunistic access when the primary network is a cellular network has been considered. The information about the positions of primary base stations is used by a maximum likelihood estimator to determine the closest active cell to a cognitive node. Then, this node can estimate the allowed transmit power that satisfies primary constraints. Evaluations have revealed that IEEE 802.11-like cognitive radio can opportunistically access cellular frequency bands under some constraints. It has also been obtained that the detection of spectrum opportunities and the protection of primary users with relatively acceptable probability is only possible under specific constraints. In particular, to detect base station activity the sensors should be close to the considered base station, meaning that a cluster of sensors should only be interested in detecting the activity of covering cells. Results have shown that the position and the distribution of the sensors can be in most cases more important than the number of these sensors, thus being important to develop models to determine the best position distribution of the sensors.
- Focusing also on opportunistic access when the primary network is a cellular network, a new approach for DSA based on stochastic models has been explored. It is particularly suitable when the primary activity patterns are very fast and then traditional DSA techniques based on sensing and localization fail to allow any transmission. The proposed approach allows a predictable and controllable QoS, which makes it suitable for applications not requiring high data rate but are sensitive to jitter and delay. Results show that the proposed approach cannot perform as well as optimal sensing- and location-based techniques for low duty cycles of primary networks. However, we believe that such techniques are very difficult to implement and stochastic-based approaches can be a good candidate for DSA problems in such scenarios. Furthermore, the proposed approach reduces power consumption because it does not require sensing.
- The use of REM in the detection and avoidance of hidden nodes has also been proposed. It is especially disruptive when deterministic or bounded latency and reliability are required within opportunistic, multi-RAT or cognitive radio deployment environments. The evaluation of the proposed approach has illustrated the ability to compensate for unknown transmitter power and propagation anomalies such as shadow fading. It is essential that the REM prediction approaches exploit the ability to combine measurements made using different references in an intelligent manner. This improves the interference predictions and reduces the complexity and power consumption required for MCDs.

- Ad Hoc networks scenario: The optimization problems in this scenario assume the existence of a number of ad hoc networks coexisting in a certain area and sharing the same spectrum. The general objective has been to guarantee to all networks the satisfaction of their requirements in terms of minimum capacity. The following aspects have been studied:
    - The considered architecture in this scenario makes use of the local REM with information at ad hoc network level and the global REM with information coming from all networks. To populate the information in both REMs, a new protocol has been proposed to enable the data dissemination of the information measured by the different nodes. Messages exchanged between nodes are transmitted using a TDMA scheme with different types of slots organized in a MAC frame.
    - A first optimization problem considered in this scenario has dealt with highly mobile autonomous networks in which interference conditions can change in a short time thus requiring frequent resource reallocation processes. Different optimization techniques, namely the EGADIA and the CPSA algorithms have been proposed to deal with the channel selection to the different links in the networks. Based on the requirements of the problem, in terms of a fast convergence to reach to a suitable solution, the CPSA fast algorithm has revealed to provide the best behaviour in this scenario.
    - Another considered problem has been the maximization of the global capacity when several flows of data are transmitted using point-to-point links. In this case, the SEGADIA algorithm has been proposed that takes into account the point-to-point link quality inside each cluster with respect to the interference from the other clusters. Results have revealed a better capability of SEGADIA with respect to EGADIA to satisfy links. Furthermore, two intra-network radio resource allocation strategies that permit to each network to attribute resources to the active data links both in case of rich and poor information obtained by REM have been also proposed.
    - The scenario in which mobile ad hoc networks act as secondary users of the spectrum used by a PU has also been considered, assuming a broadcast service in the ad hoc networks. A REM-Aided Dynamic Channel Allocation algorithm has been proposed to deal with the resource allocation in this situation. Simulation results have shown that the proposed algorithm allows a much better protection of the primary system without degrading very much the secondary performance, than the baseline algorithm from the literature that does not make use of REM.

# Acronyms

| Term | Description |
|---|---|
| 3GPP | 3rd Generation Partnership Project |
| BO | Back-Off |
| BS | Base Station |
| C-N | Cognitive Node |
| CDF | Cumulative Distribution Function |
| CPSA | Channel and Power Selection Algorithm |
| CR | Cognitive Radio |
| CRM | Cognitive Resource Manager |
| CRN | Cognitive Radio Network |
| CSG | Closed Subscriber Group |
| CSI | Channel State Information |
| DC | Duty Cycle |
| DCAA | Dynamic Channel Allocation Algorithm |
| DECT | Digital European Cordless Telephone |
| DFFR | Dynamic Fractional Frequency Reuse |
| DSA | Dynamic Spectrum Access (also Dynamic Spectrum Allocation) |
| DVB-T | Digital Video Broadcasting - Terrestrial |
| FAP | Femtocell Access Point |
| FCC | Federal Communications Commission |
| FF | Fitness Function |
| FFT | Fast Fourier Transform |
| FIFO | First In First Out |
| FSA | Frequency Selective Allocation |
| G-REM | Global REM |
| GA | Genetic Algorithm |
| GPS | Global Positioning System |
| GSM | Global System for Mobile communications |
| HeNB | Home evolved Node B |
| IA | Interleaved Allocation |
| IM | Interference Management |
| ISM | Industrial, Scientific and Medical |
| JRRM | Joint Radio Resource Management |
| KPI | Key Performance Indicator |
| L-REM | Local REM |
| LTE | Long Term Evolution |
| M2M | Machine to Machine |
| MAC | Medium Access Control |
| MBS | Macrocell Base Station |
| MCD | Measurement Capable Device |
| MCS | Modulation and Coding Scheme |
| MHT | Mean Holding Time |
| MLE | Maximum Likelihood Estimator |
| MT | Mobile Terminal |
| MUE | Macrocell User Equipment |
| NH | Network Head |

| Term | Description |
|---|---|
| NP | Non-deterministic Polinomial-time |
| NRM | Network Reconfiguration Manager |
| OAM | Operation And Maintenance |
| OFDM | Orthogonal Frequency Division Multiplexing |
| OFDMA | Orthogonal Frequency Division Multiple Access |
| P-BS | Primary Base Station |
| PC | Power Control |
| PL | Path Loss |
| PU | Primary User |
| QoS | Quality of Service |
| RA | Random Access |
| RAT | Radio Access Technology |
| RB | Resource Block |
| REM | Radio Environmental Map |
| REM-SA | REM Storage & Acquisition |
| RMSE | Root Mean Squared Error |
| RRM | Radio Resource Management |
| RSRP | Reference Signal Received Power |
| RSSI | Radio Signal Strength Indicator |
| SINR | Signal to Interference and Noise Ratio |
| SIR | Signal to Interference Ratio |
| SNR | Signal to Noise Ratio |
| SpHO | Spectrum HandOver |
| SU | Secondary User |
| TDD | Time Division Duplex |
| TDMA | Time Division Multiple Access |
| TV | TeleVision |
| TVWS | TeleVision White Space |
| Tx | Transmit |
| UE | User Equipment |
| UF | Utility Function |
| UHF | Ultra High Frequency |
| ULLA | Unified Link Layer API |
| VHO | Virtual Hand Over |
| VRR | Variable data Rate Requirements |
| WCP | Worst Case Position |
| WLAN | Wireless Local Area Network |

# References


[1] FARAMIR Deliverable D2.2 “Scenario Definitions”, http://www.ict-faramir.eu/

[2] FARAMIR Deliverable D5.1 “Conceptual Framework for enabling Measurement-based mechanisms”, http://www.ict-faramir.eu/

[3] FARAMIR Deliverable D2.4 “Final System Architecture”, http://www.ict-faramir.eu/

[4] T. Cai, J. van de Beek, B. Sayrac, S. Grimoud, J. Nasreddine, J. Riihijärvi, P. Mähönen, "Design of Layered Radio Environment Maps for RAN Optimization in Heterogeneous LTE Systems," IEEE PIMRC 2011, Toronto, Canada, September, 2011.

[5] 3GPP TS 36.300 v11.0.0, “Evolved Universal Terrestrial Radio Access (E-UTRA) and Evolved Universal Terrestrial Radio Access Network (E-UTRAN); Overall description; Stage 2 (Release 11)”, December, 2011.

[6] N.Miliou, A. Moustakas, A.Polydoros, "Interference Source Localization and Transmit Power Estimation under Log-Normal Shadowing", Proceedings of EUSIPCO 2011, Barcelona, Spain, September 2011.

[7] J. Nasreddine, N. Miliou, J. Riihijärvi, A. Polydoros, P. Mähönen, "Using Geolocation Information for Dynamic Spectrum Access in Cellular Networks," 6th ACM Workshop on Performance Monitoring and Measurement of Heterogeneous Wireless and Wired Networks ($PM^2HW^2N$ 2011) in conjunction with MSWIM 2011.

[8] www.femtofotum.org: “Interference Management in UMTS Femtocells”, December 2008.

[9] M. Yavuz, F. Meshkati, S. Nanda, A. Pokhariyal, N. Johnson, B. Raghothaman, A. Richardson, "Interference Management and Performance Analysis of UMTS/HSPA+ Femtocells", IEEE Communications Magazine, September 2009.

[10] 3GPP TR 25.967 8.0.1 (2009-03), Home Node B Radio Frequency (RF) Requirements (FDD) (Release 8), 2009.

[11] www.femtofotum.org: “Interference Management in OFDMA Femtocells”, March 2010.

[12] H. Kim, K. G. Shin, “Efficient discovery of spectrum opportunities with MAC-layer sensing in cognitive radio networks,” IEEE Transactions on Mobile Computing, vol. 7, no. 5, pp. 533 –545, May 2008.

[13] M. Sharma, A. Sahoo, K. D. Nayak, “Model-based opportunistic channel access in dynamic spectrum access networks”, in IEEE Global Telecommunications Conference (GLOBECOM 2009), December, 2009.

[14] E. G. Larsson, M. Skoglund, “Cognitive radio in a frequency-planned environment: some basic limits,” IEEE Transactions on Wireless Communications, vol. 7, no. 12, pp. 4800–4806, December, 2008.

[15] N. Hoven, A. Sahai, “Power scaling for cognitive radio”, International Conference on Wireless Networks, Communications and Mobile Computing, vol. 1, June 2005, pp. 250–255.

[16] M. Vu, N. Devroye, V. Tarokh, “The primary exclusive region in cognitive networks”, 5th IEEE Consumer Communications and Networking Conference (CCNC 2008), Jan. 2008, pp. 1014–1019.

[17] A. Sahai, R. Tandra, S. M. Mishra, N. Hoven, “Fundamental design tradeoffs in cognitive radio systems”, First international workshop on Technology and policy for accessing spectrum (TAPAS 2006). New York, NY, USA: ACM, 2006.

[18] S. Srinivasa, S. A. Jafar, “How much spectrum sharing is optimal in cognitive radio networks?”, IEEE Transactions on Wireless Networks, vol. 7, no. 10, pp. 4010 – 4018, October 2008.

[19] J. Nasreddine, A. Achtzehn, J. Riihijärvi, P. Mähönen, "Enabling Secondary Access through Robust Primary User Channel Assignment," IEEE Global Telecommunications Conference (GLOCECOM 2010), Miami, USA, December 2010.

[20] J. Nasreddine, J. Riihijärvi, P. Mähönen, "Location-based adaptive detection threshold for dynamic spectrum access," in the 4th IEEE International Symposium on New Frontiers in Dynamic Spectrum Access Networks (DySPAN 2010), Singapore, April 2010.

[21] L. Maciel, H. Bertoni, H. Xia, "Unified approach to prediction of propagation over buildings forall ranges of base station antenna height," IEEE transactions on vehicular technology, vol. 42, no. 1, pp. 41–45, 1993.

[22] R. K. Ganti, M. Haenggi, "Interference and outage in clustered wireless ad hoc networks," IEEE Transaction on Information Theory, vol. 55, pp. 4067–4086, September 2009.

[23] J. van de Beek, J. Riihijärvi, A. Achtzehn, P. Mähönen, "UHF white space in Europe - a quantitative study into the potential of the 470-790 MHz band", Proc. of IEEE DySPAN 2011, Aachen, Germany, May 2011.

[24] T. Cai, G. P. Koudouridis, C. Qvarfordt, J. Johansson, P. Legg, "Coverage and Capacity Optimization in E-UTRAN Based on Central Coordination and Distributed Gibbs Sampling," Proc. of 71st IEEE Vehicular Technology Conference (VTC 2010-Spring), Taipei, Taiwan, May 2010.

[25] 3GPP TR 36.814 v9.0.0, "Further advancements for E-UTRA physical layer aspects (Release 9)", March, 2010.

[26] I.F. Akyildiz, W.-Y. Lee, M.C. Vuran, S. Mohanty, "A Survey of Spectrum Management of Cognitive Radio Networks", IEEE Communications Magazine, April 2008, 40–48.

[27] P. Gupta, P. R. Kumar, "The capacity of wireless networks", IEEE Transactions on Information Theory, Vol. 46, No. 2, March, 2000, pp. 388-404.

[28] X. Liu, W. Wang. "On the Characteristics of Spectrum-Agile Communication Networks", IEEE Symposium on New Frontiers in Dynamic Spectrum Access Networks (DySPAN), Baltimore, MD, November 8-11, 2005.

[29] D. Palomar, M. Chiang, "A tutorial on decomposition methods for network utility maximization", IEEE Journal on Selected Areas in Communications, vol. 24, no. 8, pp. 1439–1451, August, 2006.

[30] D. Palomar, M. Chiang, "Alternative distributed algorithms for network utility maximization: Framework and applications," IEEE Transactions on Automatic Control, vol. 52, no. 12, pp. 2254–2269, December, 2007

[31] A. Vizziello, I. F. Akyildiz, R. Agusti, L. Favalli, P. Savazzi, "OFDM Signal Type Recognition and Adaptability Effects in Cognitive Radio Networks," Proc. of the IEEE Global Communications Conference (GLOBECOM 2010), Miami, Florida, USA, 6-10 Dec. 2010.

[32] R. Iyengar, K. Kar, B. Sikdar, "Scheduling Algorithms for PMP Operation in IEEE 802.16 Networks," RAWNET 2006 workshop, in Conjunction with WiOPT 06, Boston, Ma.

[33] A. Vizziello, I. F. Akyildiz, R. Agusti, L. Favalli, P. Savazzi "Cognitive Radio Resource Management exploiting Heterogeneous Primary Users", Proc. of the IEEE Global Communications conference (GLOBECOM 2011), Houston, Texas, USA, 5-9 December, 2011.

[34] B. Canberk, I. F. Akyildiz, S. Oktug, "Primary User Activity Modeling Using First-Difference Filter Clustering and Correlation in Cognitive Radio Networks," IEEE/ACM Transactions on Networking, Vol. 19, No. 1, pp. 170-183, February, 2011.

[35] C. Mohanram, S. Bhashyam, "A sub-optimal joint subcarrier and power allocation algorithm for multiuser OFDM", IEEE Communications Letters, vol. 9, no. 8, pp. 685-687, 2005.

[36] A. Vizziello, J. Pérez-Romero, "System Architecture in Cognitive Radio Networks using a Radio Environment Map", Proc. of the 4th International Conference on Cognitive Radio and Advanced Spectrum Management (CogART 2011), Barcelona, Spain, 26-29 October, 2011.

[37] M. Wellens, J. Riihijärvi, P. Mähönen, "Empirical time and frequency domain models of spectrum use", Physical Communication, vol. 2, no. 1-2, pp. 10 – 32, 2009.

[38] F. Bouali, O. Sallent, J. Pérez-Romero, R. Agustí, "Strengthening Radio Environment Maps with Primary-User Statistical Patterns for Enhancing Cognitive Radio Operation", CROWNCOM Conference, Osaka, Japan, June, 2011.

[39] F. Bouali, O. Sallent, J. Pérez-Romero, R. Agustí, "A Novel Spectrum Selection Strategy for Matching Multi-Service Secondary Traffic to Heterogeneous Primary Spectrum Opportunities", IEEE Personal, Indoor and Mobile Radio Communications conference (PIMRC), Toronto, Canada, September, 2011.

[40] M. M. Buddhikot, P. Kolodzy, S. Miller, K. Ryan, J. Evans, "DIMSUMnet: New directions in wireless networking using coordinated dynamic spectrum access", IEEE International Symposium on a World of Wireless, Mobile and Multimedia Networks (WoWMoM 2005), 2005.

[41] I. F. Akyildiz, W.-Y. Lee, M. C. Vuran, S. Mohanty, "Next generation/dynamic spectrum access/cognitive radio wireless networks: a survey", Computer Networks: The International Journal of Computer and Telecommunications Networking, Vol. 50, No. 13, pp. 2127 – 2159, 2006.

[42] N. Miliou, A. Moustakas, A. Polydoros. "Interference source localization and transmit power estimation under log-normal shadowing", European Signal Processing Conference (Eusipco 2011), 2011.

[43] A. O. Nasif, B. L. Mark. "Opportunistic spectrum sharing with multiple cochannel primary transmitters", IEEE Transactions on Wireless Communications, Vol. 8, No. 11, pp. 5702 – 5710, 2009.

[44] http://www.t-mobiletowers.com.

[45] "Second report and order and memorandum opinion and order". ET Docket No. 04-186 and ET Docket No. 02-380, FCC 08-260, November 4 2008.

[46] K. Harrison, A. Sahai, "Potential collapse of whitespaces and the prospect for a universal power rule", IEEE International Symposium on New Frontiers in Dynamic Spectrum Access Networks (DySPAN 2011), 2011.

[47] R. E. Barlow, L. C. Hunter, "Reliability analysis of a one-unit system", Operations research, Vol. 9, No. 2, pp. 200–208, March-April, 1961.

[48] L. A. Baxter, "Availability measures for a two-state system", Journal of Applied Probability, vol. 18, no. 1, pp. pp. 227–235, 1981.

[49] L. A. Baxter, "Some remarks on numerical convolution", Communications in statistics, Simulation and computation, Vol. 10, No. 3, pp. 281–288, 1981.

[50] L. A. Baxter, "Availability measures for coherent systems of separately maintained components", Journal of Applied Probability, Vol. 20, No. 3, pp. 627–636, September, 1983.

[51] H. Kim, K. G. Shin, "Efficient discovery of spectrum opportunities with mac-layer sensing in cognitive radio networks", IEEE Transactions on Mobile Computing, Vol. 7, No. 5, pp. 533 –545, May 2008.

[52] M. Sharma, A. Sahoo, K. D. Nayak, "Model-based opportunistic channel access in dynamic spectrum access networks", IEEE Global Telecommunications Conference (GLOBECOM 2009).

[53] J. Nasreddine, J. Riihijärvi, X. Li, P. Mähönen, "Exploring Opportunistic Access Techniques Using Stochastic Models: Dynamic Spectrum Access Without Sensing," IEEE MILCOM 2011.

[54] R. Cléroux, D. J. McConalogue, "A numerical algorithm for recursively defined convolution integrals involving distribution functions", Management Science, Vol. 22, No. 10, pp. 1138–1146, 1976.

[55] B. Babadi, V. Tarokh, "Gadia: A greedy asynchronous distributed interference avoidance algorithm," IEEE Transactions on Information Theory, Vol. 56, pp. 6228–6252, December 2010.

[56] S. Herry, C. Le Martret, "Parameter Determination of Secondary User Cognitive Radio Network Using Genetic Algorithm", IEEE Pacific Rim Conference on Communications, Computers and Signal Processing, Victoria, Canada, August, 2009.

[57] L. Iacobelli, F. Scoubart, D. Pirez, P. Fouillot, R. Massin, C. Lefebvre, C. Le Martret, V. Conan, "Dynamic Frequency Allocation in Ad Hoc Networks", in Cognitive Information Processing Workshop, June 2010.

[58] IEEE 802.11k-2008 standard, "IEEE Standard for Information Technology Telecommunications and Information Exchange Between Systems Local and Metropolitan Area Networks Specific Requirements Part 11: Wireless LAN Medium Access Control (MAC) and Physical Layer (PHY) Specifications Amendment 1: Radio Resource Measurement of Wireless LANs"

[59] J. Nasreddine, P. Mähönen, J. Riihijarvi et al.,"Adaptive Reconfigurable Access and Generic interfaces for Optimisation in Radio Networks – ARAGORN Document Number D 2.4 Final Specification of Generic Interfaces", 2010 http://ict-aragorn.eu/fileadmin/user_upload/deliverables/Aragorn_D24.pdf

[60] T. Farnham, P. Kulkarni, "Collaborative Radio Resource Management for femto-cell networks" Future Network and Mobile Summit, 2010

[61] J. Tiemann, S. Taranu (editors), "Architecture, Information Model and Reference Points, Assessment Framework, Platform Independent Programmable Interfaces", Deliverable D2.3 of the End to End Efficiency ($E^3$) project, September, 2009, https://ict-e3.eu/project/deliverables/full_deliverables/E3_WP2_D2.3_090930.pdf

[62] Y. Zhao, D. Raymond, C. da Silva, J. Reed, S. Midkiff, "Performance Evaluation of Radio Environment Map-Enabled Cognitive Spectrum Sharing- Networks", IEEE MILCOM, 2007.

[63] S. J. Bae, M. Y. Chung, J. So, "Handover Triggering Mechanism Based on IEEE 802.21 in Heterogeneous Networks with LTE and WLAN", IEEE Information Networking Conference (ICOIN), 2011.

[64] G. Fodor, P. Skillermark, "Performance Analysis of a Reuse Partitioning Technique for Multi-Channel Cellular Systems Supporting Elastic Services", International Journal of Communication Systems, Vol. 22, No. 3, March, 2009.